NOTICE

The quality of this microform is heavily dependent upon the quality of the original thesis submitted for microfilming. Every effort has been made to ensure the highest quality of reproduction possible.

If pages are missing, contact the university which granted the degree.

Some pages may have indistinct print especially if the original pages were typed with a poor typewriter ribbon or if the university sent us an inferior photocopy.

Reproduction in full or in part of this microform is governed by the Canadian Copyright Act, R.S.C. 1970, c. C-30, and subsequent amendments.

AVIS

La qualité de cette microforme dépend grandement de la qualité de la thèse soumise au microfilmage. Nous avons tout fait pour assurer une qualité supérieure de reproduction.

S'il manque des pages, veuillez communiquer avec l'université qui a conféré le grade.

La qualité d'impression de certaines pages peut laisser à désirer, surtout si les pages originales ont été dactylographiées à l'aide d'un ruban usé ou si l'université nous a fait parvenir une photocopie de qualité inférieure.

La reproduction, même partielle, de cette microforme est soumise à la Loi canadienne sur le droit d'auteur, SRC 1970, c. C-30, et ses amendements subséquents.

COMPUTER SIMULATIONS OF TWO-FLUID IMMISCIBLE DISPLACEMENT FLOW IN POROUS MEDIA

Dionissios Georgios Kiriakidis

A thesis submitted to the School of Graduate
Studies and Research in Partial Fulfillment
of the Requirements for the Degree of
DOCTOR OF PHILOSOPHY
in the Department of Chemical Engineering
University of Ottawa

ISBN 0-315-75076-6

UNIVERSITÉ D'OTTAWA
UNIVERSITY OF OTTAWA

Dedicated to Debbie

ITHACA

When you set out on the voyage to Ithaca,
pray that your journey may be long,
full of adventures, full of knowledge.
Of the Laestrygones and the Cyclopes
and of furious Poseidon, do not be afraid,
for such on your journey you shall never meet
if your thought remain lofty, if a select
emotion imbue your spirit and your body.
The Laestrygones and the Cyclopes
and furious Poseidon you will never meet
unless you drag them with you in your soul,
unless your soul raises them up before you.

Pray that your journey may be long,
that many may those summer mornings be
when with what pleasure, what untold delight
you enter harbors you've not seen before;
that you stop at Phoenician market places
to procure the goodly merchandise,
mother of pearl and coral, amber and ebony,
and voluptuous perfumes of every kind,
as lavish an amount of voluptuous perfumes as you can;
that you venture on to many Egyptian cities
to learn and yet again to learn from the sages.

But you must always keep Ithaca in mind.
The arrival there is your predestination.
Yet do not by any means hasten your voyage.
Let it best endure for many years,
until grown old at length you anchor at your island
rich with all you have acquired on the way.
You never hoped that Ithaca would give you riches.

Ithaca has given you the lovely voyage.
Without her you would not have ventured on the way.
She has nothing more to give you now.

Poor though you may find her, Ithaca has not deceived you.
Now that you have become so wise, so full of experience,
you will have understood the meaning of an Ithaca.

Constantine Cavafis, 1863-1933

Abstract

Two general-purpose computer programs have been developed for modelling the displacement of a wetting fluid by a non-wetting one in porous media. A microscopic approach is applied for the solution of the governing equations at the pore level. The porous medium is represented by a two-dimensional network of interconnected capillaries. One program makes use of a *stochastic approach* based on the aspects of random walks, invasion percolation and on the notion of the phase diagram for immiscible displacement. The other program makes use of a *deterministic approach* based on a relaxation technique in order to solve for the pressure field, and on certain rules for the advancement of the interface.

The series of simulations undertaken successfully predicts certain important phenomena such as: (a) monophasic flow in porous media, (b) the effects of capillary and viscous forces on the dynamic behaviour of the displacing fluid and on the oil recovery, (c) the island formation and the island size distribution as a result of the interplay of viscous and capillary forces, (d) the fractal behaviour of the displacing fluid, (e) the transition from one distinct behaviour of the displacing fluid to another, and (f) the effects of local anisotropy and heterogeneity of the porous medium on the dynamic behaviour of the displacing fluid.

The validity of the algorithms is tested by comparing the numerical results with physical experiments available in the literature. Comparisons between the two approaches reveal that (a) the stochastic approach is more efficient in terms of execution time in the computer, (b) the deterministic approach better describes the physics of the problem, and (c) the deterministic approach has more potential to be extended to other problems. It is proposed that the present programs can be used to successfully predict two-fluid immiscible displacement flow in porous media for other relevant situations.

Acknowledgments

I wish to deeply thank my thesis supervisors Drs. Evan Mitsoulis and Graham Neale for their guidance, instruction and support during the last three years.

I am also grateful to the Department of Chemical Engineering for their financial support. Furthermore, I would like to thank Drs. Olga Vizika, Alkiviades Payatakes, Peter King and Roland Lenormand for many stimulating discussions. I would like also to express my deepest thanks to my colleagues Ahmed Hannachi and Saleh Abdali as well as to Mr. William Keays for his invaluable assistance with the IBM RS/6000 computer and to my friends George Charchar and George Vonapartis.

Finally, I would like to thank my wife Debbie for her love, patience and support during the last three years and also to express my deepest thanks to our family in Thessaloniki, Greece and in Montreal.

Contents

List of Tables

List of Figures

Nomenclature

A	flow cross-sectional area, m^2
A_t	total area of islands (-)
b	thickness of Hele-Shaw cell, m
Ca_{DLA}	capillary number at the DLA limit (-)
Ca_{INV}	capillary number at the invasion percolation limit (-)
Ca_{PF}	capillary number at the plug flow limit (-)
C_{1-5}	proportionality constants (-)
d	spatial dimension (-)
D	characteristic length, m
D_f	fractal dimension (-)
D_h	hypercsaling exponent (-)
E	sweep efficiency (-)
f	areal density of islands (-)
G	flow conductivity of a channel, $m^3\ s^{-1}\ Pa^{-1}$
g	acceleration due to gravity, $m^2\ s^{-2}$
h	length of lattice unit and thickness of the network, m
i_p	number of a pore in the network (-)
i_x, i_y	coordinates of a pore in the network (-)
J_i	Bessel function (-)
K	proportionality constant (-)
k	step of the random walk (-)
L	length of a porous medium, m
l_{ij}	length of a channel connecting pores i,j, m
M	viscosity ratio, (-)
M_{DLA}	viscosity ratio at the DLA limit, (-)
M_{PF}	viscosity ratio at the pluig flow limit, (-)
m(q)	number of islands within a size range q, (-)

$m(r_f)$	mass of an object as a function of its size r_f, kg
n	number of occupied sites (-)
$n(s_p)$	number of islands of size s_p (-)
N_B	Bond number (-)
N_{Ca}	Capillary number (-)
N_{Re}	Reynolds number (-)
$N_{p;b}$	number of pores/channels in the network (-)
$N_{x;y}$	number of pores in the x/y direction (-)
p	transition probability of the random walk (-)
P	pressure, Pa
$P_{i;d}$	pressure in the invading/displaced fluid, Pa
$P_{i;j}$	pressure in pore i/j, Pa
P_C	capillary pressure, Pa
$P_{C_{i,j}}$	capillary pressure in a channel connecting pores i,j, Pa
q	characteristic number of the size range of the islands, (-)
Q	volumetric flow rate of injected fluid, $m^3\ s^{-1}$
Q_i	volumetric flow rate in channel i, $m^3\ s^{-1}$
Q_{ij}	volumetric flow rate in the channel connecting pores i,j, $m^3 s^{-1}$
r	channel radius, m
r_f	size, m
r_o	average channel radius, m
R	pore radius, m
$s_{NW;W}$	saturation of the NW/W fluid (-)
s_p	size of an island (-)
u(x,k)	probability of the random walk (-)
V	velocity, $m\ s^{-1}$
$\overline{V}$	average velocity, $m\ s^{-1}$
V_C	critical velocity, $m\ s^{-1}$
$V_{i;d}$	velocity in the invading/displaced fluid, $m\ s^{-1}$
W	width of the Hele-Shaw cell, m
x	position of random walk (-)
$x_{NW;W}$	fraction of the NW/W fluid (-)
z	characteristic microscopic length, m

GREEK LETTERS

α	exponent of the island size distribution (-)
β	relaxation parameter (-)
γ	interfacial tension, $N\ m^{-1}$
δP	pressure change, Pa
$\delta P_{NW;W}$	intraphase pressure drop in the NW/W fluid, Pa m^{-1}
δx	displacement distance, m
ΔP	pressure difference, Pa
$\Delta \rho$	density difference, $kg\ m^{-3}$
ϵ	porosity of the porous medium (-)
η	instability growth rate, $m\ s^{-1}$
θ	contact angle, rad
κ	permeability of the porous medium, m^2
$\kappa_{ri;rd}$	relative permeability of the invading/displaced fluid (-)
$\kappa_{rNW;rW}$	relative permeability of the NW/W fluid (-)
λ	dispersion of the uniform size distribution (-)
$\lambda_{NW;W}$	mobility of the NW/W fluid, $m^2\ Pa^{-1}\ s^{-1}$
μ	fluid viscosity, Pa s
$\mu_{i;d}$	viscosity of the invading/displaced fluid, Pa s
$\mu_{NW;W}$	viscosity of the NW/W fluid, Pa s
μ_e	effective viscosity, Pa s
$\rho_{i;d}$	density of the invading/displaced fluid, $kg\ m^{-3}$
$\rho(r_f)$	density of an object as a function of its size r_f, $kg\ m^{-3}$
σ	wavelength of a perturbation, m
ϕ	sticking probability (-)
$\phi_{NW;W}$	sticking probability for NW/W contacts (-)
χ, ζ	cylindrical coordinates
ψ	phase transition probability (-)
ω	stability index (-)

Chapter 1

INTRODUCTION

1.1 The Physics of Flow in Porous Media

The study of the physics of flow in porous media is very important in many engineering and scientific applications. Phenomena and processes such as ground water hydrology, water purification, filtration, packed column distillation, oil displacement in underground reservoirs, ceramic engineering, catalysis and powder metallurgy all rely strongly upon it as fundamental to their individual problems (Scheidegger 1974, Dullien 1979, Greenkorn 1983, Lake 1989). Among these, two-fluid flow in underground reservoirs is certainly one of the most important processes, and it is the area on which this thesis is focused.

Oil is produced from natural deposits which are found underground in the interstices of porous rock formations like sand, sandstone, limestone and dolomite. In most cases, the recovery of oil from underground reservoirs is attained in three different stages: *primary*, *secondary* and *tertiary recovery* (Jha 1973, Lake 1989).

During the *primary* recovery stage the oil flows spontaneously through the pro-

duction well due to the high oil pressure in the reservoir. However, the reservoir pressure eventuallly subsides and a considerable amount (75-95%) of the original oil in place (OOIP) remains unrecovered. The recovery of the remaining oil is the subject of *enhanced oil recovery* (E.O.R.) processes.

During the *secondary* recovery stage water is usually injected to displace the oil out of the reservoir. At the end of this stage an amount of 60 to 80% of OOIP typically remains unrecovered with obvious strong implications to the world economy. The principal cause of the low secondary recovery is the *fingering* of the displacing fluid (water) within the displaced fluid (oil) in the oil reservoir.

The most common technique used during the *tertiary* recovery stage is flooding with aqueous solutions of alkalis, polymers and/or surfactants in order to reduce fingering and increase sweep efficiency (Stalkup 1970, Paterson et al. 1984, Lake 1989, Nasr-el-Din et al. 1990, Tayal and Narayan 1990, Symons et al. 1990).

The problem of two-fluid displacement flow in porous media is very complicated due to various factors and pore-scale phenomena that come into play, such as fluid viscosities, flow rate, interfacial tension (between immiscible fluids), reservoir morphology and wettability, formation and instability of blobs of residual oil, propagation of these blobs, film flow, advancement of the interface during the immiscible displacement and others. This problem has been a very active area of research for the last few decades. Many attempts have been made to explain the dynamic behaviour of the displacing fluid and the cause of fingering in order to provide a better understanding of the mechanisms of two-fluid flow in porous media and to

ultimately improve the efficiency of enhanced oil recovery processes. Two general approaches have been followed:

(a) The first approach is based on the development of averaged continuum equations, which involve physical parameters to be determined by experiments. This approach is useful for *macroscopic* modelling and predictions if the various parameters are known. However, this approach does not account for microscopic phenomena nor for the morphology of the porous medium. Therefore, it may not provide accurate and quantitative predictions when phenomena at the pore-scale play a significant role.

(b) The second approach is based on *microscopic* equations. According to this approach the porous medium is represented by a network of interconnected capillaries whose radii possess a specific size distribution. Many of the microscopic phenomena are incorporated and described and some others are idealized. Many studies have been conducted on two-fluid flow in Hele-Shaw cells (see Section 2.1) in order to gain an understanding of certain fundamental phenomena which occur in porous media as well.

In this thesis the second approach is followed. Network models of porous media are employed in order to study the immiscible displacement of a wetting fluid by a non-wetting fluid in a porous medium. Two computer simulation algorithms have been developed and are discussed. They are based on two different mathematical approaches. According to the first mathematical approach, the governing equations are reinterpreted in terms of hypothetical particles (random walkers) and the algorithm is referred to as *stochastic*. According to the second mathematical approach,

the governing equations are solved directly (deterministically) and the algorithm is referred to as *deterministic*. Both algorithms are used to study and to improve our understanding of the effects of various factors on the behaviour of displacement processes. Numerical experiments are compared with physical ones available in the literature in order to test the validity of the algorithms.

1.2 Outline of the Thesis

Chapter 2: Certain important definitions are provided and the governing equations for flow in porous media and in Hele-Shaw cells are presented. A literature review of studies in fluid displacement and the objectives of the present study are also presented.

Chapter 3: The porous medium is represented by a two-dimensional network of interconnected capillaries. The stochastic approach based on the aspects of random walks, invasion percolation and on the notion of the phase diagram is described. The deterministic approach based on a relaxation technique for solving for the pressure field and on certain rules for the advancement of the interface is also described for both monophasic and biphasic flow in porous media.

Chapter 4: Monophasic flow is studied and the permeability of the medium is plotted against the average channel radius and the dispersion of the size distribution. Results of the simulations for two-fluid immiscible displacement are presented by using both approaches and are compared with experiments available in the literature. The effects of viscous and capillary forces on the dynamic behaviour of the displacing fluid, on the oil recovery, on the island formation, on the island size

distribution and on the fractal behaviour of the cluster of the displacing fluid are presented. The effects of the local anisotropy on the dynamic behaviour of the displacing fluid and the effects of the network size on the oil recovery are also presented. Certain implications of the results of the simulations are discussed. Finally, comparisons between the mathematical approaches applied in the present study and other approaches applied in previous studies reveal the differences, the potentials, the improvements and the limitations.

Chapter 5: The conclusions of the present study are summarized and certain recommendations are made for future work based on the subject of flow in porous media.

Chapter 2

THEORY

2.1 Important Definitions

The following definitions will be used throughout this study:

-**Porous Medium**: a structure which contains spaces, so-called pores or voids, free of solid, embedded in the solid matrix (see Figure 2.1). The porous medium is characterized by the *porosity*, ϵ, and the *permeability*, κ, which are dependent on the pore geometry but are independent of the properties of the penetrating fluid when the fluid is Newtonian.

-**Wetting and Non-Wetting Fluid**: when one fluid is slowly displacing another immiscible fluid in a capillary tube or a porous medium, the fluid for which the *contact angle*, θ, between the tube and the interface is smaller than $\pi/2$ is termed the *wetting fluid*, (W), while the other one is termed the *non-wetting fluid*, (NW) (see Figure 2.2)

-**Meniscus**: the interface between two immiscible fluids in a capillary tube or a porous medium.

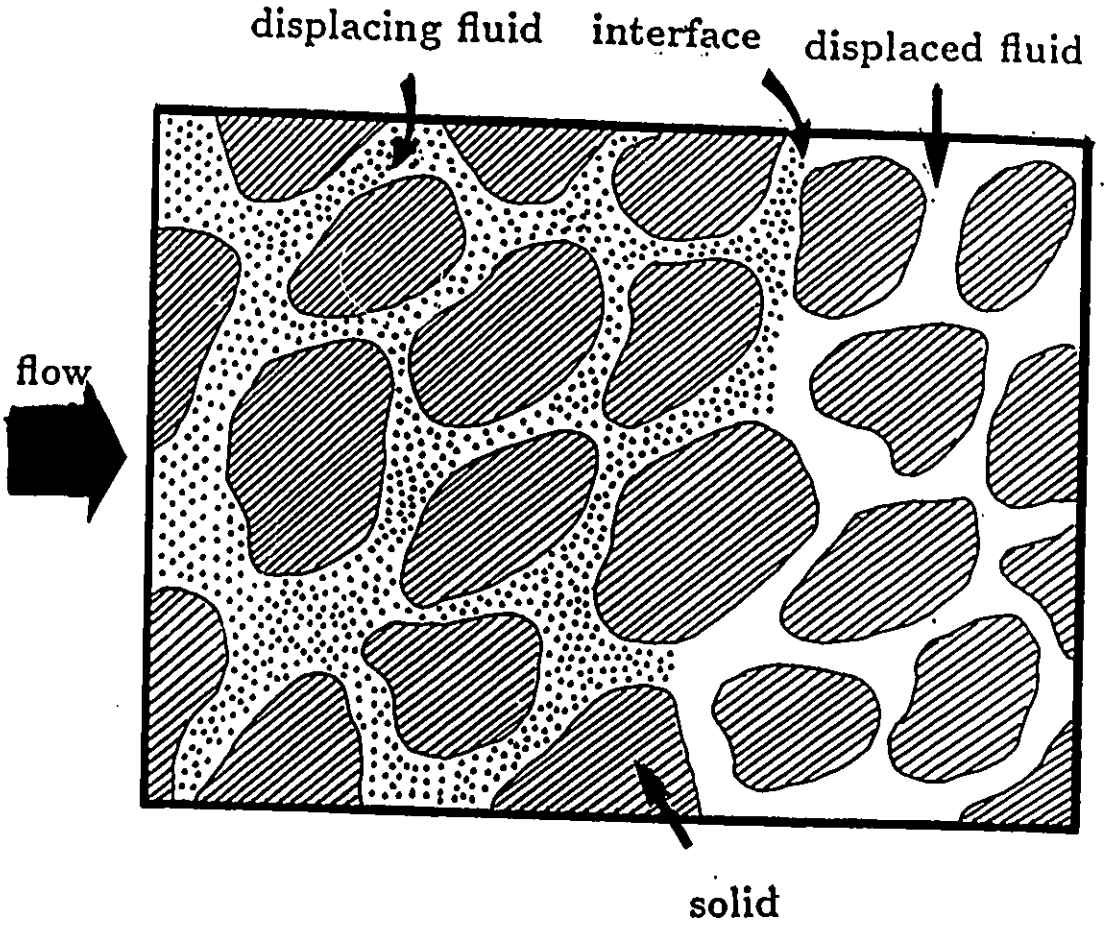

Figure 2.1: Two-phase flow in a porous medium under the influence of a pressure gradient.

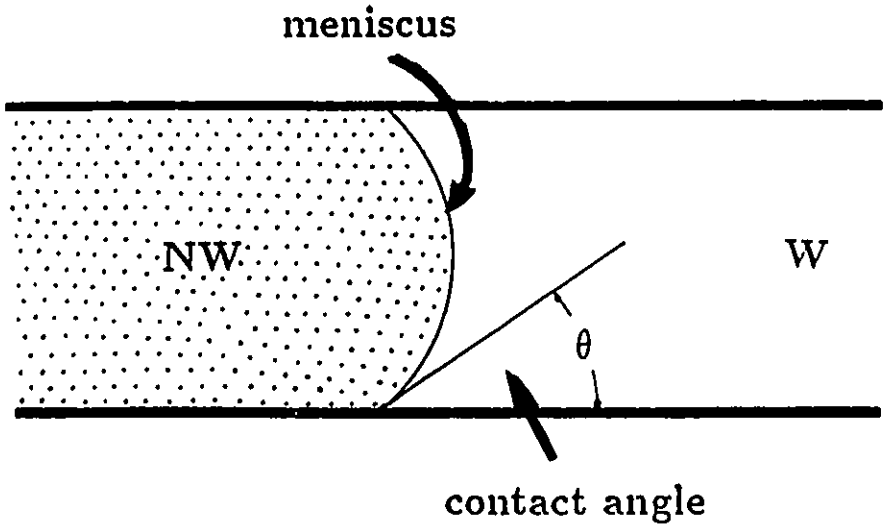

Figure 2.2: The meniscus and the contact angle for two immiscible fluids in a capillary.

-**Capillary Pressure (P_C)**: defined by

$$P_C = P_{NW} - P_W \tag{2.1}$$

where P_{NW} and P_W are the pressures at the interface in the non-wetting and wetting fluids, respectively. At static equilibrium, the capillary pressure in a cylindrical channel of radius r is given by

$$P_C = \frac{2\gamma cos\theta}{r} \tag{2.2}$$

where γ is the interfacial tension and θ the contact angle.

-**Drainage**: the displacement of a wetting fluid by a non-wetting fluid under the influence of a pressure gradient.

-**Imbibition**: the spontaneous displacement of a non-wetting fluid by a wetting fluid in the presence or absence of a pressure gradient.

-**Network or Lattice**: a structure, which is a simplified representation of the porous medium, composed of *sites* (pores) multiconnected by *bonds* (channels). In general, the diameter of the sites is larger than that of the bonds in a two-dimensional network (see Figure 2.3a). The mathematical representation of a network is seen in Figure 2.3b and it is a simplification of a network obtained by assigning no dimensions to the sites and bonds.

-**Connectivity or Co-ordination number**: is the number of nearest neighbours connected to a site of the network.

-**Ordered Networks**: are networks whose coordination number is identical to the number of nearest neighbours for each site. Networks which do not satisfy the above

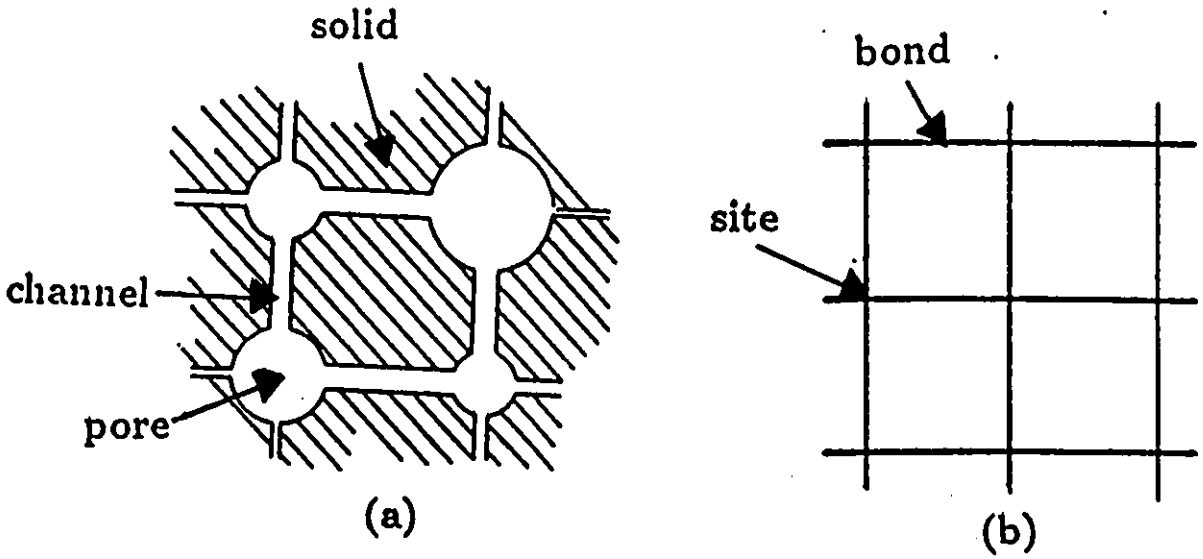

Figure 2.3: (a) Idealized representation of a two-dimensional porous medium by a network and (b) mathematical representation of the network by a lattice.

condition are termed as *disordered.*

-**Hele-Shaw Cell**: an idealized cell made of two horizontal, parallel plates with a small separation distance (see Figure 2.4, Hele-Shaw 1898). Two-phase flow in Hele-Shaw cells is considered to be strictly two-dimensional, since the separation distance, b, is very small compared to the other dimensions, W and L.

-**Viscosity Ratio (M)**: the ratio of the viscosity μ_i of the invading (displacing) fluid to the viscosity μ_d of the displaced fluid

$$M = \frac{\mu_i}{\mu_d} \tag{2.3}$$

-**Reynolds Number (N_{Re})**: the ratio of inertial to viscous forces defined by

$$N_{Re} = \frac{\rho \overline{V} D}{\mu} \tag{2.4}$$

where ρ is the fluid density, μ the fluid viscosity, $\overline{V}$ a characteristic (average) velocity and D a characteristic length. For flow in most porous media, due to low velocities, $N_{Re} < 1$.

-**Capillary Number (N_{Ca})**: the ratio of viscous to capillary forces defined as

$$N_{Ca} = \frac{Q\mu_i}{\gamma A} \tag{2.5}$$

where Q is the volumetric flow rate of the invading (displacing) fluid, μ_i the viscosity of the displacing fluid, γ the interfacial tension and A the cross-sectional area of the porous medium normal to the flow direction. In general, at low capillary numbers ($N_{Ca} << 1$) capillary forces dominate, while at capillary numbers close to one, viscous forces become dominant.

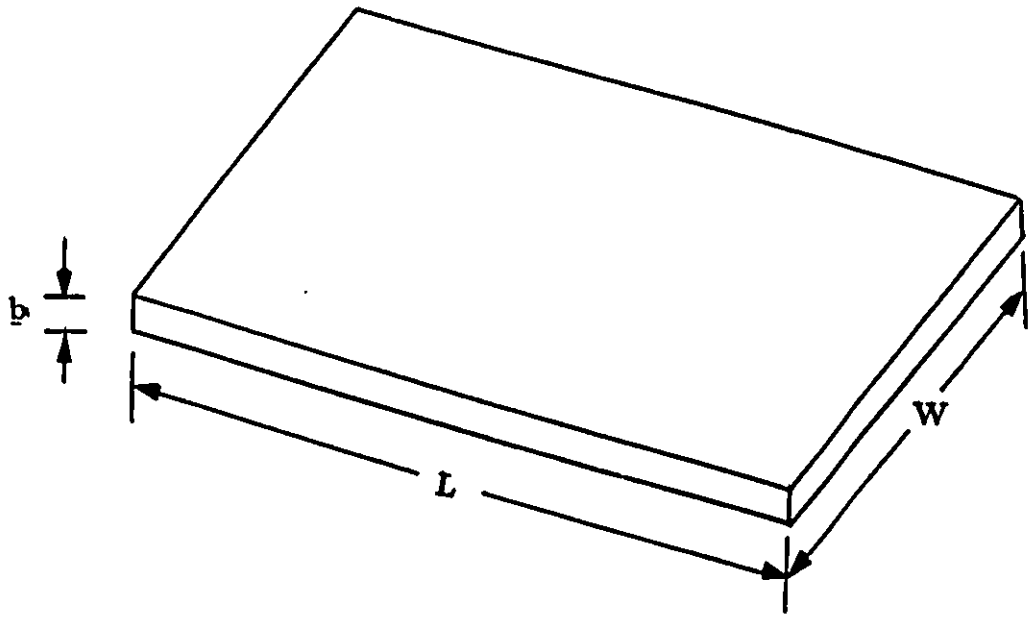

Figure 2.4: A Hele-Shaw cell.

-Bond Number (N_B): the ratio of buoyancy to capillary forces defined as

$$N_B = \frac{gz^2\Delta\rho}{\gamma cos\theta} \tag{2.6}$$

where $\Delta\rho$ is the density difference between the two fluids, g the acceleration due to gravity and z a characteristic microscopic length.

-Wettability: the tendency or preference of a fluid to spread on a solid surface in the presence of another fluid. A quantitative measure of the wettability is the contact angle, θ. For most of the last 50 years, a large body of engineering practice has been based on the assumption that most petroleum reservoirs are very strongly water-wet (VSWW). The rationale for assuming VSWW conditions was that water originally occupied the pore space; as oil accumulated, water was retained by capillary forces in the finer pores and as films on pore surfaces overlain by oil. Wettability behaviour other than VSWW was observed in reservoir core samples, but it was often ascribed to artifacts related to core recovery and testing procedures. The majority of reservoir measurements have been made on cleaned core samples with refined oil or air as the non-wetting phase to give results for, or equivalent to, VSWW conditions. Mounting evidence on the effects of crude oil on the wetting behaviour (Cuiec 1990) has now led to wide acceptance of the conclusion that most reservoirs are at wettability conditions other than VSWW. Reservoir wettability is not a simply defined property (Morrow 1990). Classification of reservoirs as water-wet or oil-wet is a gross oversimplification. Measurements show that reservoir wettability can cover a broad spectrum of wetting conditions that range from VSWW to strongly oil-wet. Within this range, complex mixed-wettability conditions given by combinations of preferentially water-wet and oil-wet surfaces have

been identified.

-**Permeability**: the ease with which a fluid flows through a porous medium. In a network, the permeability depends upon the pore geometry, size, size distribution and topology.

-**Homogeneous and Heterogeneous Porous Media**: a porous medium is termed *homogeneous* with respect to one of its properties, if that property is independent of location, otherwise it is termed *heterogeneous* (Ryan and Neale 1975).

-**Isotropic and Anisotropic Porous Media**: a porous medium is termed *isotropic* with respect to one of its properties if that property is independent of direction, otherwise it is termed *anisotropic.*

-**Viscous Fingering**: the phenomenon which occurs in general at low viscosity ratios ($M \leq 1$) and high capillary numbers. The displacing, less viscous fluid tends to channel inside the displaced fluid (see Figure 2.5). Viscous fingering is caused by interfacial instabilities, which are created, and subsequently grow due to viscosity differences and heterogeneities in the oil reservoir.

During the displacement of a fluid of viscosity μ_d and density ρ_d by another fluid of viscosity μ_i and density ρ_i in a homogeneous porous medium with permeability κ, Darcy's equation for one-dimensional flow is expressed as (Homsy 1987)

$$\frac{dP}{dx} = \frac{-\mu V}{\kappa} - \rho g \tag{2.7}$$

where V is the superficial (mean) velocity, P the pressure and μ, κ, ρ and g as previously defined.

Figure 2.5: Viscous fingering of the invading fluid (black) displacing the displaced fluid (white) in a porous medium.

Consider a sharp interface or a zone where the density and the viscosity change rapidly. Then the pressure difference on the displaced fluid as a result of a virtual displacement δx of the interface is

$$\delta P = [(\mu_d - \mu_i)V/\kappa + (\rho_d - \rho_i)g]\delta x \tag{2.8}$$

If the net pressure difference is positive, then any small displacement will amplify, leading to an instability. Thus a combination of unfavorable density and/or viscosity ratios and flow direction can conspire to render the displacement unstable. For example, for downward vertical displacement of a dense, viscous fluid by a lighter, less viscous one gravity is a stabilizing force, while viscosity is destabilizing, leading to a critical velocity V_C above which there is no instability:

$$V_C = \frac{\kappa(\rho_d - \rho_i)g}{(\mu_i - \mu_d)} \tag{2.9}$$

There are three other obvious cases depending upon the signs of $\rho_i - \rho_d$ and $\mu_d - \mu_i$: one in which gravity drives the instability and viscosity stabilizes it, and the other two cases when both basic forces are either stabilizing or destabilizing.

A simpler statement may be made when the gravity force is absent, i.e. in a horizontal displacement. In this case, instability always results when a more viscous fluid is displaced by a less viscous one. Thus the two basic forces responsible for instability are gravity and viscosity.

Experimental studies on viscous fingering were carried out by van Meers (1957) and Paterson (1981). However, the phenomenon of viscous fingering is often referred to as *the Saffman-Taylor instability*, in recognition of the work conducted by Saffman and Taylor (1958). The phenomenon of viscous fingering was studied at about the

same time by Chuoke et al. (1959), who predicted a critical flow rate above which interfacial instabilities grow leading to viscous fingering in the presence of the interfacial tension. They also provided an equation for the wavelength of the fingers. Paterson's work was carried out in a Hele-Shaw cell for the radial displacement of glycerine by air. For short times, there is a reasonable agreement with the expectations of Saffman and Taylor (1958). Paterson predicted the finger wavelength and the number of fingers for initial growth and the size of fingers for intermediate growth.

Later, Ni et al. (1986) extended Paterson's work to porous media. Peters and Flock (1981) determined the onset of instabilities in terms of a dimensionless group, which includes the critical flow rate predicted by Chuoke et al. (1959). Large-scale numerical simulations have been provided by Tryggavson and Aref (1983), DeGregoria and Schwartz (1985) and Schwartz (1986). Most authors made use of perturbation theory and some calculated the finger wavelength of the fingers at maximum growth rate. Experimental studies by Nittman et al. (1986) and Park and Homsy (1985) have shown that the single finger is subject to a tip-splitting instability. Homsy (1987) gives an excellent overview of most of the theoretical and experimental work mentioned above.

-**Capillary Fingering**: this phenomenon occurs at very low flow rates (low capillary number) due to heterogeneities within the porous medium. The interface tends to follow the paths of least resistance in the case of drainage. This resistance is provided by the capillary pressure (Equation 2.2), which opposes advancement of the interface. Therefore, the interface moves preferentially through the largest pores

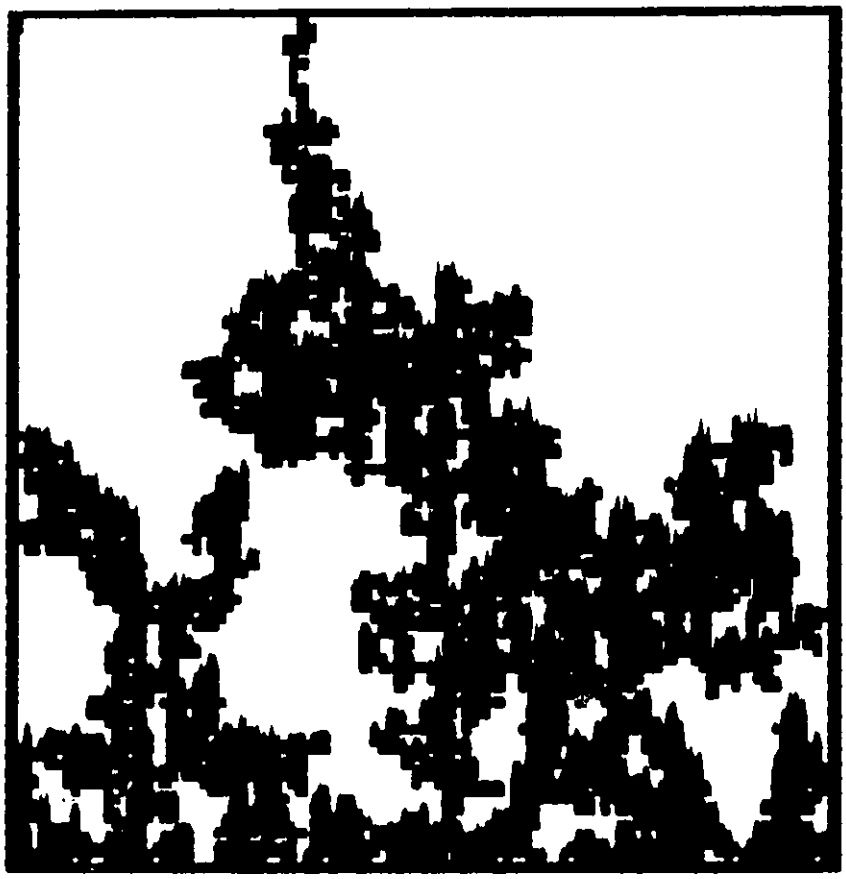

Figure 2.6: Capillary fingering of the invading fluid (black) displacing an immiscible fluid (white) in a porous medium.

since they provide the lowest capillary pressure. Contrary to drainage, imbibition is facilitated by a high capillary pressure.

During an immiscible displacement at low flow rates, fingers tend to grow in all directions, even backwards, causing trapping of the displaced phase (see Figure 2.6). Capillary fingering is very often identified with *invasion percolation*, which is a stochastic theory used to describe capillary fingering. The invasion percolation theory is discussed in the next section.

-**Stable Displacement**: this occurs at high flow rates and high viscosity ratios. The interface moves as a flat front resulting in high oil recovery (see Figure 2.7). Stable displacement is often referred to as plug flow, on account of its flat front. However, even in this case instabilities are created due to heterogeneities and they are of the scale of a few pores.

-**Residual Oil**: is the oil which remains trapped and unrecovered at the end of the displacement. It is distributed within the porous medium in groups of oil-filled pores completely surrounded by the invading phase (water). A group of trapped pores is often referred to as an oil blob, oil island or ganglion (Payatakes 1982, Payatakes and Dias 1984).

-**Connate or Initial Water**: is the water, or generally speaking the invading phase, initially in place occupying remote regions of the pore space completely surrounded by oil (Paterson et al. 1984)

-**Oil Sweep Efficiency**: is the fraction of the volume of oil recovered at the end of the displacement process. The sweep efficiency in this study is identical to the

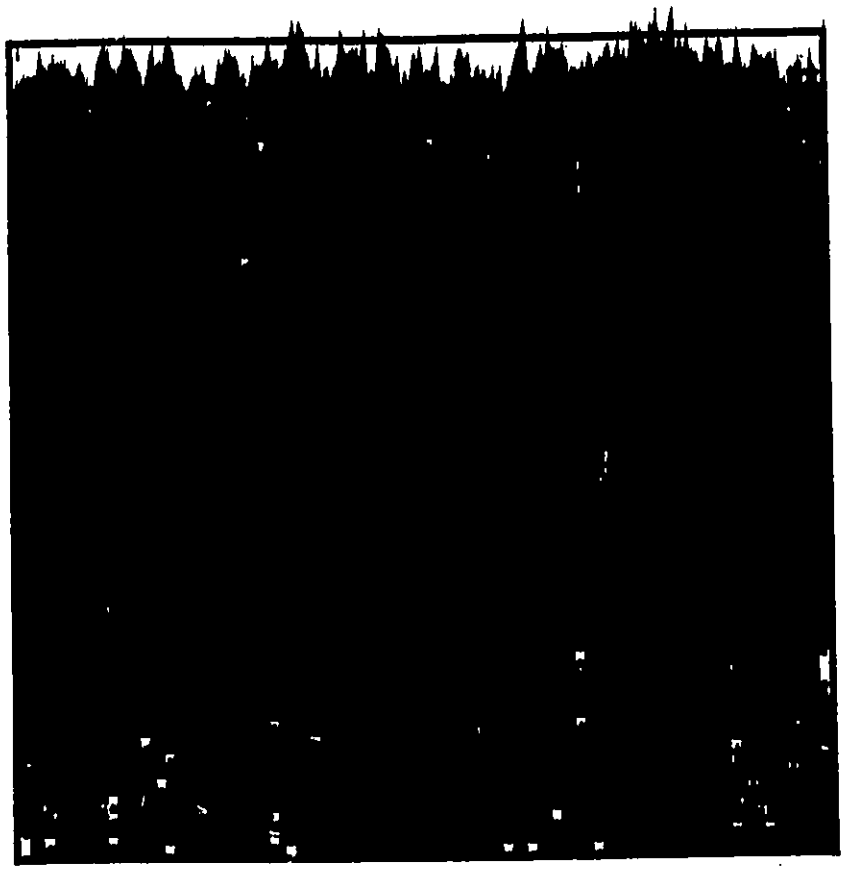

Figure 2.7: Plug flow behaviour of the invading fluid (black) displacing another fluid (white) in a porous medium.

fraction of the pores of the network invaded by the displacing fluid.

-**Fractals**: are objects which appear to be ramified and irregular and are scale-invariant. The concept of fractals was developed by Mandelbrot (1982,1989) as an attempt to describe highly irregular and disordered objects.

Consider firstly a circular or spherical object of mass m and radius r_f (Figure 2.8) The object can be either solid (uniform density) or full of holes, but in either case we assume that the density does not depend on the size of the object. Therefore, if the radius of the object is increased from r_f to $2r_f$, the mass of the object is increased by a factor of 2^2 (if the object is circular) or by 2^3 (if the object is spherical). The relationship between the mass and length is thus of the form:

$$m(r_f) \propto r_f^d \tag{2.10}$$

where d is the so-called *spatial dimension*. An object whose mass-length relation satisfies Equation (2.10) is said to be *compact*.

The relationship between the mass of an object and its characteristic length r_f can be defined more generally than in Equation (2.10). One way to define the *fractal dimension*, D_f, is by the equation

$$m(r_f) \propto r_f^{D_f} \tag{2.11}$$

Fractals are objects that satisfy Equation (2.11) with a value of D_f less than the spatial dimension, d. Their density is thus not the same for all r_f but scales as

$$\rho(r_f) \propto r_f^{(D_f - d)} \tag{2.12}$$

Since the fractal dimension, D_f, is lower than the spatial dimension, d, a fractal

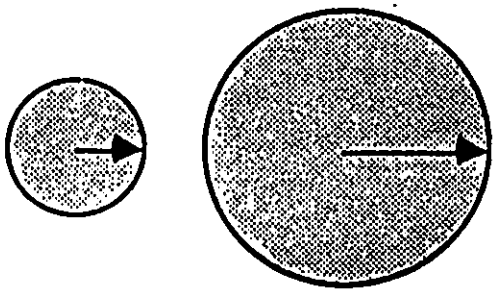

Figure 2.8: Two circular objects with radius r_f and $2r_f$, respectively. The number of dots per unit area in each circle is uniform.

object becomes less dense at larger length scales. This scale-dependence of the density is a quantitative measure of the notion that fractals are ramified objects.

2.2 Governing Equations

2.2.1 Flow in Porous Media

Flow in a a porous medium is described by Darcy's equation (Darcy 1856), provided that the Reynolds number, N_{Re}, is very small. For single-phase flow and in the absence of gravity, Darcy's equation takes the form

$$V = -\frac{\kappa}{\mu}\nabla P \tag{2.13}$$

where V is the superficial velocity, P the pressure, μ the fluid viscosity and κ the permeability of the porous medium.

For two-phase flow, a generalized form of Darcy's equation is applied (Lake 1989, Dullien 1979)

$$V_i = -\frac{\kappa\kappa_{ri}(s)}{\mu_i}\nabla P_i \tag{2.14}$$

$$V_d = -\frac{\kappa\kappa_{rd}(s)}{\mu_d}\nabla P_d \tag{2.15}$$

where the subscripts i and d signify the injected and displaced fluids, respectively. The saturation, s, is defined as the fraction of the total void space occupied by one fluid in the volume over which the average is taken. The volume is a small section of a larger displacement, but is still of macroscopic size. P_i and P_d denote the pressures in the injected and displaced fluids, respectively; κ_{ri} and κ_{rd} are the so-called relative permeabilities and are assumed to be dependent only upon the

saturation. The relative permeability represents the factor by which the flow rate is reduced for two-fluid flow (Equations 2.14, 2.15) compared with the single flow value (Equation 2.13). The sum of the relative permeabilities of several phases in a porous medium is always less than unity.

2.2.2 Flow in a Hele-Shaw Cell

Flow in a Hele-Shaw cell is described by an equation similar to Darcy's equation, namely

$$V = -\frac{b^2}{12\mu}\nabla P \tag{2.16}$$

Equations (2.13) and (2.16) are equivalent, since the term $b^2/12$ can be replaced by an effective permeability. Thus, single-phase Hele-Shaw flow is analogous to two-dimensional incompressible flow in porous media. It might be supposed that the same analogy would hold for viscous fingering in porous media. However, this analogy fails in the case of flow of immiscible fluids, since flow in porous media in this case is truly multiphase, as opposed to two-phase, and the forces associated with the propagation of menisci through the pore space comprising the medium cannot be neglected and are not modelled in the Hele-Shaw geometry. Furthermore, the geometry of the solid matrix can influence the fingering patterns observed and also a Hele-Shaw cell does not allow for the phenomenon of residual oil. Nevertheless, the case of Hele-Shaw flow is of fundamental interest in its own right and permits us to establish some useful concepts.

2.3 Literature Review of Studies in Fluid Displacement

Theoretical studies of both a stochastic and a deterministic nature have been undertaken to describe miscible and immiscible fluid displacements in porous media and Hele-Shaw cells. Experimental studies have also been carried out to confirm theoretical predictions.

Witten and Sander (1981,1983) developed an algorithm better known as DLA (*Diffusion-Limited Aggregation*), in order to simulate diffusion-limited aggregation growth. The most effective way to study such a process is to let *random walkers* wander over an arbitrary lattice and to stick on the growing cluster upon first contact. Computer simulations by Meakin (1983a,b) confirmed these findings in terms of the fractal dimension, which characterizes the structure of the cluster. Later, Meakin and Tolman (1989) improved the DLA algorithm by including anisotropy in three- and four-dimensional lattices. Ball and Brandy (1985) studied large-scale lattice effects in DLA by using Witten and Sander's classical algorithm. DLA with radial anisotropy was studied by Meakin and Vicsek (1987) in an attempt to simulate fingering in liquid crystals. The above studies were confirmed by experimental measurements on the growth of metal aggregates by Matsushita et al. (1984) and by Weitz and Oliveira (1985). Most of the above studies included measurements of the fractal dimension, D_f.

Paterson (1984) noticed the similarities between DLA patterns and viscous fingering in porous media at very low viscosity ratios. Paterson considered the Laplace

equation for the pressure

$$\nabla^2 P = 0 \tag{2.17}$$

which follows from Equation (2.13) and from the continuity equation for incompressible fluids

$$\nabla \cdot V = 0 \tag{2.18}$$

with the condition that the pressure P is zero at the interface and inside the displacing fluid in the absence of interfacial tension and gravity. Another condition is that the permeability κ is constant, which is the case for homogeneous and isotropic porous media. Paterson also suggested another model to simulate the displacement at high values of the viscosity ratio. This model is called *anti-DLA*. According to this model, the Laplace equation is considered only in the displacing fluid, and random walkers are allowed to wander only in this fluid and to stick upon contact with the interface. Paterson (1987) also simulated flow within porous media containing heterogeneities (which occur when a zone of different permeability is present in the porous medium) by changing the lattice spacing in order to account for the boundary conditions. These conditions are satisfied when the permeability is proportional to the size of the local lattice spacing. The DLA and the anti-DLA models as they are applied to fluid displacement imply negligible pressure gradients in the displacing and displaced fluids, respectively.

Following Paterson's work further studies were performed for both porous media and Hele-Shaw cells. Maloy et al. (1985) carried out experiments in porous media by displacing a high-viscosity fluid by air. Their results confirmed the analogy between DLA and viscous fingering in porous media introduced by Paterson. Paterson's work

was also confirmed by experiments in Hele-Shaw cells carried out by Lenormand et al. (1981), Nittmann et al. (1985,1986), and Stanley and Nittmann (1986) for linear displacement. Daccord et al. (1986) carried out studies for two-fluid, radial displacement in Hele Shaw cells and Sherwood and Nittmann (1986) studied the effect of the viscosity ratio on DLA. All of the above studies revealed a value for the fractal dimension very close to the 1.73 which is characteristic of the original DLA model, although end-effects were apparent in linear displacement.

At about the same time additional studies were carried out on DLA. Tang (1985) modified the DLA model and allowed for a number of visits of the random walkers at an interfacial site before the interface advances to that site. Meakin and Deutch (1986) proposed a model similar to the anti-DLA one, called *Diffusion-Limited Annihilation.*

The effects of the interfacial tension on viscous fingering were studied by McLean and Saffman (1981) in a Hele-Shaw cell. They developed a streamline technique and they determined the shape of the interface as a solution of a non-linear integro-differential equation. Vicsek (1984) by using the DLA model incorporated the interfacial tension in terms of a sticking probability, which was dependent upon the local curvature of the interface. Szep et al. (1987) examined the connection between DLA and dendritic growth by incorporating the interfacial tension in a similar way. Liang (1986), based on Kadanoff's (1985) approach, included the effect of the interfacial tension by letting the random walker evaporate from the cluster after a contact with the interface with a probability proportional to the pressure discontinuity at the interface, which is equal to the capillary pressure. Recently,

Fernandez and Albarran (1990) made an attempt to incorporate the interfacial tension in the simulation of the displacement of a viscous fluid by an inviscid fluid in a Hele-Shaw cell. Their study is based on some of Kadanoff's ideas.

The DLA studies mentioned above were limited to very low viscosity ratios. However, several attempts have been made to include the effects of a finite viscosity ratio. Sahimi and Yortsos (1985) and Siddiqui (1989) simulated two-fluid displacement in a Hele-Shaw cell at finite viscosity ratios by letting random walkers stick on the interface with a probability which depends upon the viscosity ratio and the local curvature of the interface. They expressed the sticking probability, ϕ, by

$$\phi = \frac{\frac{1}{M} - 1}{\frac{1}{M} + 1} + f(N_{Ca}, W) \tag{2.19}$$

where $f(N_{Ca}, W)$ is a term accounting for the interfacial tension and the curvature which is quite similar to that proposed by Vicsek (1984) and Szep et al. (1987). M. King and Sher (1987) included finite viscosity ratios in two-fluid miscible flow in porous media by solving the coupled non-linear, partial differential equations describing multiphase and multicomponent fluid flow in a porous medium. This was based on an approach similar to an earlier study by Turkevitch and Sher (1985).

Most of the studies mentioned above made use of some aspects of the original DLA model and were applied to both porous media and to Hele-Shaw cells. At this point some major distinctions between two-fluid displacements in porous media and in Hele-Shaw cells should be made:

(a) In a porous medium the interfacial tension acts through the microscopic curvature in individual pores and not through the macroscopic curvature as is

the case in Hele-Shaw cells.

(b) In a porous medium the interface between the two fluids is not sharp, but there is a region where both fluids are present. Therefore, the flow is not described by Darcy's equation but rather by the modified equations (2.14,15).

(c) The randomness due to the microstructure of the porous medium is absent in Hele-Shaw cells.

(d) Trapped islands of unrecovered displaced phase are observed in porous media but not in Hele-Shaw cells.

Other stochastic as well as deterministic studies have been carried out in order to simulate two-fluid displacement flow in porous media. Chan et al. (1988) developed a model in which the random nature of the porous medium is incorporated into a numerical simulation scheme based on the discretization of the continuum fluid-mechanical equations following earlier work carried out by Chan et al. (1986). Their model does not take into account the effects of the interfacial tension and it is valid only for very low values of the viscosity ratio. Chen and Wilkinson (1985) made use of the electrical analog of flow in porous media developed by Fatt (1956a,b,c) and by using a Gauss-Seidel over-relaxation technique solved for the pressure field only in the displaced fluid. Their algorithm is applied at low viscosity ratios and at the limit of vanishing interfacial tension. However, they showed the transition from dendritic growth to DLA as the porous medium becomes heterogeneous. Siddiqui and Sahimi (1987) showed that DLA and viscous fingering are not equivalent in heterogeneous or topologically disordered porous media. P. King (1987) confirmed

the above studies with simulations of two-fluid, radial displacement flow at different viscosity ratios. DeGregoria (1985,1986) developed a model similar to Chen and Wilkinson's in order to describe two-fluid displacement in homogeneous porous media at finite viscosity ratios. At the same time, Sherwood and Nittmann (1986) developed a model in order to describe the transition from DLA to plug flow at the limit of vanishing interfacial tension. Sherwood (1986), based on DeGregoria's and Sherwood and Nittmann's work, studied the distribution of the size of trapped areas of the displaced fluid during two-fluid, radial displacement in porous media at the limit of vanishing interfacial tension.

From the above studies and other observations on both three- and two-dimensional media the following have been observed:

(a) Wetting properties are important. There is a qualitative difference in fingering when the invading fluid does or does not wet the medium. In the former case fingering is characterized by some macroscopic continuum scale, whereas in the latter fingering is more likely to be confined to the pore scale.

(b) Characteristic macroscopic scales, if present, decrease with increasing capillary number.

(c) When the invading fluid is non-wetting, the resulting pattern is "a probe of the topology of the microstructure and is characteristic of percolation behaviour, with a backbone that may have a fractal character" (Homsy 1987)

(d) There is simultaneous flow of both phases in a zone behind a displacement front, assuming such a front may be identified.

The *percolation theory* has been used to describe capillary fingering. It was introduced by Hammersley (1957). Kirkpatrick (1973) extended the percolation theory in order to describe transport in porous media. Results presented by Kirkpatrick for cubic networks were limited by the fact that all the bonds of the network that were allowed to conduct flow had the same conductivity. Larson et al. (1977, 1981a,b) made an attempt to determine the relative amounts of invaded areas and the characteristic size of trapped areas. However, this approach, known as *classical percolation theory*, fails to describe trapping of the displaced fluid.

Later, Chandler et al. (1982) followed a different approach from the classical percolation theory. According to this approach, the porous medium is represented by a network of interconnected capillaries with radii following a uniform size distribution. Therefore, capillaries with the smallest radius will provide the highest capillary pressure. Chandler et al. (1982) interpreted the above considerations in a stepwise Monte-Carlo process. The algorithm starts from an initial interface at one end of the lattice. Random numbers are assigned to the interfacial bonds representing the radii of the capillaries and the interface moves along the bond with the largest random number (rank) in the case of drainage. Concequently, random numbers are reassigned to the interfacial bonds and the previous steps are repeated until the interface reaches the other end of the network. Trapping of the displaced fluid is taken into account at each step of the process by checking for trapped areas. This algorithm predicts fingering and trapping at all length scales, leading to high residual saturation of the dislplaced fluid. Chandler et al. (1982) calculated a fractal dimension ($D_f = 1.83$) which was different from the value of the fractal

dimension ($D_f = 1.89$) predicted by the classical percolation theory.

Wilkinson and Willemsen (1983), motivated by the above work of Chandler et al., introduced a new form of percolation theory known as *Invasion Percolation.* Invasion percolation is a dynamic model which describes the displacement process at constant flow rate rather than at constant applied pressure, which was the case of the previous studies carried out by Larson et al. (1983), deGennes and Guyon (1978) and Lenormand and Bories (1980). It is this feature which leads to the dynamic rule of advancing the interface at the point of least resistance, as opposed to advancing all interfaces up to some chosen threshold resistance. In the presence of the trapping rule, the distinction between constant flow rate and constant pressure difference becomes very important, at least from the point of view of simulation, because invasion percolation implies a unique time sequence of advances of the interface, and hence a unique way of deciding whether or not a given portion of the displaced fluid becomes trapped. By contrast, at a given applied pressure, the interface can advance in many places, and different time orderings can lead to different trapping configurations. Invasion percolation provides a value for the fractal dimension which is very close to 1.82. The difference between this value and 1.89, which is the value of the fractal dimension predicted by the classical percolation theory, is due to trapping of the displaced fluid. Lenormand and Zarcone (1985a) confirmed the findings of invasion percolation by experiments in network models. They measured a fractal dimension of the invading cluster which was very close to the value predicted by invasion percolation.

Additional studies on invasion percolation were carried out by Wilkinson and Bar-

sony (1984) in two and three dimensions to obtain critical quantities of the percolation cluster. McCarthy (1987), based on invasion percolation theory, computed the critical points and critical exponents of percolation on a random lattice which is the dual of a Voronoi network. Ramakrishnan and Wasan (1986), based on the percolation theory, carried out studies on two-fluid displacement flow in a porous medium. They used the Bernoulli percolation model for an infinite lattice in order to interpret the capillary behaviour of the medium and to calculate the capillary pressure-saturation relationship. Later, Wilkinson (1986) suggested that some percolation ideas are consistent with the multiphase Darcy equations. Wilkinson observed some critical behaviours of the relative permeability and capillary pressure curves. By using these results, he made predictions for the shape of the fluid saturation profiles near the percolation threshold in the presence of buoyancy or viscous pressure gradients. Yanuka et al. (1986) modelled the fluid displacement in three dimensions, based on the classical percolation theory. However, this method is time-consuming and does not take trapping of the displaced fluid into account. Laidlow et al. (1988) examined the two-fluid displacement of a compressible fluid. Mohanty et al. (1987) developed a deterministic model to predict imbibition displacement flow in porous media in the capillary fingering region. By using a two-dimensional network, they predicted the saturation of the displaced fluid. Most recently a percolation model was proposed by Bakurof et al. (1990) to describe oil displacement in porous media. An excellent introduction and overview on percolation theory is given by Stauffer (1985).

Lenormand and Zarcone (1985b), following an earlier experimental technique of

Lenormand et al. (1983), demonstrated the transition from capillary fingering to viscous fingering at low viscosity ratios and from capillary fingering to plug flow at high viscosity ratios. Lenormand (1986a) explained the fluid displacement in network models and the different transitions as well as the differences between imbibition and drainage displacements.

Up to this point the three distinct behaviours of immiscible displacement (viscous fingering, capillary fingering and plug flow) have been mentioned together with some numerical and experimental studies that have been carried out.

Lenormand (1985) mapped the domains of validity of the three types of immiscible displacement of a wetting fluid by a non-wetting fluid onto the plane having axes representing the capillary number and the viscosity ratio. This mapping has been called the *phase diagram* for immiscible displacement (see Figure 2.9). According to the phase diagram, each domain corresponds to a different basic mechanism for linear displacement (i.e. the displacement that occurs when the displacing fluid is injected along one side of the network and the displaced fluid is recovered along the opposite side) in which only one kind of force is acting the other two being negligible. Therefore, the flow pattern of the displacing fluid is the result of the interplay of three kinds of forces:

(a) viscous forces in the displacing fluid

(b) viscous forces in the displaced fluid

(c) capillary forces at the interface.

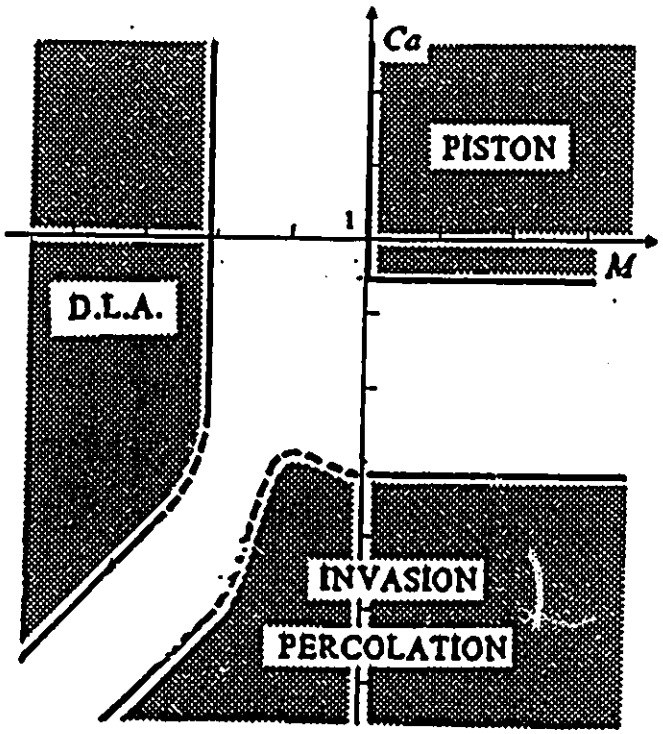

Figure 2.9: The phase diagram for drainage displacement in a porous medium (Lenormand 1985). Piston, Invasion Percolation and DLA correspond to stable displacement (plug flow), capillary fingering and viscous fingering at a low viscosity ratio, M.

Lenormand (1986b) extended the phase diagram to three-dimensional porous media. Later, Leclerc and Neale (1988) developed a model in order to describe the transition between the three distinct behaviours mapped on the phase diagram. Their study made use of the DLA and anti-DLA models as well as the notion of the phase diagram. Viscous fingering at low viscosity ratios and plug flow are modelled by random walkers released from within the wetting and non-wetting fluid, respectively. Leclerc and Neale chose a sticking probability equal to the normalized ratio of an intraphase pressure drop to the capillary pressure. At high flow rates the sticking probability is close to one and walkers stick upon first contact with the interface. At low flow rates and low viscosity ratios, random walkers are allowed to wander in the displacing fluid (anti-DLA). In the capillary fingering region, random walkers wander only within the displacing fluid and, upon sticking, the interface is allowed to move to its neighbouring sites depending upon the sticking probability. This algorithm, although successfully describing the transitions on the phase diagram, does not take into account trapping of the displaced fluid nor the local anisotropy of the porous medium, since random walkers move with equal transition probabilities (=0.25) at each step. In addition, the algorithm does not predict the transition from DLA to plug flow. Therefore, the flow pattern of the displacing (non-wetting) fluid results rather from the randomness of the random walkers and the next-to-nearest neighbour contacts of the interface as well as the diagonal steps of the random walkers. In addition, the structure and the anisotropy of the porous medium are ignored.

According to Lenormand (1989a), the main drawback of the basic stochastic mod-

els is in the modelling of displacements at finite viscosity ratios in the transition from DLA- to plug flow limits. In addition, many questions about the role of the interfacial tension still remain unanswered and no attempt has been successfully made to incorporate the interfacial tension in the DLA model. The DLA model as applied by Paterson (1984) accounts for miscible displacement, i.e. at the limit of vanishing interfacial tension at a very high capillary number.

The deterministic models mentioned above make use of the electrical analog of the flow in porous media, and for Newtonian fluids the problem is reduced to the solution of a set of linear equations for the pressure. However, difficulties arise when capillary effects due to the interfacial tension are taken into account. From the mathematical point of view, the threshold due to the capillary pressure leads to a non-linear problem: the system of equations used to solve for the pressure at each node requires knowledge of which channel will next be invaded by the menisens, and this knowledge itself requires the value of the pressure at each node.

In order to avoid difficulties due to this non-linearity, different approaches have been used. All of these approaches consist of replacing the non-linear problem by a set of linear problems. Koplik and Lasseter (1986) used a trial technique in which all possible combinations of elementary displacements are investigated. For each case the problem becomes linear. Instead of the threshold value for the pressure at each cylindrical channel, Payatakes (1982), Payatakes and Dias (1984), Dias and Payatakes (1986a,b) and Vizika (1989) used the more realistic representation of a conical pore. These studies examined microdisplacement of a non-wetting fluid by a wetting one, and the mobilization of oil ganglia. However, due to the

pore geometry, the capillary pressure changes along a channel and many steps are required to resolve the motion of the interface in a single channel. The above methods are time consuming and limited to small networks.

Lenormand et al. (1988) developed a model which takes the capillary pressure into account and allows simulations of large networks (100×100). According to their approach, if the pressure drop between two nodes is less than the capillary pressure, the flow rate in this channel is taken to be zero for diphasic flow. Lenormand et al. (1988) used a relaxation technique to solve for the pressure on a network represented by cylindrical capillaries. The pores (nodes) are spherical and represent the porosity of the network. According to this approach motion of the interface is considered only in the pores. Therefore, a pore may contain both fluids whereas a channel contains either one of the fluids.

Most recently, Blunt and P. King (1991a,b) followed a similar approach to perform large scale simulations. They solved the linear problem by using a Gauss-Seidel overrelaxation technique. Motion of the interface is considered only in the pores in a similar way as in the previous study (Lenormand et al. 1988). However, pores may be invaded by both fluids. This approach allowed them to perform large scale simulations in three-dimensional networks and to predict the relative permeability as a function of saturation for different capillary numbers and viscosity ratios. These predictions show that the relative permeability is a function of the viscosity ratio and the capillary number. Their results are in agreement with the predictions made previously Leverett (1941), Odeh (1959), Tuber (1971) and Lefebvre du Prey (1973).

Lenormand (1989b), based on previous numerical and experimental studies, improved the concepts of the phase diagram. In that work, Lenormand presented some quantitative equations for the limits of the phase diagram by considering some principles of the invasion percolation theory and simplifications of the physical problem.

The limits of the DLA region are expressed by the following equations:

$$Ca_{DLA} = C_1\lambda(h/L)^{7/4}(r_o/h)^3M \tag{2.20}$$

$$M_{DLA} = C_2(h/L) \tag{2.21}$$

The limits of the plug flow (piston) region are

$$Ca_{PF} = C_3\lambda(r_o/L)^3 \tag{2.22}$$

$$M_{PF} \simeq 1 \tag{2.23}$$

The limits of the invasion percolation region are

$$Ca_{INV} = C_4\lambda(h/L)^{11/4}(r_o/h)^3 \qquad M > M_{PF} \tag{2.24}$$

$$Ca_{INV} = C_5\lambda(r_o/L)^{7/4}(r_o/h)^3 \qquad M < M_{DLA} \tag{2.25}$$

In the above equations λ denotes the dispersion of a uniform size distribution of the channels, L the length of the network, r_o the average channel radius, h the length of the network lattice unit, and $C_1 - C_5$ are proportionality constants.

2.4 Objectives

The objective of the present study is to develop efficient numerical models which would be capable of simulating the displacement of a wetting fluid by a non-wetting fluid in a porous medium represented by a two-dimensional network of interconnected capillaries.

Two computer programs will be developed, one based on a stochastic and the other on a deterministic approach for solving the governing equations at the pore level.

The stochastic approach will be applied to predict the transition from one behaviour of the displacing fluid to another by making use of the DLA, anti-DLA and invasion percolation models modified in order to incorporate the local anisotropy and heterogeneity of the porous medium. This approach will enable predictions of the effects of viscous and capillary forces on:

(a) the dynamic behaviour of the displacing fluid and the oil recovery,

(b) the island formation and the island size distribution,

(c) the fractal behaviour of the displacing fluid.

The deterministic approach will be applied to predict the transition from one behaviour of the displacing fluid to another by applying certain rules for the advancement of the interface inside the channels while neglecting the pore space. The deterministic approach will enable predictions of:

(a) the effects of viscous and capillary forces on the dynamic behaviour of the displacing fluid and on the oil recovery,

(b) the effects of local anisotropy and heterogeneity of the porous medium on the dynamic behaviour of the displacing fluid.

Finally, this study will provide a direct comparison between the two general approaches used for the modelling of flow in porous media with previous theoretical and experimental studies. The simulations are expected to reveal important implications on enhanced oil recovery processes by providing insight into certain significant aspects of the physics of flow in porous media.

Chapter 3

MODELLING OF FLOW IN POROUS MEDIA

This chapter describes the network representation of a two-dimensional porous medium and the stochastic and deterministic approaches for the modelling of the displacement of a wetting fluid by a non-wetting fluid in a porous medium.

3.1 The Network Representation of a Porous Medium

As has been mentioned in Section 2.1, a network model of a porous medium is a mathematical representation. The purpose of such a model is the representation of a porous medium which retains the most important characteristics and properties of the porous medium but does not retain the complexity of its structure. Therefore, the mathematical treatment of the physical phenomena is facilitated.

The network which is used in the present study consists of spherical pores multi-connected by cylindrical channels. The pore and the channel radii follow a uniform size distribution. This approximation has been made by many authors (Chandler

et al. 1982, Lenormand et al. 1988, Blunt and P.King 1990a, and others). Dias and Payatakes (1986a,b) and Vizika (1989) made a more realistic approximation of representing the porous medium by a network of conical pores However, this last approximation makes the problem more complicated and limited to small networks. In addition, phenomena such as viscous and capillary fingering cannot be distinguished in the scale of a few pores. Therefore, large networks are required in order to study the above phenomena and to describe a macroscopic behaviour of the oil reservoir with respect to these phenomena and the transition from one to another.

A two-dimensional network is characterized by the number of pores in each direction, N_x and N_y, the thickness of the network, and the distance between the centers of two adjacent pores, h (constant), and the pore and channel radii.

The total number of pores in the network is

$$N_p = N_x N_y \tag{3.1}$$

and the total number of channels is

$$N_b = (2N_x + 1)N_y + N_x \tag{3.2}$$

For the notation of the pores and the channels, consider a pore in the network with coordinates (i_x, i_y), where i_x is in the flow direction. Then this pore is numbered as follows

$$i_p = i_x N_y + i_y \tag{3.3}$$

To number the four channels connected to the pore i_p consider the schematic representation of Figure 3.1. According to this representation the channel notation is

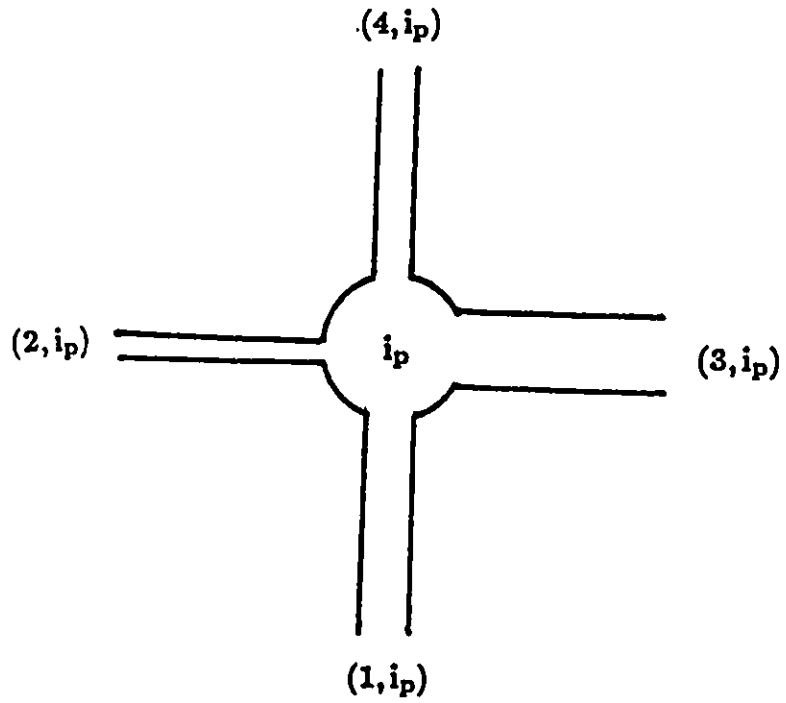

Figure 3.1: Representation and numbering of the channels connecting a pore with the network.

as follows:

$$(1, i_p) = 2i_x N_x - i_y N_y$$

$$(2, i_p) = 2(i_x - 1)N_x + i_y$$

$$(3, i_p) = 2i_x N_x + i_y$$

$$(4, i_p) = 2i_x N_x + i_y - N_y + 1 \tag{3.4}$$

A channel connects two pores. Then according to the notation, the channel $(2,i_p)$ is identical with the channel $(3,i_p - N_y)$. The length, l_{ij}, of a channel connecting the pores i and j is given by

$$l_{ij} = h - R_i - R_j \tag{3.5}$$

where R_i is the pore radius and h the distance between the centers of two adjacent pores.

In the following sections two computer network simulators are described.

3.2 The Stochastic Approach

The displacement of a wetting fluid by a non-wetting fluid in a porous medium is described. Flow of both phases is described by Darcy's equation (Equation 2.13), provided that the Reynolds number, N_{Re}, is very low.

The continuity equation for incompressible fluids (Equation 2.18) in conjunction with Darcy's equation for each phase (Equations 2.14, 2.15) becomes

$$\nabla \cdot (\frac{K K_{ri;d}}{\mu_{i;d}} \nabla P_{i;d}) = 0 \tag{3.6}$$

where all of the terms in Equation (3.6) have been defined in Chapter 2.

Assuming that the wetting fluid initially occupies 100% of the available pore space in the porous medium, and that none of this fluid remains undisplaced in the zone invaded by the non-wetting fluid, the above equation for a homogeneous and isotropic porous medium reduces to Laplace's equation for the pressure (Equation 2.17).

Considering the displacement of a viscous fluid by a less viscous one, one may approximate P=constant in the less viscous fluid (Paterson 1984). The DLA model describes the movement of a random walker (Shreider 1963, Rudnick and Gaspari 1987) in the context of diffusion-limited aggregation, so that for a constant flux of walkers from a source far away from the aggregate (to which the walkers eventually stick) Laplace's equation must be satisfied

$$\nabla^2 u = 0 \tag{3.7}$$

where u(x,k) is the probability that a walker is at point x at the kth step with the condition u=0 on the boundary of the aggregate. The aggregate grows with a velocity, V, proportional to ∇u. Therefore:

$$V = K\nabla u \tag{3.8}$$

where K is proportionality constant.

Modelling of viscous fingering according to the DLA model is based on the similarities between Equations (2.13) and (3.8) and (2.17) and (3.7). Therefore, the displacement of a viscous fluid by a less viscous fluid can be described by releasing

random walkers from the recovery side and letting them stick upon contact in the interface. In a similar way, the displacement of a fluid by a more viscous one can be described by the anti-DLA model (Paterson 1984).

To take into account the capillary pressure at the interface, an early approach (Kiriakidis et al. 1991a) made use of a sticking probability which is given by

$$\phi_{NW;W} = \frac{\delta P_{NW;W}}{\delta P_{NW;W} + P_C} \tag{3.9}$$

where $\delta P_{NW;W}$ is a pressure difference in the non-wetting/wetting fluid, referred to as the intraphase pressure drop (Leclerc and Neale 1988), and P_C the capillary pressure.

The pressure difference $\delta P_{NW;W}$ is determined by following a simplifying assumption made by Lenormand (1985a). Thus, at the limit of stable displacement (plug flow), flow of both fluids occurs through N_y parallel channels of radius r_o, which is the average channel radius. Darcy's equation for single-phase flow becomes:

$$\frac{Q}{A} = \frac{\kappa}{\mu}\frac{\Delta P}{L} \tag{3.10}$$

where Q is the flow rate, L the length of the porous medium, ΔP the pressure difference, A the flow cross-sectional area and κ and μ as previously defined. Then, according to Lenormand's assumptions and by approximating the effective permeability of the porous medium to each fluid by the permeability of the porous medium, the pressure difference in each fluid for A=2Lr_o is given by

$$\delta P_{NW;W} = \frac{QL\mu_{NW;W}}{2\kappa r_o L} \tag{3.11}$$

In the DLA limit, flow of the displacing, non-wetting fluid is assumed to occur in one single channel of length L and radius r_o. On the other hand, flow of the displaced

fluid is assumed to occur in N parallel channels of radius r_o. Then, from Equation (3.10) for A=2Lr_o and A=πr_o^2 we have

$$\delta P_{NW} = \frac{QL\mu_{NW}}{\pi\kappa r_o^2} \tag{3.12}$$

$$\delta P_W = \frac{QL\mu_W}{2\kappa L r_o} \tag{3.13}$$

The sticking probability, $\phi_{NW;W}$, expresses the susceptibility of the interface to rearrangements after first contact, provided that $\delta P_{NW;W}$ is not too high with respect to the capillary pressure, since in the case of drainage the capillary pressure opposes advancement of the interface. When P_C is close to $\delta P_{NW;W}$, walkers will tend to avoid narrow channels. On the other hand, when P_C is negligible compared to $\delta P_{NW;W}$, the sticking probability approaches unity and the limit of vanishing interfacial tension is obtained.

To model capillary fingering an approach similar to an earlier one (Leclerc and Neale 1988) has been followed. Each pore is connected with four nearest-neighbours. The number of active bonds for percolation for each pore is obtained by performing four coin-toss trials per site with a probability which is equal to the non-wetting sticking probability, ϕ_{NW}.

The above approach, although providing a satisfactory description of the dynamic behaviour of the invading fluid, ignores certain aspects of the physics of the displacement. In particular, the local anisotropy of the porous medium is taker into account only by a sticking probability via the capillary pressure which is inversely proportional to the channel radius. In addition, the equations which determine the

intraphase pressure drop appear rather simplistic and the pressure field is ignored.

In a later study (Kiriakidis et al. 1990a,b, 1991b), a different approach was adopted by considering the flow conservation equation for incompressible flow in each pore expressed by

$$\sum_{i=1}^{4} Q_i = 0 \tag{3.14}$$

where Q_i is the flow rate in any channel connecting a pore with its four nearest neighbours. Then, considering a pore i in each of the two phases and assuming that flow in the channels is described by the Poiseuille Equation, the flow rate in the channel connecting pores i and j is expressed by

$$Q_{ij} = G_{ij}(P_i - P_j) \tag{3.15}$$

where G_{ij} is the flow conductivity of the channel, defined as

$$G_{ij} = \frac{\pi {r_{ij}}^4}{8\mu l_{ij}} \tag{3.16}$$

where l_{ij} is the length of the channel connecting pores i, j. Then, the flow conservation equation may be written as

$$\sum_{j=1}^{4} G_{ij}(P_i - Pj) = 0 \tag{3.17}$$

or

$$P_i = \frac{\sum_{j=1}^{4} G_{ij} P_j}{\sum_{j=1}^{4} G_{ij}} \tag{3.18}$$

The last equation is equivalent to equation (2.26) and it is satisfied by a random walker which is launched from a site i and moves to each neighbouring site with a transition probability given by

$$p = \frac{G_{ij}}{\sum_{j=1}^{4} G_{ij}} \tag{3.19}$$

The random walker subsequently sticks upon contact with the interface.

To make an approach for the sticking probability consider the rate of growth of a perturbation (Peters and Flock 1981) which is given by

$$\eta \propto e^{\omega t} J_m(\sigma, \zeta) cos(\zeta \chi) \tag{3.20}$$

where η is the frontal perturbation velocity, σ the wavelength, J_m the Bessel function of the first kind, t the time, ζ and χ the cylindrical coordinates, ω the stability index and m an integer number (m=0,1,2...). The stability index is given by

$$\omega = \frac{\sigma[(\frac{1}{\lambda_W} - \frac{1}{\lambda_{NW}})V - (\rho_{NW} - \rho_W)gcos(\tau)] - \sigma^3\gamma}{(\frac{1}{\lambda_W} + \frac{1}{\lambda_{NW}})} \tag{3.21}$$

where $\lambda_{NW;W}$ is the mobility of the non-wetting/wetting fluid and τ the angle between the flow direction and the horizontal plane.

Considering the above equation in the absence of buoyancy forces and in the limit of vanishing interfacial tension, one can write

$$\omega \propto \frac{\frac{1}{\lambda_W} - \frac{1}{\lambda_{NW}}}{\frac{1}{\lambda_W} + \frac{1}{\lambda_{NW}}} \tag{3.22}$$

or

$$\omega \propto \frac{\frac{\lambda_{NW}}{\lambda_W} - 1}{\frac{\lambda_{NW}}{\lambda_W} + 1} \tag{3.23}$$

In the simulation of the two-fluid, immiscible displacement the sticking probability is taken to be

$$\phi_W = \frac{\frac{\lambda_{NW}}{\lambda_W} - 1}{\frac{\lambda_{NW}}{\lambda_W} + 1} \tag{3.24}$$

The mobility of each fluid can be expressed by

$$\lambda_{NW;W} = \frac{\kappa \kappa_{rNW;rW}}{\mu_{NW;W}} \tag{3.25}$$

and assuming the following dependence of the relative permeability, $\kappa_{rNW;rW}$, on the saturation, $s_{NW;W}$

$$\kappa_{rNW;W} = s^2_{NW;W} \tag{3.26}$$

the sticking probability can then be determined from Equation (3.24).

Considering Equation (3.24), when ϕ_W approaches unity the stability index, ω, becomes very high and the perturbations tend to grow further forming fingers of the invading fluid. Simulating a displacement process by random walkers, walkers launched from within the displaced fluid (DLA) tend to enhance instability growth. The rate of growth of an instability depends on the viscosity ratio and it is higher at low viscosity ratios since the stability index is high. As the viscosity ratio approaches unity the stability index tends to zero leading to a flat front.

In the capillary fingering region the capillary forces dominate and motion of the interface occurs smoothly, and in the case of drainage through the path of least resistance, which is provided by the capillary pressure. Since the pore diameters are, in general, larger than the channel diameters, the capillary pressure is expected to be higher when the interface is located in the channels. Therefore, what controls motion of the interface is the local pore structure and geometry. At any given stage of the displacement the interface does not see the exit. An approach very similar to that of Chandler et al. (1982) has been followed here. Random numbers are assigned at the beginning of the simulation to all of the channels, corresponding

to their radius. At any step the interface advances through the channel with the largest random number (largest radius) and automatically fills the corresponding pore which was initially occupied by the displaced fluid. This procedure is repeated until the interface reaches the recovery side. At this point it is important to note two major characteristics of this approach:

(a) At any given step of the simulation, only one pore is filled with the invading fluid which is equivalent to a constant flow rate condition (Wilkinson and Willemsen 1983).

(b) The random numbers corresponding to the channel radii are assigned only once and they are maintained constant throughout the simulation.

To consider the immiscible displacement of a wetting fluid by a non-wetting one in the transition regions (DLA-capillary fingering, plug flow-capillary fingering and DLA-plug flow) the phase diagram is taken into account and in particular the equations which express its limits (Equations 2.20-25). According to this approach, displacements at low viscosity ratios are described by the DLA model when

$$N_{Ca} > Ca_{DLA} \tag{3.27}$$

where Ca_{DLA} is the capillary number at the DLA limit. In this case only wetting walkers approach the interface, moving with a transition probability, p, and sticking in the interface with a sticking probability, ϕ_W. In this region viscous forces in the displacing fluid and capillary forces at the interface are negligible compared to the viscous forces in the displaced fluid.

For displacements in the transition region between DLA and capillary fingering, i.e. when

$$Ca_{DLA} > N_{Ca} > Ca_{INV} \tag{3.28}$$

where Ca_{INV} is the capillary number at the capillary limit, both viscous forces in the displaced fluid and capillary forces at the interface are significant. In this region, the interface moves according to both the DLA and the invasion percolation model with a phase transition probability given by

$$\psi = \frac{O(Ca_{DLA}) - O(N_{Ca})}{O(Ca_{DLA}) - O(Ca_{INV})} \tag{3.29}$$

where "O" denotes the order of the capillary number as approximated by the logarithm (Kiriakidis et al. 1990b).

For displacements in the capillary region ($N_{Ca} < Ca_{INV}$) only capillary forces are significant and advancement of the interface occurs by the invasion percolation mechanism.

In a similar way, the transition from plug flow to capillary fingering is modelled with a phase transition probability expressed by

$$\psi = \frac{O(Ca_{PF}) - O(N_{Ca})}{O(Ca_{PF}) - O(Ca_{INV})} \tag{3.30}$$

An attempt to model the transition from DLA to plug flow limits has also been made. In this region viscous forces in both fluids are significant and they are taken into account. Therefore, both the anti-DLA and DLA mechanisms are used with a phase transition probability, ψ, given by

$$\psi = \frac{O(M_{PF}) - O(M)}{O(M_{PF}) - O(M_{DLA})} \tag{3.31}$$

Summarizing the stochastic approach, the following points should be noted:

(a) Heterogeneities and anisotropy of the porous medium are taken into acount by the transition probability of the random walkers which depends on the flow conductivity of the channels.

(b) The sticking probability of the wetting walkers depends on the mobility ratio and provides a measure of the tendency for instability growth.

(c) Capillary effects are taken into account only in the transition regions towards capillary fingering. The phase transition probability provides a measure of the significance of the capillary forces with respect to the viscous forces. In the transition regions and the capillary region motion of the interface occurs by following the invasion percolation mechanism.

(d) Regions of the displaced fluid that are completely surrounded by the invading fluid are not invaded, since the fluids are incompressible.

At this point some aspects of the stochastic solution to the problem are discussed. Solution of the problem, i.e. determination of the pressure field, necessitates the solution of an elliptic equation. In a deterministic method, the pressure field, the velocity and the fluid motion are calculated and implemented explicitly. However, in a stochastic method this is not the case. Instead, the solution of the elliptic equation for the pressure is modelled by random walkers. This technique is known to converge to the correct pressure field after a large number of walkers are averaged (Shreider 1963). This last condition is satisfied either by allowing the random walkers to

stick to the interface with a sticking probability or by having an interfacial pore visited at least N_v times before the interface advances to this pore. A discussion on this subject has been presented by Siddiqui and Sahimi (1987) with references to a number of proposed approaches in the literature.

A logical question that arises is how N_v is related to the physical problem and how large it should be in order to approach the correct solution to the problem. These questions still remain unanswered. In the present work N_v is arbitrarily equated to N_{LIM}=2. Higher values of N_v result in a dramatic increase in the execution time of the algorithm.

The flow diagram of the computer algorithm based on the stochastic model is given in Figure 3.2. The simulation commences by assigning the pore and channel radii (according to a uniform size distribution), the length, L, the number of pores, N_x and N_y and the thickness h. The input data (flow rate, viscosities, interfacial tension, contact angle) are fed in and the limits of the phase diagram are calculated from the physical properties of the fluids and the geometrical characteristics of the porous medium. Then, depending upon the capillary number of the displacement and the limits of the phase diagram, one of the mechanisms described above is followed. When random walkers reach the boundary walls they are either killed (absorbing boundaries) or reflected (reflecting boundaries). A very important and time consuming part of the algorithm is the test for trapped areas at each step in the simulation. These regions are checked by tracing the perimeter of such areas. The algorithm finally stops when the interface reaches the recovery side. The efficiency of the displacement process is obtained from the calculation of the fraction of invaded

Figure 3.2: The Stochastic Algorithm for modelling of two-fluid immiscible displacement flow in a porous medium.

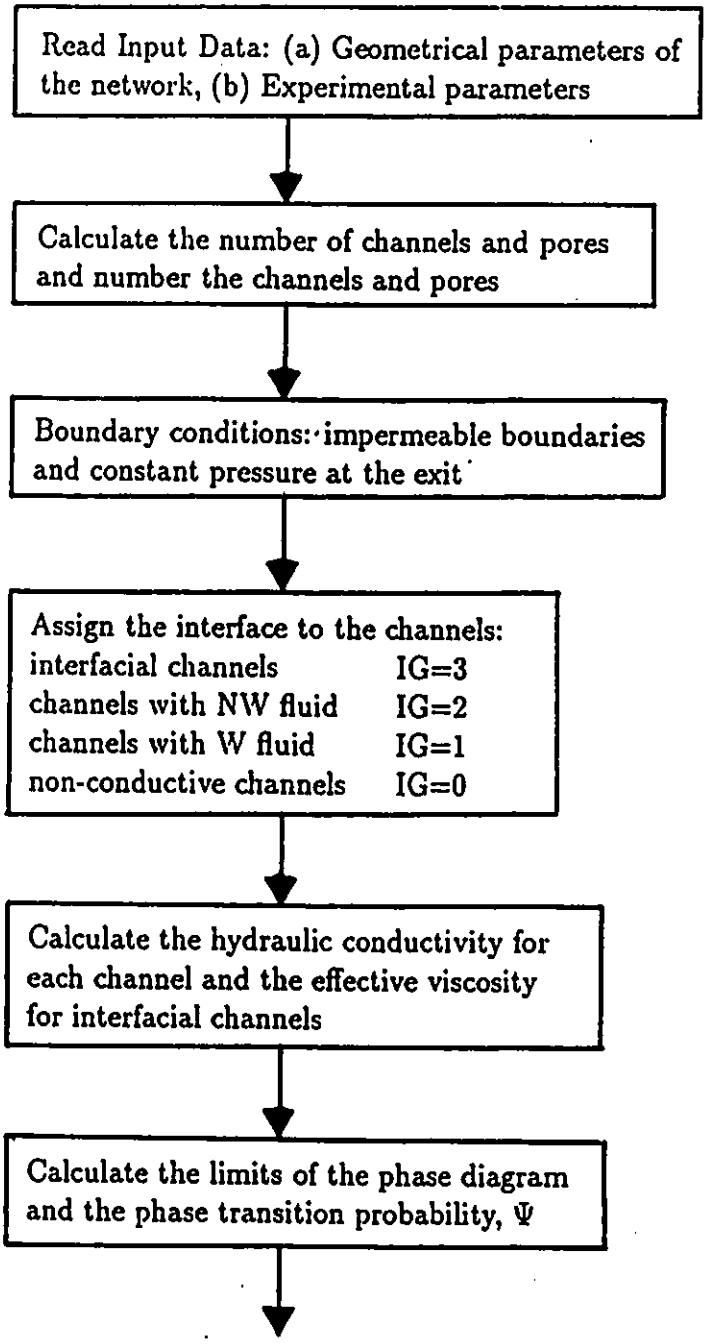

con'd ...

...con'd

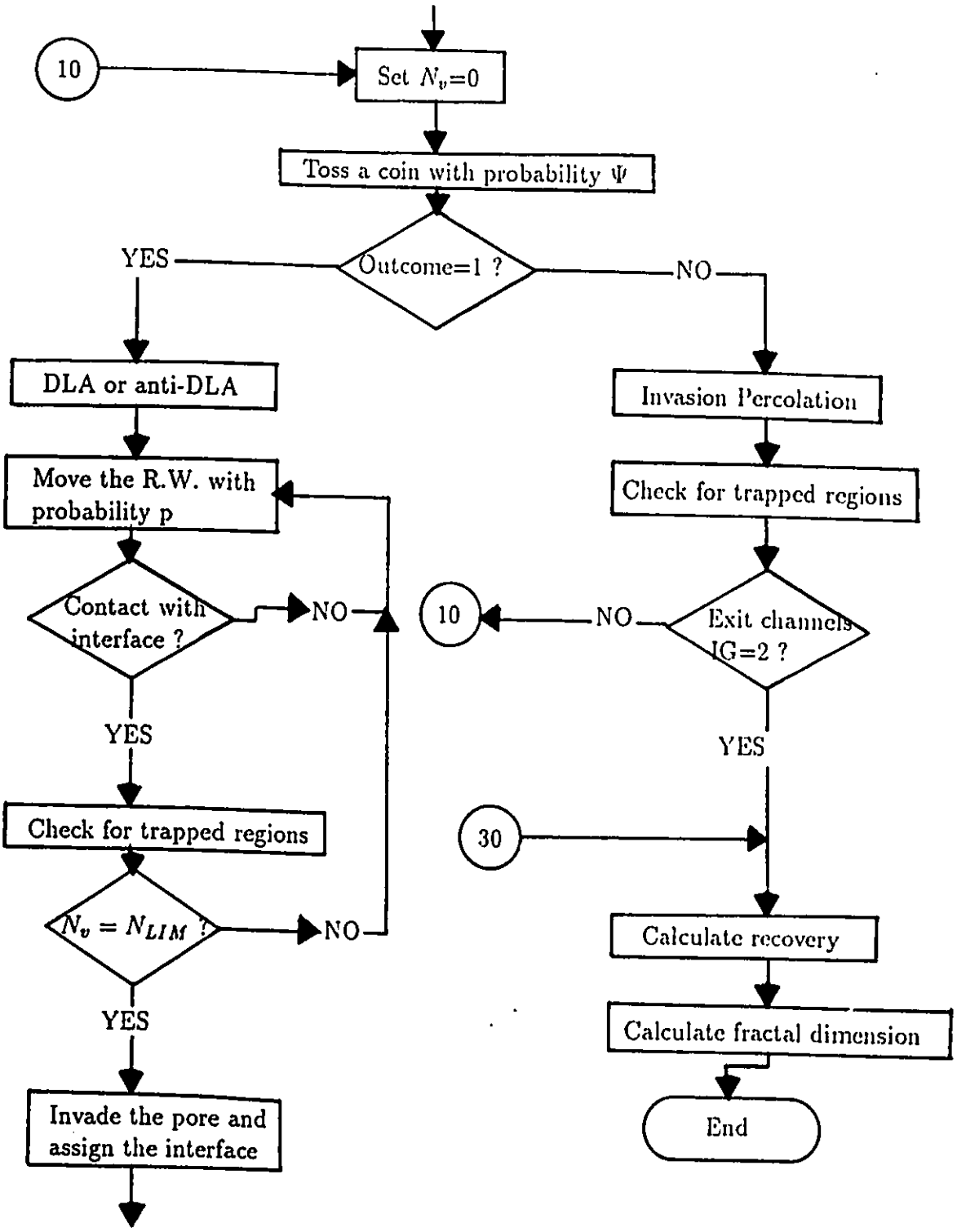
10
Set N_v=0
Toss a coin with probability Ψ
YES
Outcome=1 ?
NO
DLA or anti-DLA
Move the R.W. with probability p
Contact with interface ?
NO
YES
Check for trapped regions
$N_v = N_{LIM}$?
NO
YES
Invade the pore and assign the interface
Invasion Percolation
Check for trapped regions
10
NO
Exit channels IG=2 ?
YES
30
Calculate recovery
Calculate fractal dimension
End

con'd ...

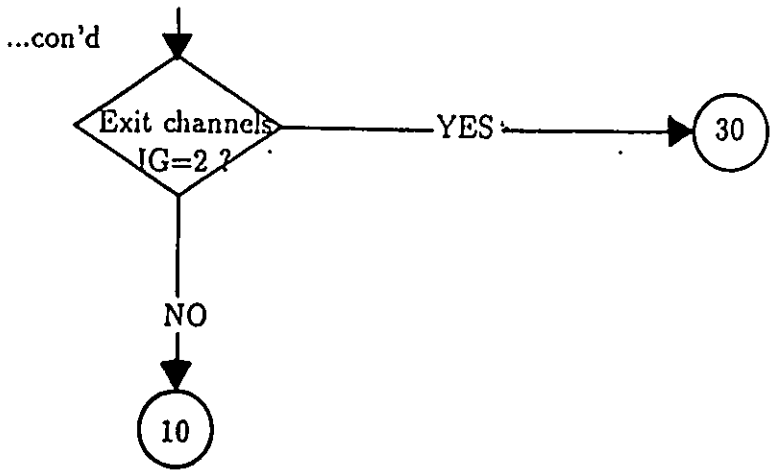
...con'd
Exit channels
IG=2 ?
YES
30
NO
10

pores.

The simulations were implemented in a computer program written in standard FORTRAN 77 language. Standard IMSL routines were used extensively, in particular GGBN (binomial distribution; weighted-coin tosses) and GGUBFS(pseudo-uniform random number generator). The runs for the simulations were performed in the University of Ottawa's AMDAHL 5860 mainframe computer (CMS operating system).

3.3 The Deterministic Approach

3.3.1 Monophasic Flow - Permeability of the Porous Medium

The permeability, κ, of a porous medium, represented by a network of multiconnected channels whose radii follow a size distribution, is determined by considering monophasic flow of a Newtonian fluid of known viscosity and injected at a constant flow rate.

The flow rate in a channel is assumed to obey the Poiseuille equation and the flow conservation equation for incompressible flow at each pore is described by Equation (3.13). The injection pressure is determined by a flow conservation equation in the injection side of the network and the pressure in the recovery side is maintained constant at an arbitrary value.

The problem to be solved consists of $N_p + 1$ linear equations, with unknowns being

the N_p nodal pressures and the injection pressure. The problem is solved by using a Gauss-Seidel successive overrelaxation technique. The pressure P_i in a pore i is determined by

$$P_i = (1-\beta)P_i + \frac{\sum_{j=1}^{4} G_{ij}P_j}{\sum_{j=1}^{4} G_{ij}} \tag{3.32}$$

where β is the overrelaxation parameter (=1.7), P_j the pressure at any neighbouring pore and G_{ij} as previously defined.

The solution of the problem determines the injection pressure and therefore the pressure difference, ΔP. The permeability, κ, is determined according to Equation (3.10) as follows

$$\kappa = \frac{Q\mu L}{A\Delta P} \tag{3.33}$$

where all the quantities have been defined before.

3.3.2 Two-Fluid Displacement Flow

The immiscible displacement of a wetting fluid by a non-wetting one is modelled by a deterministic network simulator which is described below. The model is based on the following assumptions:

(a) Both fluids are Newtonian and incompressible.

(b) Poiseuille equation describes flow in the channels.

(c) Dynamic effects on the contact angle due to the flow are neglected.

(d) Gravity effects are neglected.

(e) The pressure drop occurs only in the channels.

(f) The pores are filled completely with either the invading (non-wetting) fluid or the displaced (wetting) fluid. However, the channels may contain both fluids.

Initially the wetting fluid is in place in the network and occupying the entire pore space. The non-wetting fluid is injected at a constant flow rate in the injection side and the pressure in the recovery side is kept constant. No-flow conditions are imposed in the lateral boundaries.

Flow in a channel where both fluids are present, is expressed by the Poiseuille equation as follows (Dias and Payatakes 1986a)

$$Q_{ij} = \frac{\pi r_{ij}^4}{8 l_{ij} \mu_e} (P_i - P_j - P_{C_{ij}})^+ \tag{3.34}$$

where Q_{ij} is the flow rate, P_i and P_j the pressures in the pores i and j which are filled with the non-wetting and the wetting fluids, respectively, $P_{C_{ij}}$ the capillary pressure, μ_e an effective viscosity and l_{ij}; r_{ij} as previously defined. In this equation the + sign denotes the positive part, meaning that Q_{ij}=0 as long as $(P_i - P_j) \leq P_{C_{ij}}$; otherwise, the expression for the flow rate is the one for biphasic flow in a channel with a pressure jump at the interphase.

The effective viscosity in an interfacial channel is given by (P.King 1987)

$$\mu_e = x_{NW} \mu_{NW} + x_W \mu_W \tag{3.35}$$

where $x_{NW;W}$ is the volumetric fraction of the non-wetting/wetting fluid in the channel. The use of this expression for the effective viscosity is restricted to very small displacements of the interface inside the channel since the fraction $x_{NW;W}$ changes with the position of the interface in the channel.

Flow in the bulk fluids is modelled by the equations describing monophasic flow, i.e. by the flow conservation equation at each pore. However, the flow in interfacial channels no longer depends linearly on the pressure difference as can be seen from Equation 3.34. The flow is zero up to a threshold value corresponding to the capillary pressure. To illustrate the above considerations, consider the very simple model proposed by Lenormand et al. (1988) consisting of two parallel channels, a case that can be studied analytically. The radii of the capillaries are r_1 and r_2 ($r_1 > r_2$), P_{C_1} and P_{C_2} are the two capillary thresholds ($P_{C_1} < P_{C_2}$) and G_1 and G_2 are the flow conductivities. The non-wetting fluid is injected at a constant flow rate Q at a uniform (but changing) injection pressure, P, with a constant pressure at the exit (P=0). It is also assumed that the fluids have the same viscosity.

Initially, the two menisci are located at the entrance of each channel (Figure 3.3a). The problem then is to determine the pressure P at the entrance as a function of the total flow rate Q. The total flow rate is given by

$$Q = G_1(P - P_{C_1})^+ + G_2(P - P_{C_2})^+ \tag{3.36}$$

As long as P is smaller than P_{C_1} then each of the two terms in the above equation is zero and there is no displacement. When P is between P_{C_1} and P_{C_2}, only the first term is not zero, and displacement occurs only in the first channel whose flow conductivity is G_1, which is the slope in Figure 3.3b. When $P > P_{C_2}$ displacement occurs in both channels. The slope in Figure 3.3b is $G_1 + G_2$. This simple model describes the physics of the displacement of a wetting fluid by a non-wetting fluid in a porous medium represented by a network of interconnected channels.

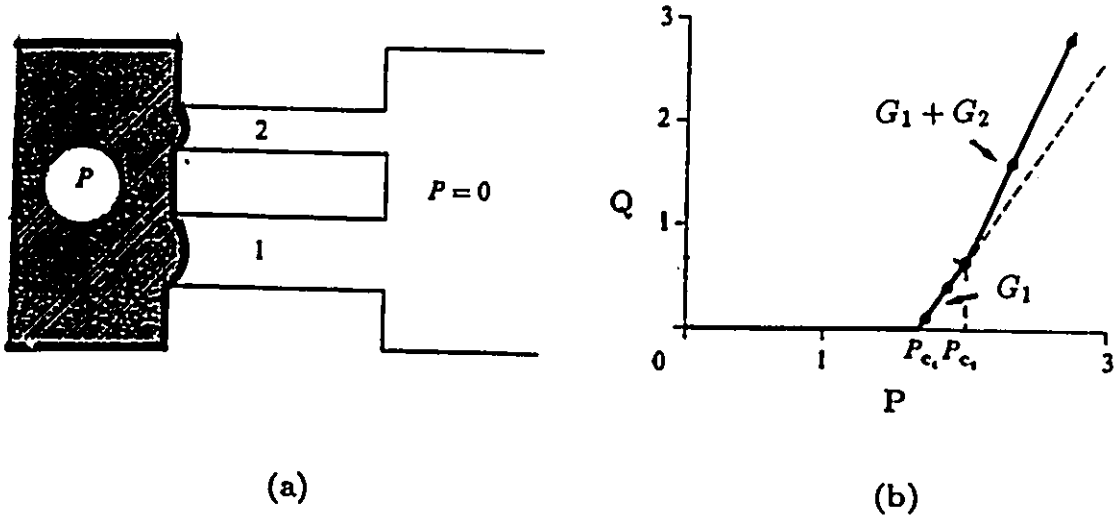

Figure 3.3: Displacement of a wetting fluid (white) by a non-wetting fluid (black) in two parallel capillaries: (a) initial configuration, (b) non-linear relationship between the flow rate, Q, and the injection pressure, P

The solution of the non-linear problem is approximated by a relaxation technique. The solution of the linear, monophasic problem provides an initial guess for the non-linear problem. The injection pressure is then modified by including the capillary pressure. At each step, the pressure at each pore is updated through the flow conservation equation. When the threshold pressure is not reached in interfacial channels, their flow conductivities are set equal to zero and no flow is conducted through those channels. The relaxation procedure stops when a satisfactory stability is obtained. Then, the flow rate in each interfacial channel is calculated by using the Poiseuille equation. A time step is calculated so that only one channel is completely filled with the non-wetting fluid. Then, the interface is advanced in all the interfacial channels according to the flow rate and the time step. The interface is frozen in channels where the threshold pressure is not reached. As soon as the non-wetting fluid fills an interfacial channel it fills automatically the corresponding pore. At this stage the volumetric fractions of the fluids, the flow conductivity of and the effective viscosity in the interfacial channels are calculated. New interfacial channels are assigned around the recently invaded pore. At this stage of each step it is possible that interfacial channels are found between two pores filled with the non-wetting fluid. In this case, the flow conductivity of these channels is set equal to zero for the rest of the simulation. A trapping rule is used at this stage to check for trapped pores occupied by the wetting fluid. These pores are recorded and the flow conductivity of the channels which connect these pores with the rest of the network are set equal to zero for the rest of the simulation. The above procedure is repeated at each step until one of the exit channels (channels connected to the recovery side) is invaded by the non-wetting fluid. At this point, the fraction of the invaded pores

is calculated as well as the oil recovery from the invaded pores and channels.

The present algorithm can also be used to describe the dynamic behaviour of the invading fluid in the presence of connate regions of this fluid in the porous medium. The connate phase occupies the pores and channels which connect these pores. It is assumed that the connate regions are immobile and that there is no flow within these regions. Therefore, the pressure field is not calculated within these regions. Channels containing the connate phase are taken to be non-conductive (G=0).

The simulation proceeds as it was described before. At any step of the simulation, the algorithm checks to see if there is a channel with connate phase connected to the newly filled pore. If there is one, the region of the connate phase to which this channel belongs is identified and this region becomes part of the invading phase. The flow conductivities of the channels previously containing the connate phase are calculated and new interfacial channels are assigned to the new front. These steps are repeated throughout the simulation.

The two-fluid immiscible displacement of a wetting fluid by a non-wetting fluid in a disordered porous medium can be described by the deterministic algorithm described in this section. Sites with a co-ordination number less than four are assumed to have fictitious bonds of zero conductivity. Thus the disordered network is equivalent to an ordered network which contains a number of non-conductive bonds. In the simulation, the flow conductivity of fictitious channels is set equal to zero throughout the simulation. The simulation proceeds in exactly the same way as it was described before.

In conclusion, the deterministic model described above simulates the displacement of a wetting fluid by a non-wetting one in a porous medium represented by a network of interconnected channels. The algorithm is based on a simple model proposed by Lenormand et al. (1988). The problem is non-linear due to the capillary pressure involved in the calculation of the flow rate in interfacial channels. The solution of the non-linear problem is approximated by a relaxation technique which is used in order to determine the pressure field. In interfacial channels where the threshold pressure, which is represented by the capillary pressure, is not reached the interface is frozen. Advancement of the interface is resolved only inside the channels and only one pore is invaded by the non-wetting fluid at any given step.

A flow diagram of the computer algorithm is presented in Figure 3.4. The simulations were implemented in a computer program written in standard FORTRAN 77 language. The runs for the simulations were performed in the University of Ottawa's AMDAHL 5860 mainframe computer (CMS operating system) and in the IBM RS/6000 computer (Unix operating system).

Figure 3.4: The Deterministic Algorithm for modelling of two-fluid immiscible displacement flow in a porous medium.

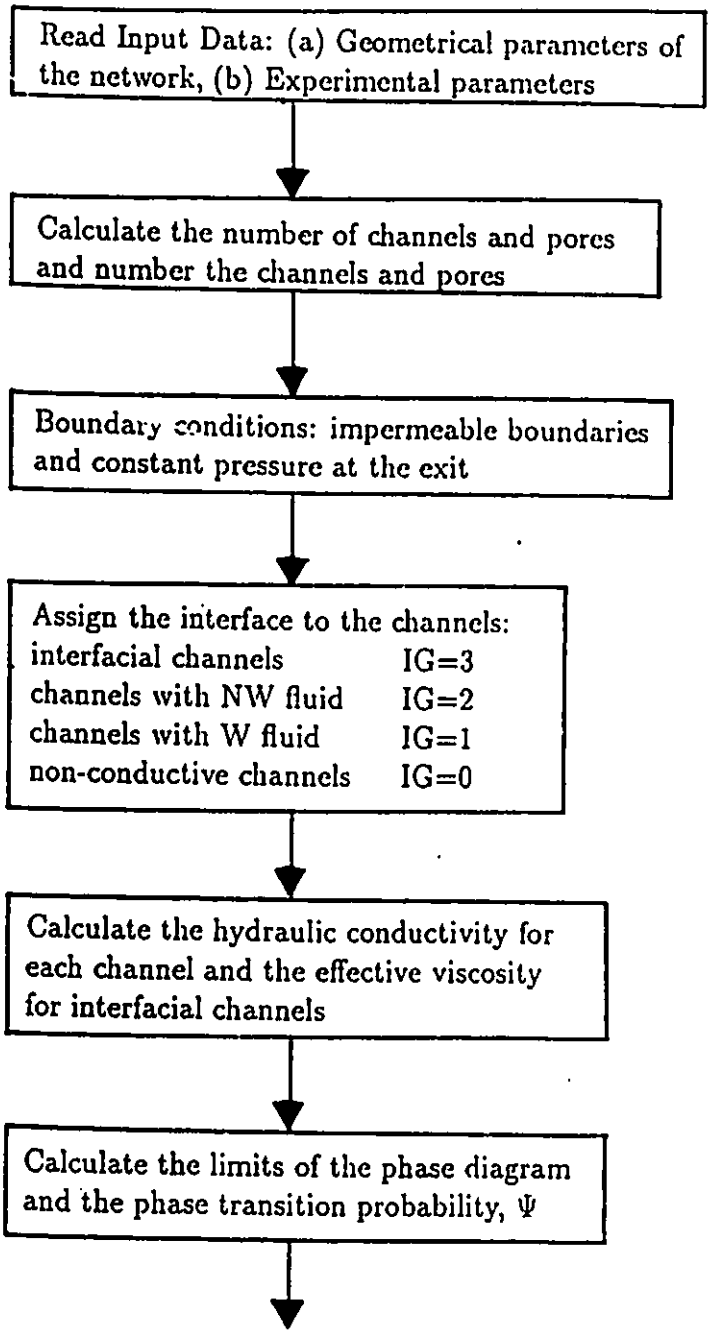

con'd ...

...con'd

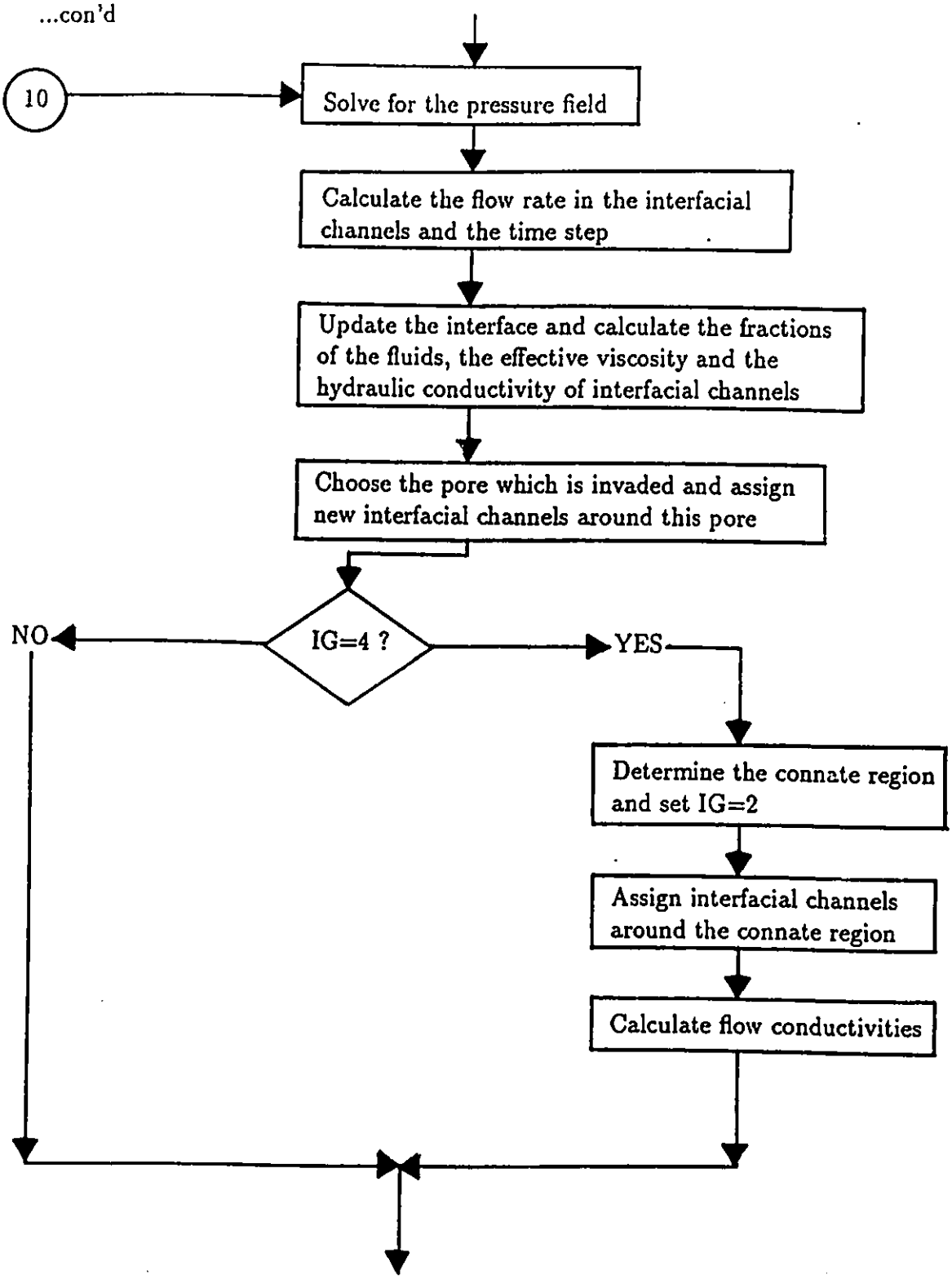
10
Solve for the pressure field
Calculate the flow rate in the interfacial channels and the time step
Update the interface and calculate the fractions of the fluids, the effective viscosity and the hydraulic conductivity of interfacial channels
Choose the pore which is invaded and assign new interfacial channels around this pore
IG=4 ?
NO
YES
Determine the connate region and set IG=2
Assign interfacial channels around the connate region
Calculate flow conductivities

con'd ...

... con'd

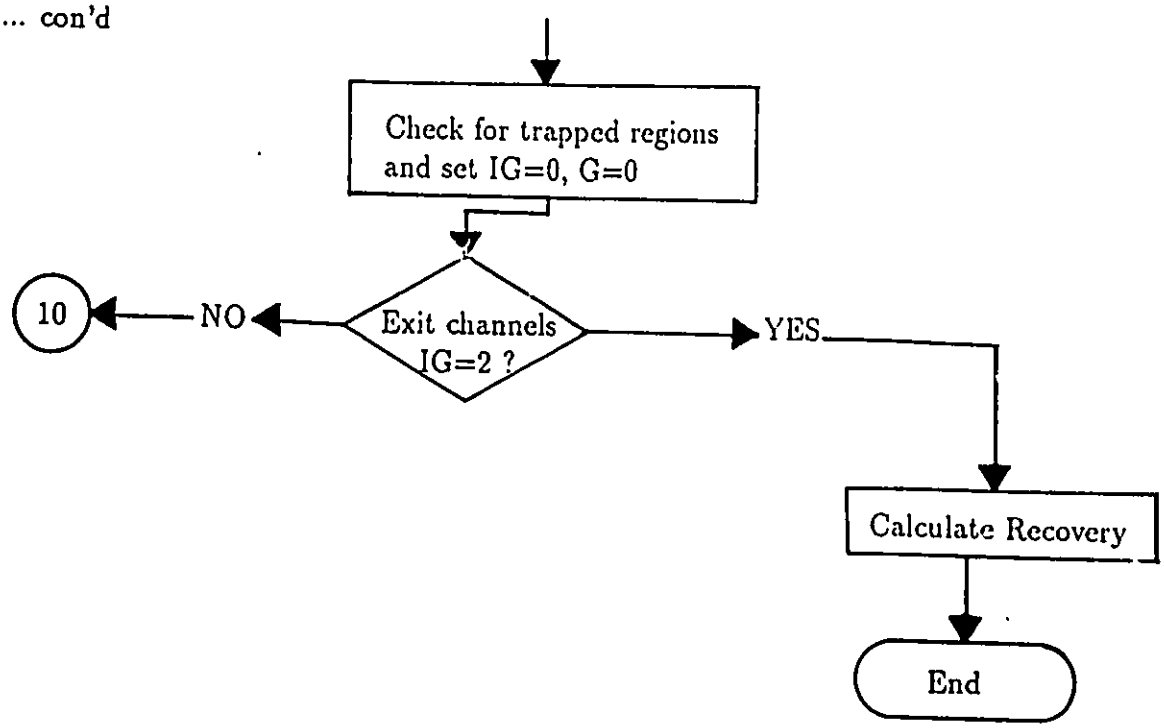
Check for trapped regions
and set IG=0, G=0
Exit channels
IG=2 ?
NO
10
YES
Calculate Recovery
End

Chapter 4

RESULTS AND DISCUSSION

This chapter presents simulations of flow in porous media and an extensive comparison of the present approaches with previous attempts at modelling two-fluid immiscible displacement flow in porous media.

4.1 Results of the Simulations

4.1.1 Monophasic Flow - Permeability

The deterministic algorithm is used in order to study monophasic flow in a porous medium and to calculate the permeability of the porous medium as it has been described in Section 3.3. The permeability of the porous medium is calculated as a function of the average channel radius, r_o, and the dispersion, λ, of the uniform size distribution of the channel radii. For these calculations a network of size 50×50 is used and the permeability of the network, κ, is determined from Equation (3.33) after solving for the pressure field in the network.

The permeability of the network, κ, is presented as a function of the average channel radius, r_o, and the dispersion, λ, in Figures 4.1 and 4.2, respectively. From Figure

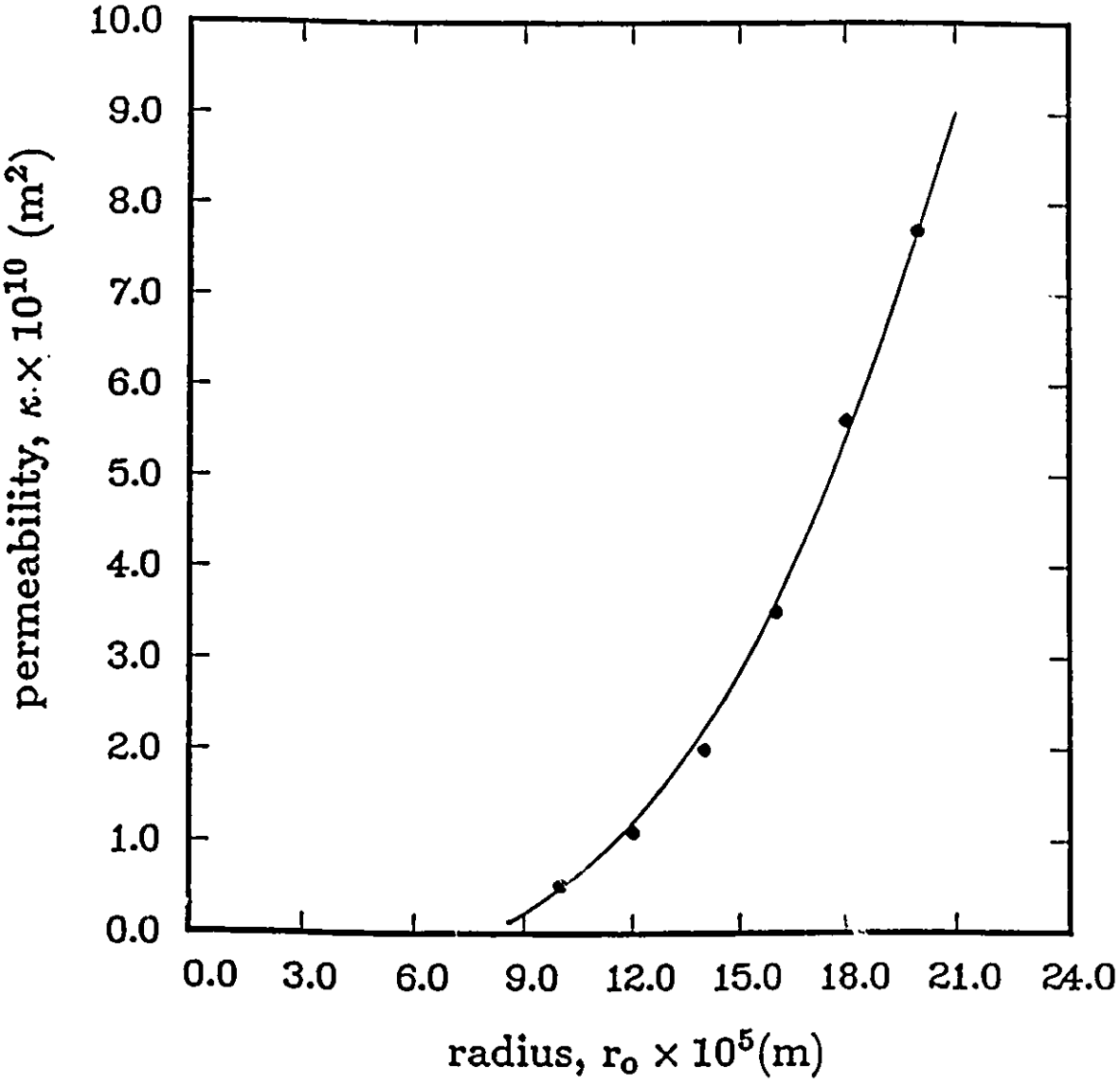

Figure 4.1: The permeability, κ, of a network of interconnected capillaries as a function of the average channel radius, r_c, for dispersion, λ=0.5.

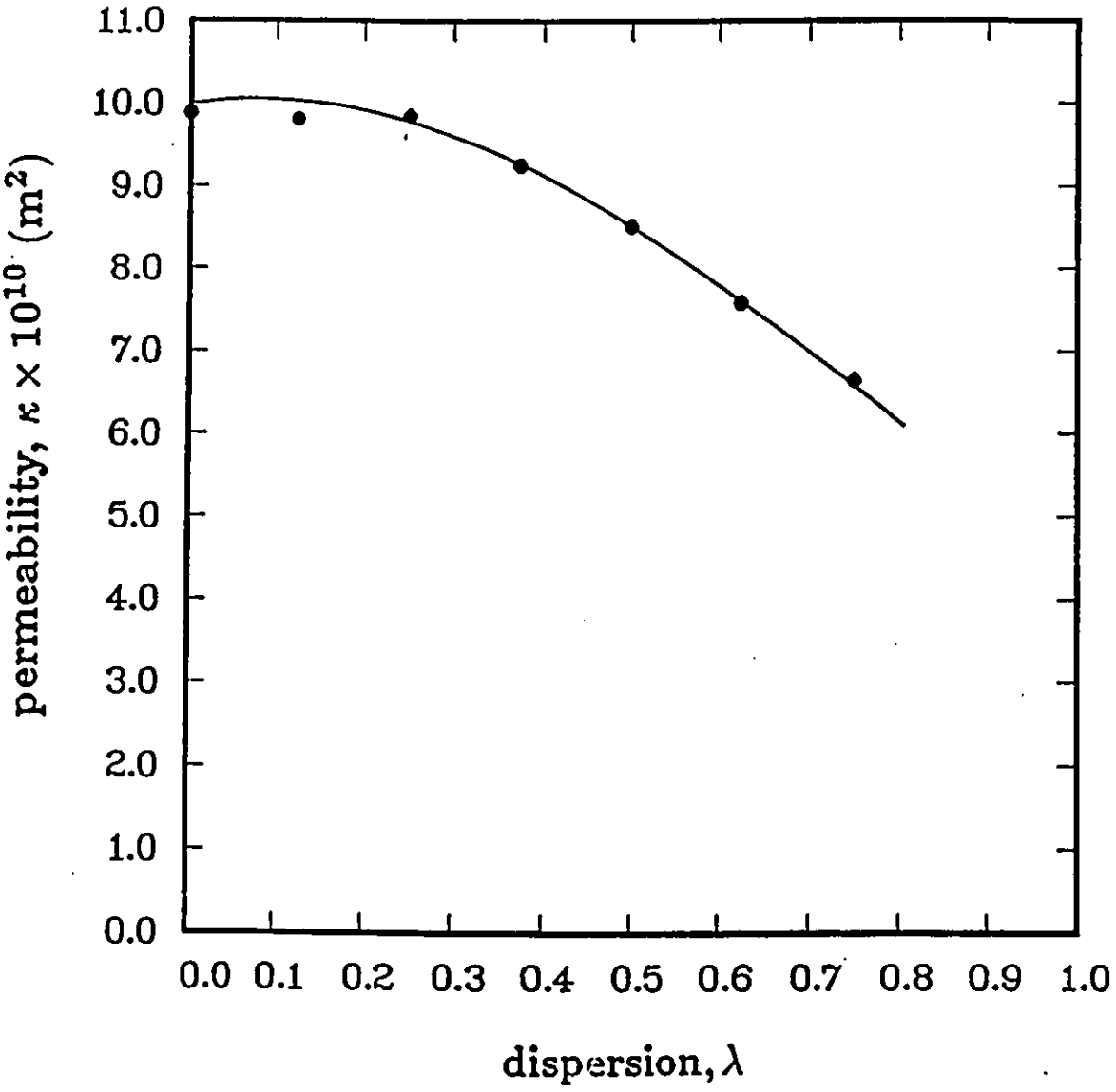

Figure 4.2: The permeability, κ, of a network of interconnected capillaries as a function of the dispersion, λ, for $r_o = 2.0 \times 10^{-4}$m.

4.1 it is observed that the permeability of the network increases almost linearly for $r_o > 10^{-4}$m, while for lower values of r_o the increase is more gradual. From Figure 4.2 it is observed that the local anisotropy of the network, expressed in terms of the dispersion, results in a decrease of the permeability.

4.1.2 Validity of the Algorithms

Numerical results of the simulations are compared with the numerical and experimental results of Lenormand et al. (1988) in order to test the validity of the algorithms.

A network of 100x100 is used, similar to that used by Lenormand et al. (1988). The radii of the channels are chosen from a uniform size distribution $[(1-\lambda)r_o, (1+\lambda)r_o]$ with $r_o = 2.3 \times 10^{-4}m$ and λ= 0.56. Three cases are considered: (a) the transition from DLA to capillary fingering, (b) the transition from plug flow to capillary fingering, and (c) the transition from DLA to plug flow.

Using the stochastic algorithm simulations were repeated 4-6 times for each set of data by using a different random seed number. Simulations by the time-consuming deterministic algorithm were performed only once for each set of data. Results of the simulations by using the stochastic algorithm are presented in Tables 4.1 and 4.2 and sample runs in Figures 4.3-4.6. Figure 4.6 shows a sample run in the capillary region at different stages of the simulation.

Results of the simulations by using the deterministic algorithm are presented in Tables 4.3 and 4.4 and sample runs in Figures 4.7-4.11. Figures 4.10 and 4.11

Table 4.1: Results of the Simulations (Stochastic Algorithm)

Figure	M	N_{Ca}	E	D_f
4.3a	2.0×10^{-5}	5.0×10^{-6}	0.15-0.18	1.53-1.57
4.3b	2.0×10^{-5}	5.0×10^{-7}	0.17-0.19	1.55-1.58
4.3c	2.0×10^{-5}	1.0×10^{-7}	0.18-0.20	1.58-1.62
4.3d	2.0×10^{-5}	1.0×10^{-8}	0.20-0.23	1.61-1.65
4.3e	2.0×10^{-5}	5.0×10^{-9}	0.25-0.31	1.67-1.73
4.3f	2.0×10^{-5}	1.0×10^{-9}	0.26-0.37	1.72-1.77
4.4a	5.0	3.0×10^{-1}	0.91-0.93	1.94-1.95
4.4b	5.0	3.0×10^{-3}	0.89-0.91	1.93-1.94
4.4c	5.0	5.0×10^{-5}	0.78-0.80	1.87-1.90
4.4d	5.0	1.0×10^{-5}	0.71-0.74	1.84-1.86
4.4e	5.0	2.0×10^{-6}	0.43-0.52	1.77-1.81
4.4f	5.0	2.0×10^{-7}	0.26-0.37	1.72-1.77

Table 4.2: Results of the Simulations (Stochastic Algorithm)

Figure	N_{Ca}	M	E
4.5a	1.0	2.0×10^{-5}	0.15-0.18
4.5b	1.0	2.0×10^{-3}	0.15-0.18
4.5c	1.0	2.0×10^{-2}	0.20-0.22
4.5d	1.0	1.0×10^{-1}	0.27-0.35
4.5e	1.0	1.0	0.45-0.55
4.5f	1.0	10.0	0.91-0.94

present two sample runs in the DLA and viscous fingering regions, respectively, at different time steps.

The sample runs in Figures 4.3 and 4.4 and Figures 4.7 and 4.8 are at almost identical conditions in terms of the capillary number, N_{Ca}, and the viscosity ratio, M, as those of Lenormand et al. (1988) in Figures 4.12-4.14. A visual comparison immediately reveals a good qualitative agreement. The sweep efficiency (fraction of pores invaded by the displacing, non-wetting fluid) is plotted against the capillary number and the viscosity ratio in Figures 4.15-4.17.

In Figure 4.15 the sweep efficiency starts from a plateau at high values of the capillary number and approaches another plateau at low values of the capillary number. The agreement of these predictions with experiments is good. However, the deterministic algorithm predicts a lower plateau for the sweep efficiency in the capillary region. At high values of the capillary number the fingers grow towards the exit with very little growth in other directions, i.e. backwards (Figure 4.7a). At lower values of the capillary number side-branches are formed and even grow backwards as a result of the action of the interfacial tension (Figures 4.7c,d and Figures 4.3c,d). In some cases, small regions of oil become trapped as a result of the finger growth. However, these regions are of the pore scale. In this region viscous and capillary forces are comparable and the flow pattern of the invading fluid is a result of the interplay of these forces. Finally at very low values of the capillary number (Figures 4.3f, 4.7f), capillary forces become dominant and the motion of the interface is a result of the local anisotropy and microstructure of the porous medium. Fingers grow in all directions leading to large trapped regions of

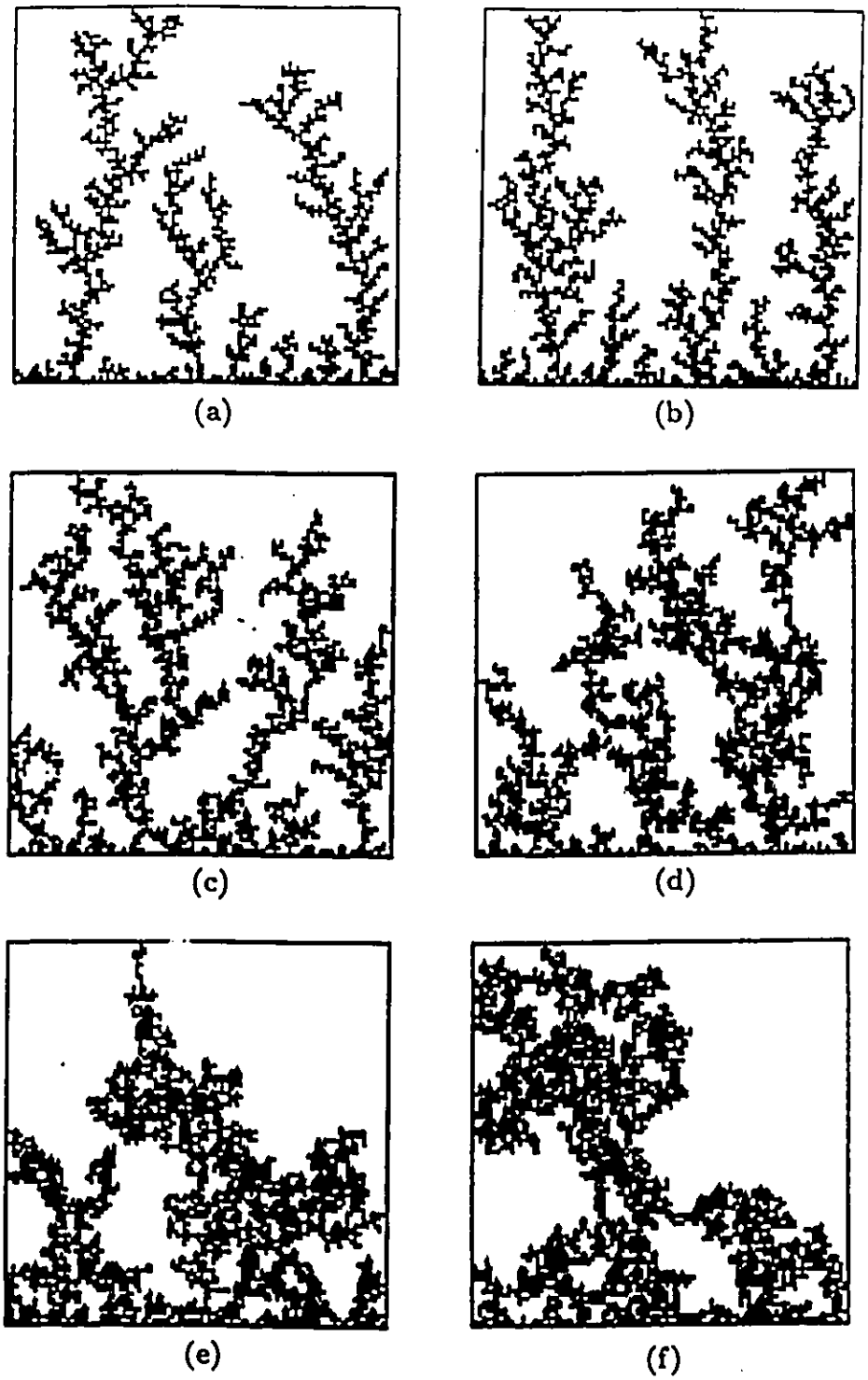

Figure 4.3: Stochastic simulations of immiscible displacement of a wetting fluid (white) by a non-wetting fluid (black) at $M = 2.0 \times 10^{-5}$ for: (a) $N_{Ca} = 5.0 \times 10^{-6}$. (b) $N_{Ca} = 5.0 \times 10^{-7}$, (c) $N_{Ca} = 1.0 \times 10^{-7}$, (d) $N_{Ca} = 1.0 \times 10^{-8}$, (e) $N_{Ca} = 5.0 \times 10^{-9}$. (f) $N_{Ca} = 1.0 \times 10^{-9}$.

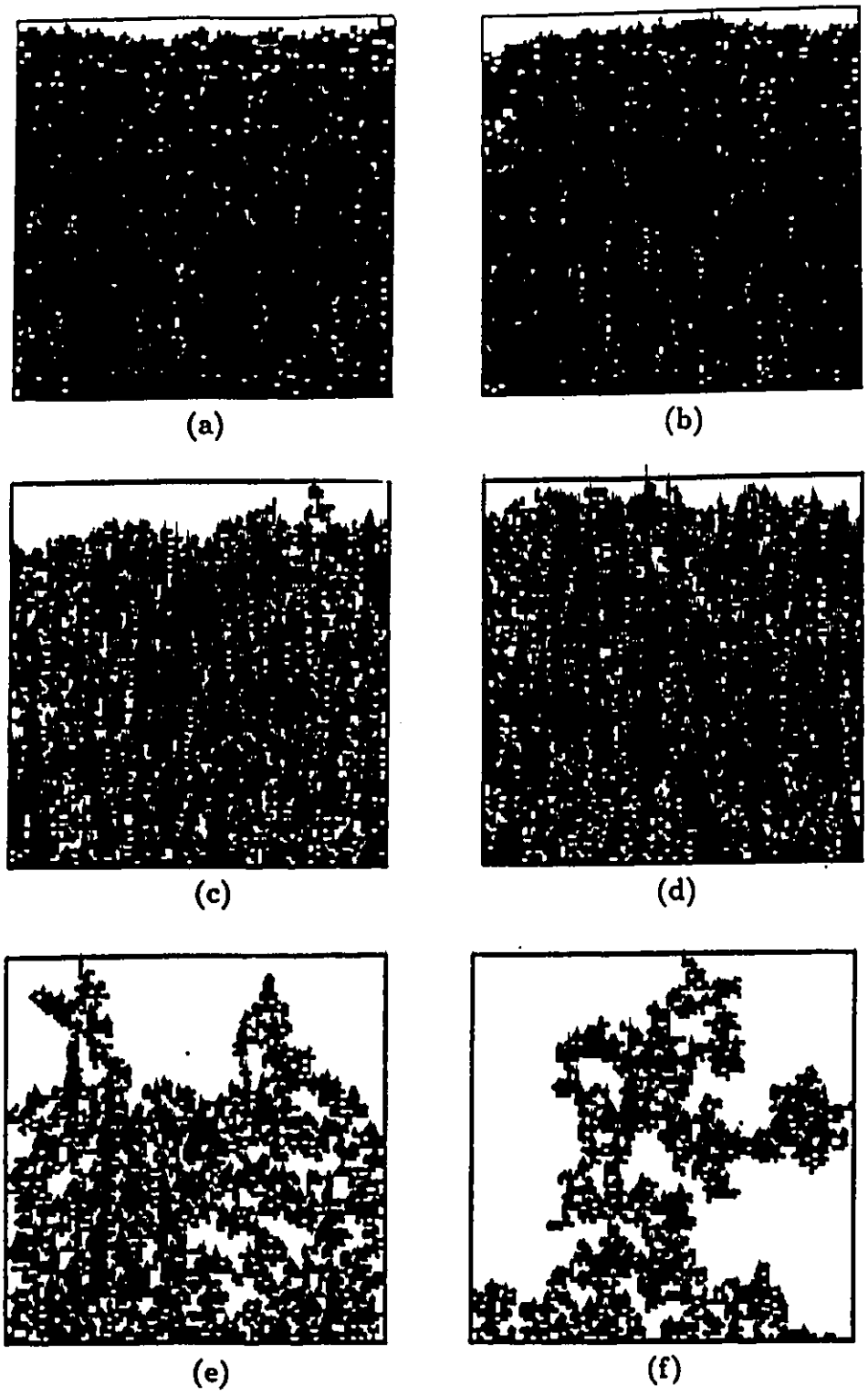

Figure 4.4: Stochastic simulations of immiscible displacement of a wetting fluid (white) by a non-wetting fluid (black) at M=5.0 for: (a) $N_{Ca} = 3.0 \times 10^{-1}$. (b) $N_{Ca} = 3.0 \times 10^{-3}$, (c) $N_{Ca} = 5.0 \times 10^{-5}$, (d) $N_{Ca} = 1.0 \times 10^{-5}$, (e) $N_{Ca} = 2.0 \times 10^{-6}$. (f) $N_{Ca} = 2.0 \times 10^{-7}$.

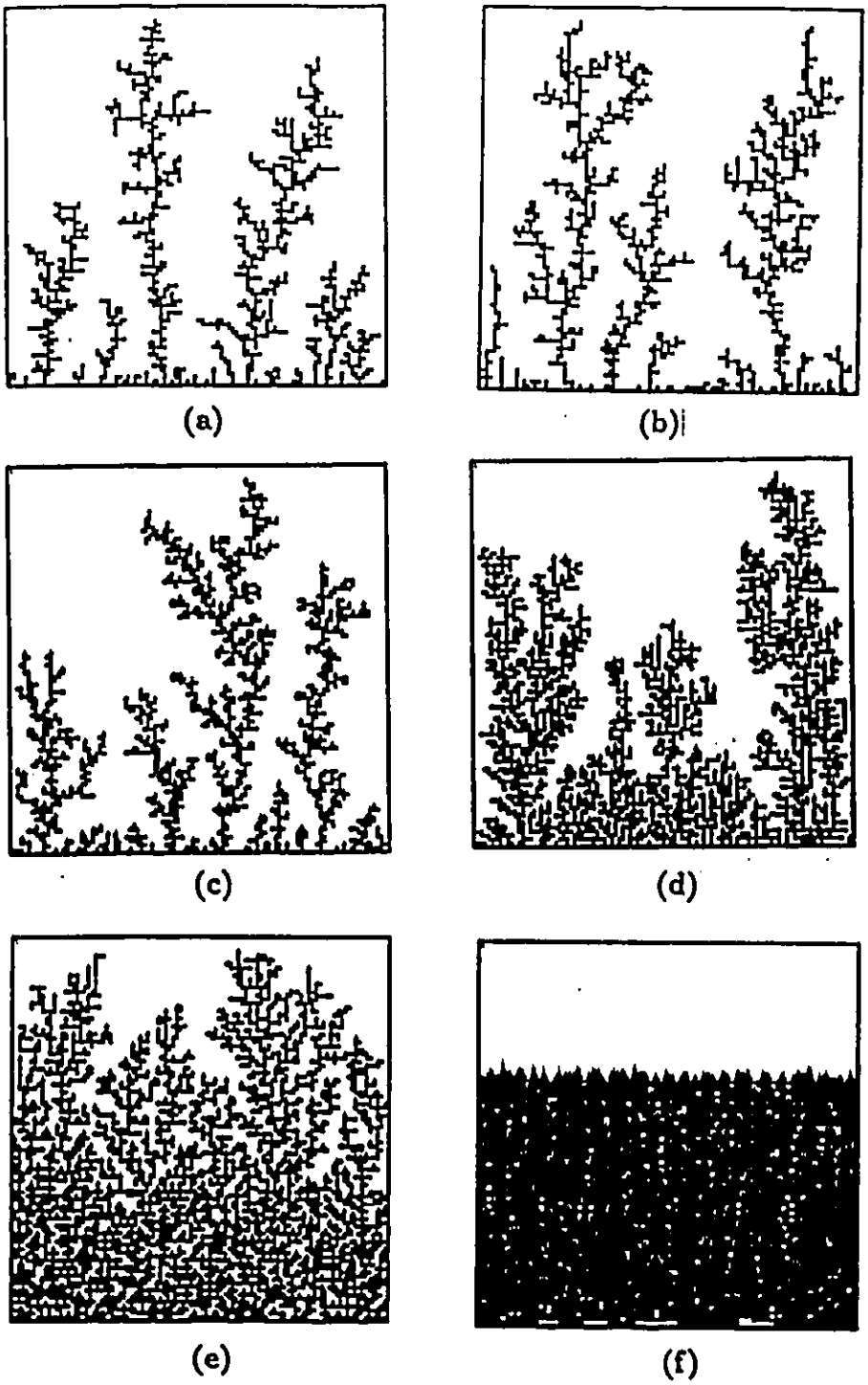

Figure 4.5: Stochastic simulations of immiscible displacement of a wetting fluid (white) by a non-wetting fluid (black) at $N_{Ca} = 1.0$ for: (a) $M = 2.0 \times 10^{-5}$, (b) $M = 2.0 \times 10^{-3}$, (c) $M = 2.0 \times 10^{-2}$, (d) $M = 1.0 \times 10^{-1}$, (e) M=1.0, (f) M=10.0.

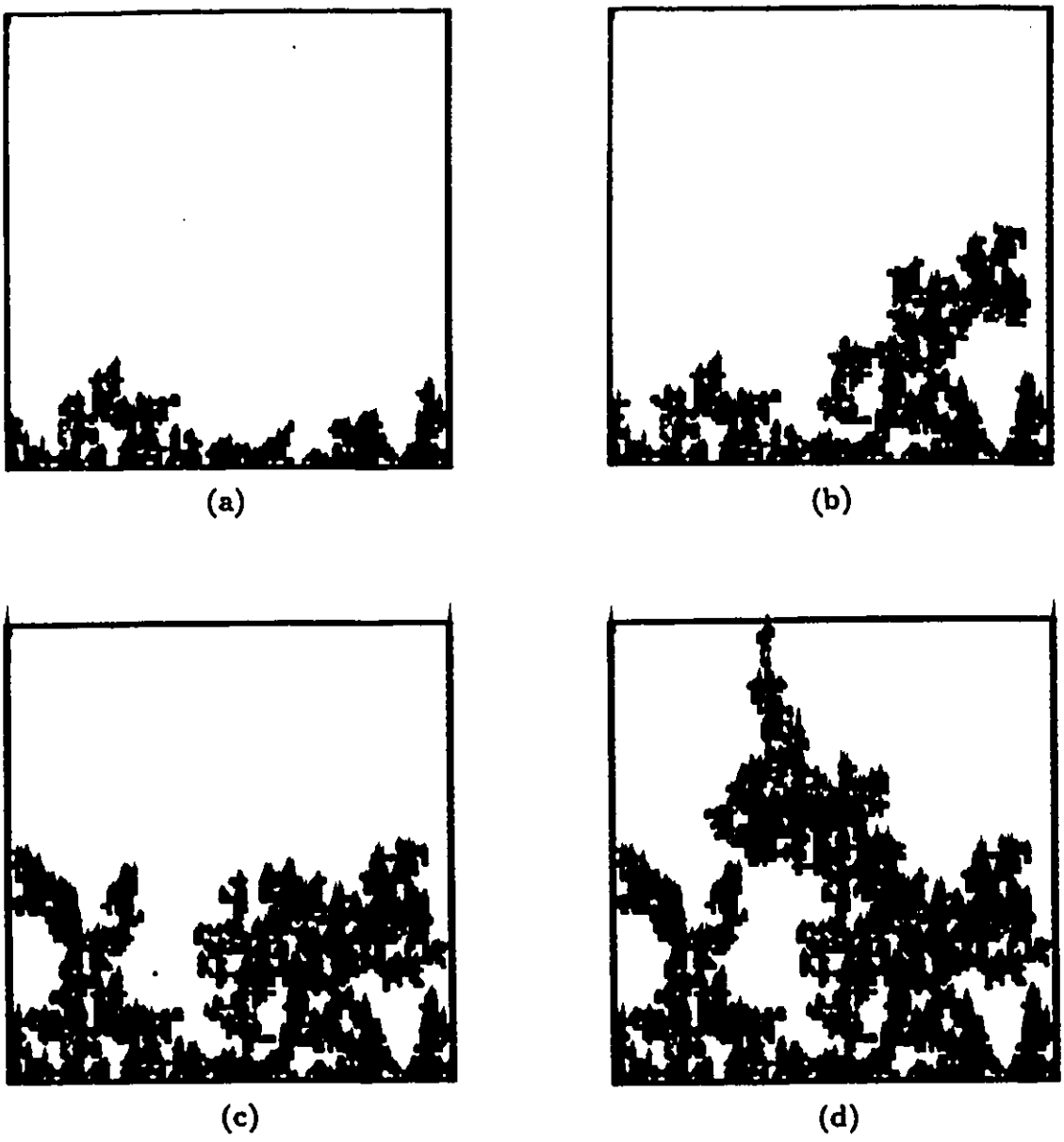

Figure 4.6: Stochastic simulations of capillary fingering (M=5.0, N_{Ca}=1.0×10^{-7}) at different stages: (a) 720 steps, (b) 1440 steps, (c) 2160 steps, (d) 2880 steps.

Table 4.3: Results of the Simulations (Deterministic Algorithm)

Figure	M	N_{Ca}	E
4.7a	2.0×10^{-5}	2.0×10^{-6}	0.15-0.16
4.7b	2.0×10^{-5}	7.0×10^{-7}	0.14-0.15
4.7c	2.0×10^{-5}	2.0×10^{-7}	0.17-0.18
4.7d	2.0×10^{-5}	3.0×10^{-8}	0.18-0.20
4.7e	2.0×10^{-5}	1.0×10^{-8}	0.20-0.22
4.7f	2.0×10^{-5}	1.0×10^{-9}	0.22-0.25
4.8a	5.0	3.0×10^{-1}	0.91-0.92
4.8b	5.0	3.0×10^{-3}	0.80-0.82
4.8c	5.0	5.0×10^{-5}	0.60-0.63
4.8d	5.0	5.0×10^{-6}	0.34-0.37
4.8e	5.0	7.0×10^{-7}	0.22-25
4.8f	5.0	7.0×10^{-8}	0.22-25

Table 4.4: Results of the Simulations (Deterministic Algorithm)

Figure	N_{Ca}	M	E
4.9a	1.0	2.0×10^{-5}	0.15-0.16
4.9b	1.0	1.0×10^{-2}	0.19-0.20
4.9c	1.0	1.0×10^{-1}	0.46-0.48
4.9d	1.0	1.0	0.77-0.78
4.9e	1.0	5.0	0.91-0.92
4.9f	1.0	80.0	0.91-0.92

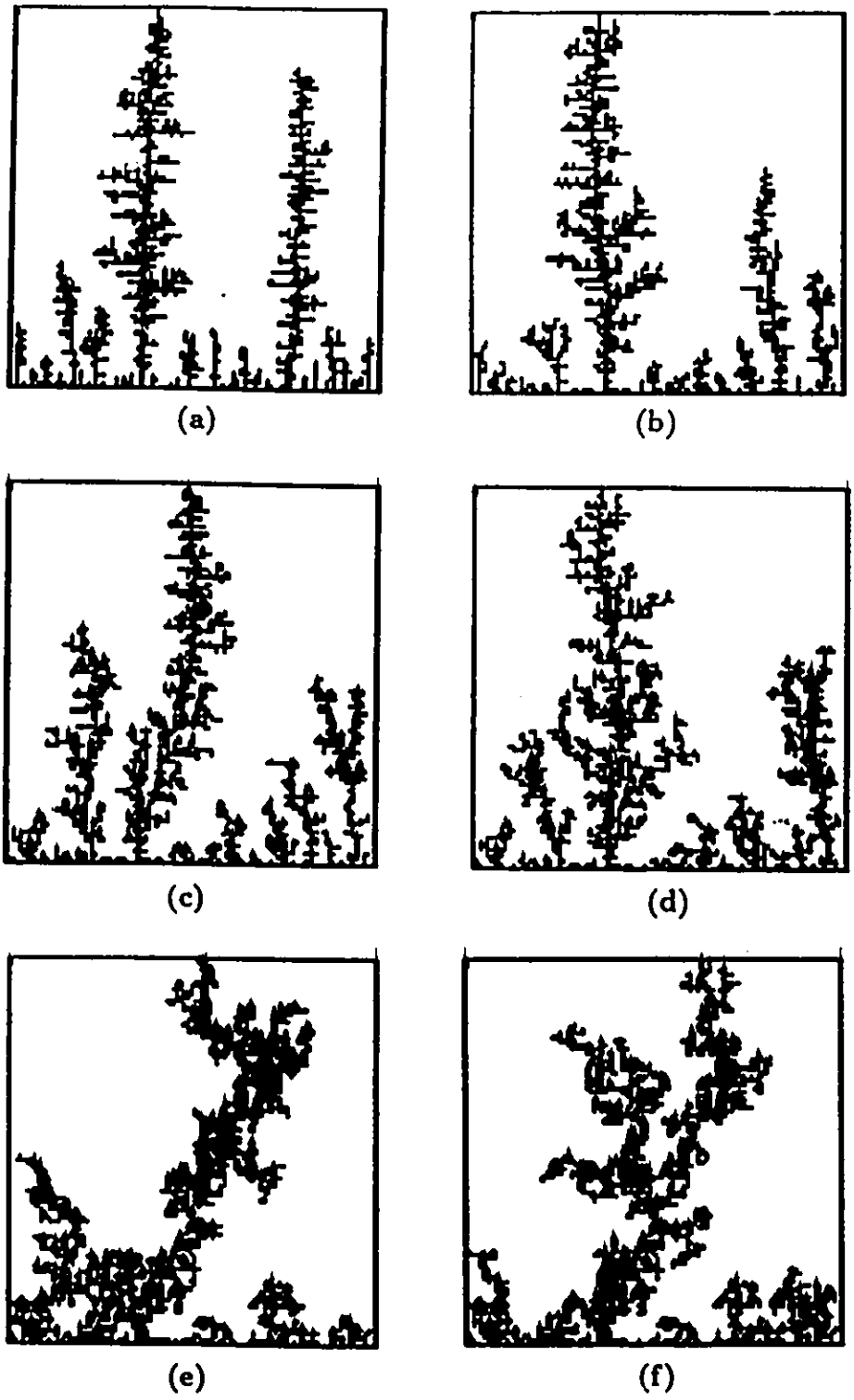

Figure 4.7: Deterministic simulations of immiscible displacement of a wetting fluid (white) by a non-wetting fluid (black) at $M = 2.0 \times 10^{-5}$ for: (a) $N_{Ca} = 7.0 \times 10^{-6}$. (b) $N_{Ca} = 7.0 \times 10^{-7}$. (c) $N_{Ca} = 2.0 \times 10^{-7}$, (d) $N_{Ca} = 3.0 \times 10^{-6}$. (e) $N_{Ca} = 1.0 \times 10^{-8}$. (f) $N_{Ca} = 1.0 \times 10^{-9}$.

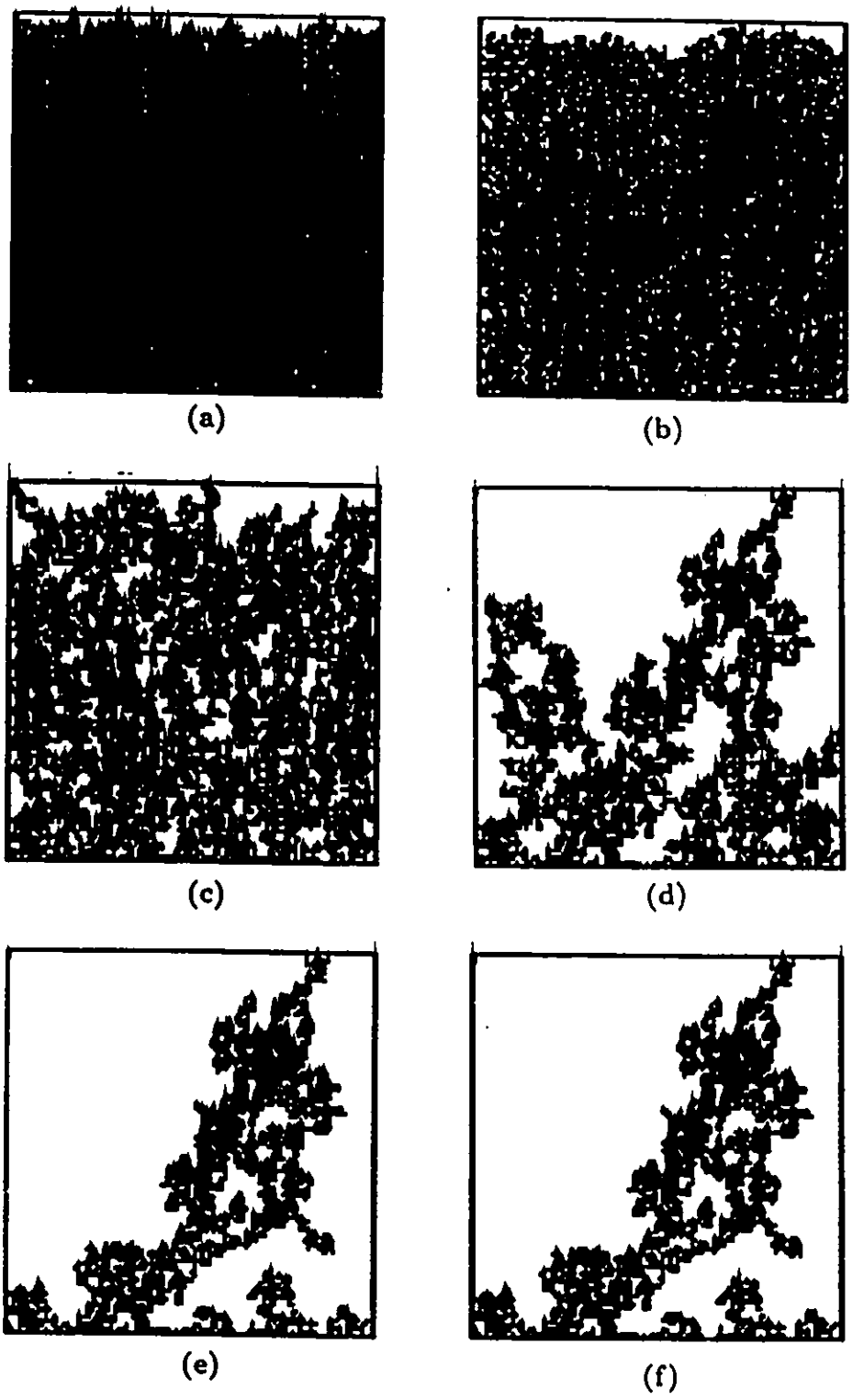

Figure 4.8: Deterministic simulations of immiscible displacement of a wetting fluid (white) by a non-wetting fluid (black) at M=5.0 for: (a) $N_{Ca} = 3.0 \times 10^{-1}$, (b) $N_{Ca} = 3.0 \times 10^{-3}$, (c) $N_{Ca} = 5.0 \times 10^{-5}$, (d) $N_{Ca} = 5.0 \times 10^{-6}$, (e, $N_{Ca} = 7.0 \times 10^{-7}$, (f) $N_{Ca} = 7.0 \times 10^{-8}$.

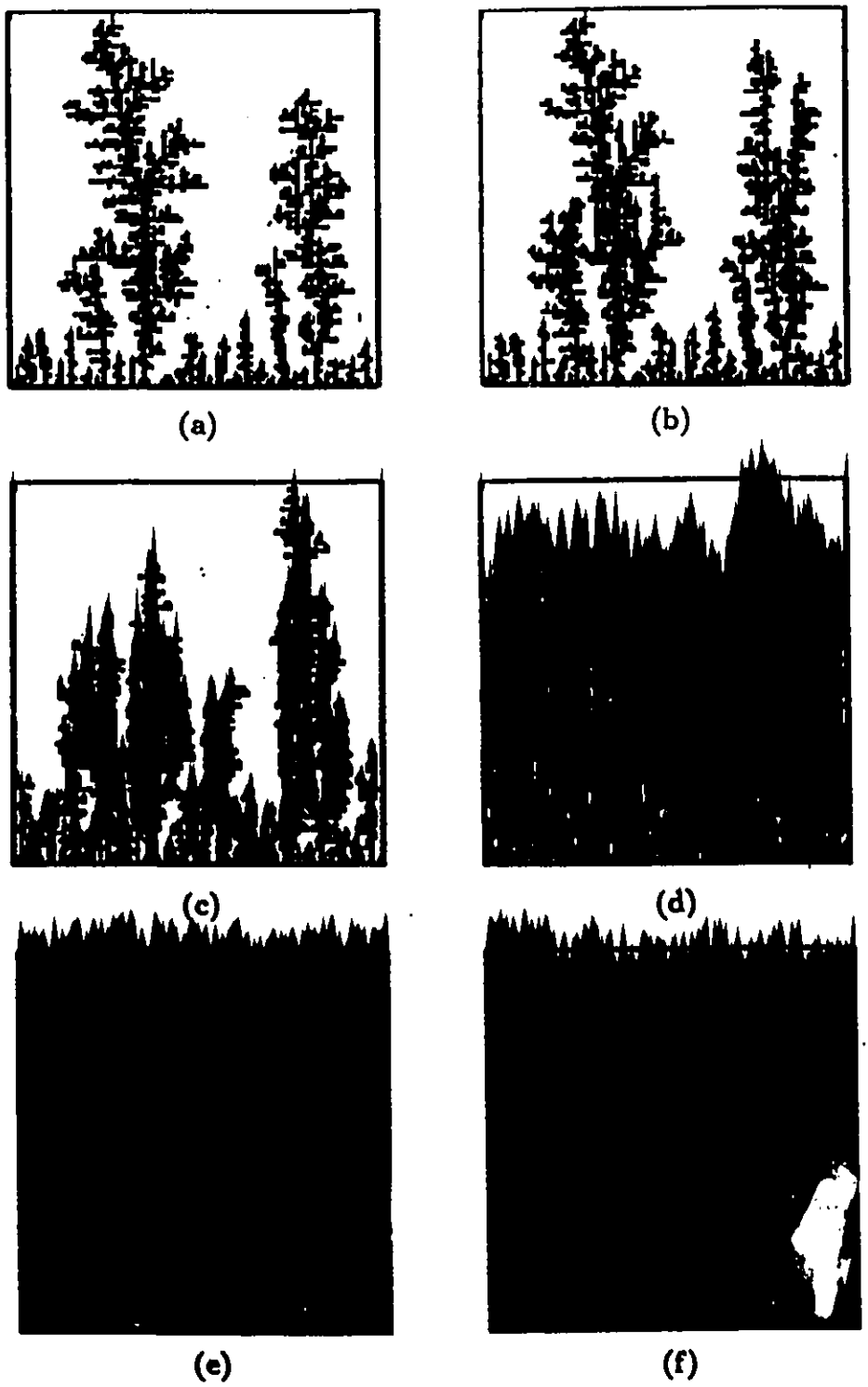

Figure 4.9: Deterministic simulations of immiscible displacement of a wetting fluid (white) by a non-wetting fluid (black) at $N_{Ca} = 1.0$ for: (a) $M = 2.0 \times 10^{-5}$, (b) $M = 1.0 \times 10^{-2}$, (c) $M = 1.0 \times 10^{-1}$, (d) M=1.0. (e) M=5.0. (f) M=80.0.

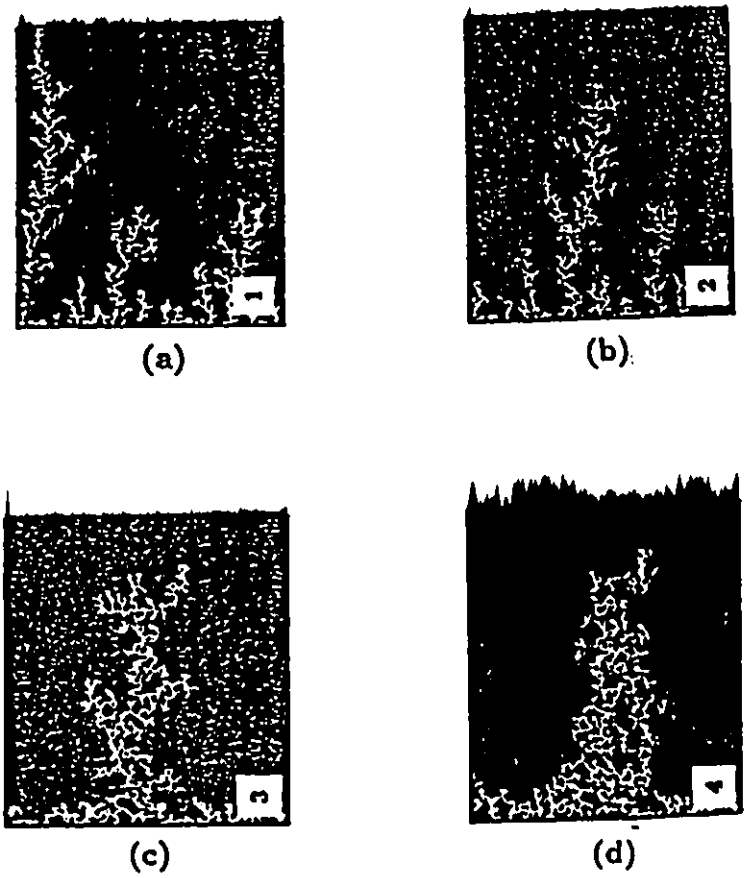

Figure 4.10: Experimental results (Lenormand et al. 1988) of immiscible displacement of a wetting fluid (black) by a non-wetting fluid (white) at $M = 2.0 \times 10^{-5}$ for: (a) $N_{Ca} = 5.0 \times 10^{-7}$, (b) $N_{Ca} = 2.0 \times 10^{-7}$, (c) $N_{Ca} = 2.0 \times 10^{-8}$, (d) $N_{Ca} = 2.0 \times 10^{-9}$.

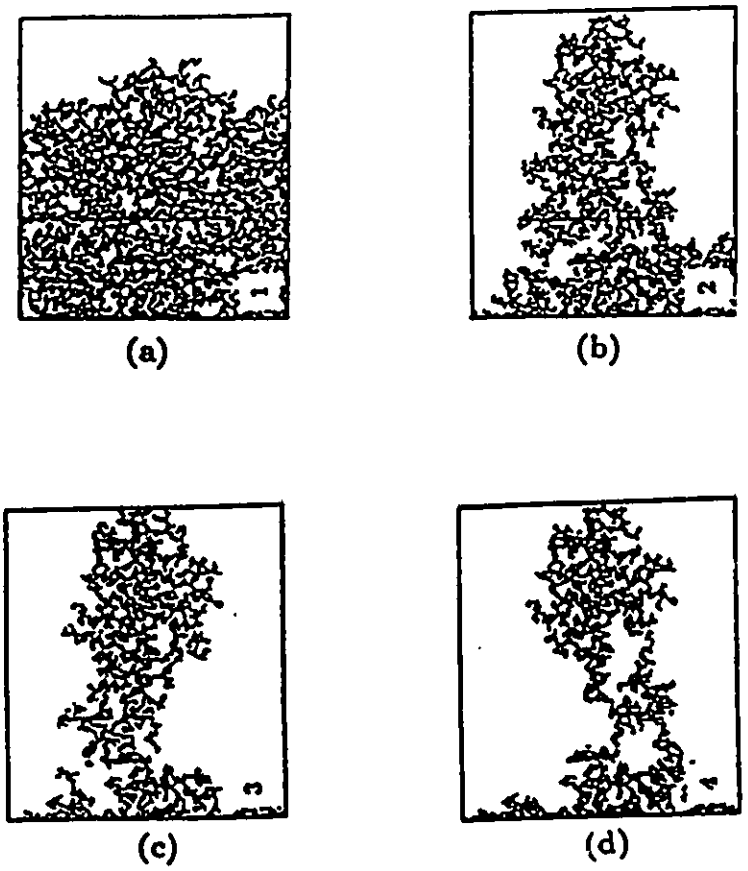

Figure 4.11: Experimental results (Lenormand et al. 1988) of immiscible displacement of a wetting fluid (white) by a non-wetting fluid (black) at M=5.0 for: (a) $N_{Ca} = 1.0 \times 10^{-1}$, (b) $N_{Ca} = 7.0 \times 10^{-7}$, (c) $N_{Ca} = 2.0 \times 10^{-8}$, (d) $N_{Ca} = 2.0 \times 10^{-9}$.

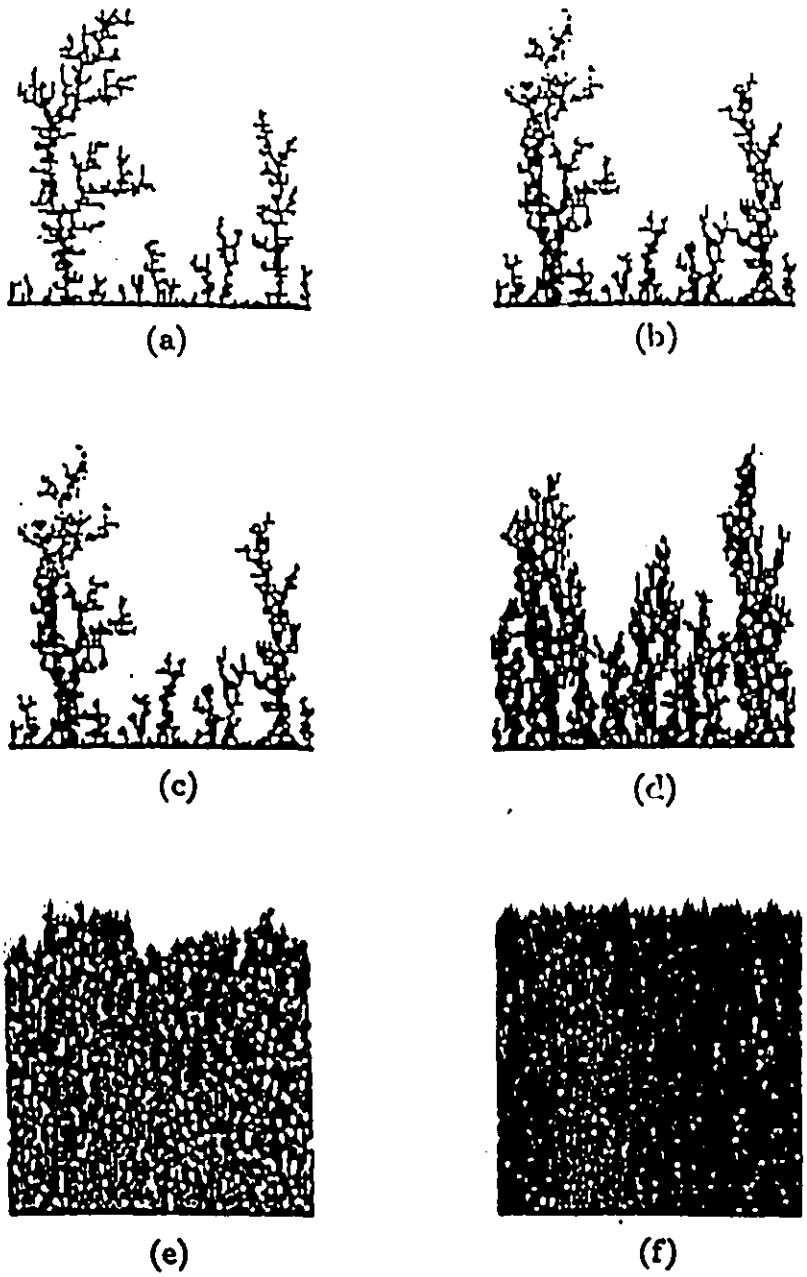

Figure 4.12: Deterministic simulations (Lenormand et al. 1988) of immiscible displacement of a wetting fluid (white) by a non-wetting fluid (black) at $N_{Ca} = 1.0$ for: (a) $M = 1.0 \times 10^{-4}$, (b) $M = 1.0 \times 10^{-3}$, (c) $M = 2.0 \times 10^{-2}$, (d) $M = 1.0 \times 10^{-1}$, (e) M=1.0, (f) M=100.0.

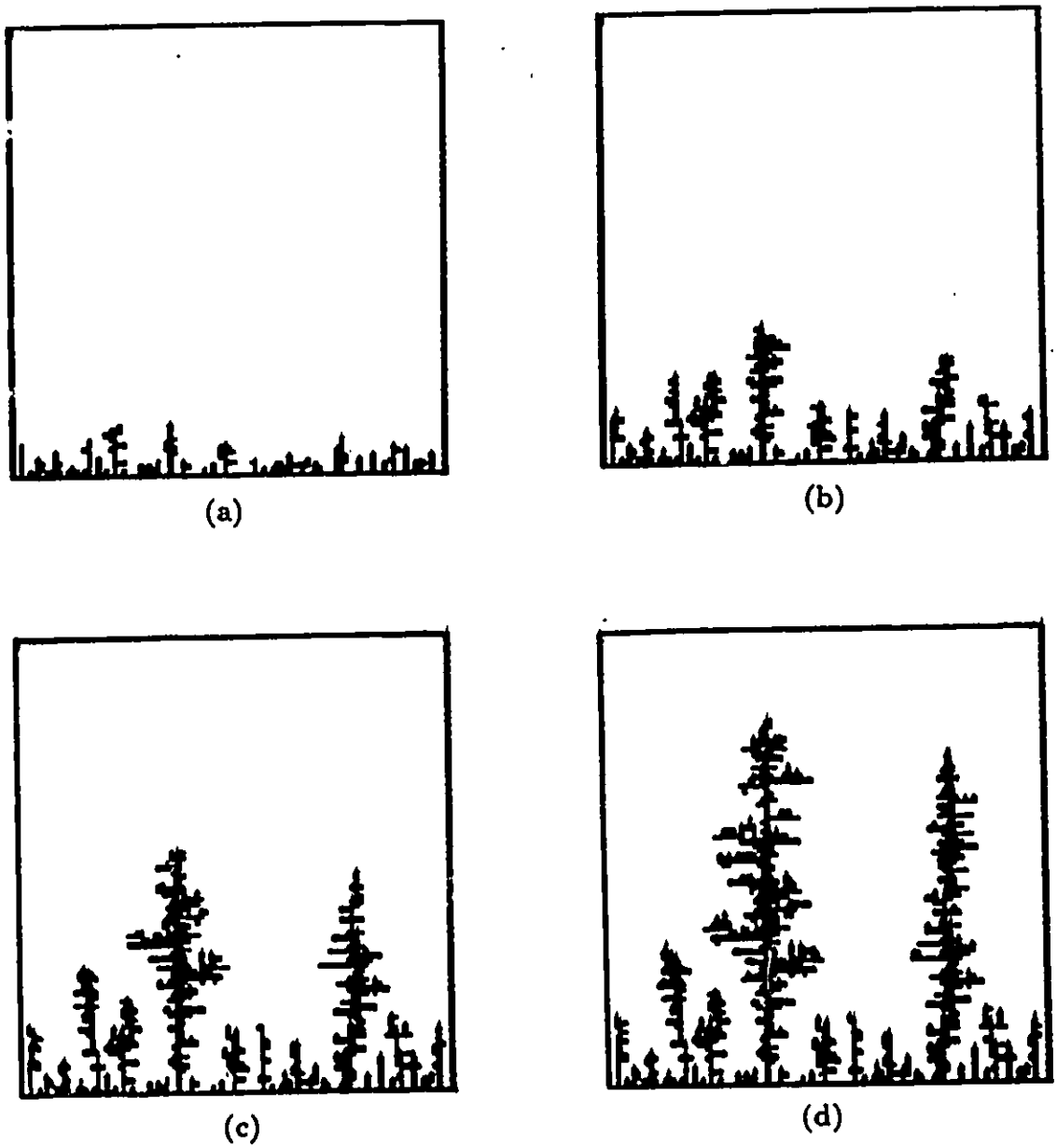

Figure 4.13: Deterministic simulations of DLA (M=2.0 $\times 10^{-5}$, N_{Ca}=7.0 $\times 10^{-6}$) at different stages: (a) 420 steps, (b) 840 steps, (c) 1260 steps, (d) 1600 steps.

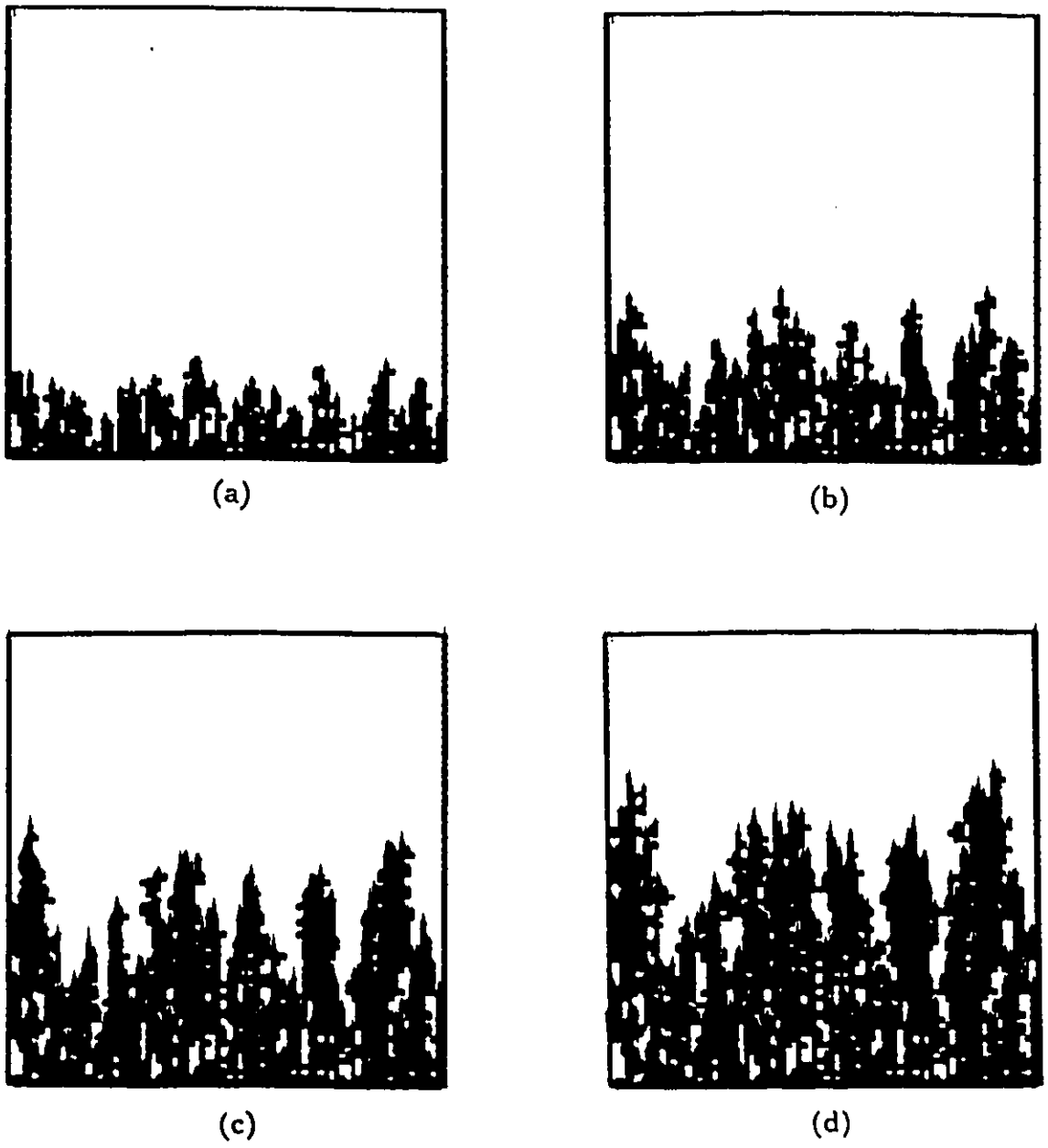

Figure 4.14: Deterministic simulations of viscous fingering (M=0.5, N_{Ca}=1.0 $\times 10^{-3}$) at different stages: (a) 720 steps, (b) 1440 steps, (c) 2160 steps, (d) 2800 steps.

the displaced fluid.

In Figure 4.16 the sweep efficiency starts from a plateau at low values of the capillary number and approaches another plateau at high values of the capillary number. The agreement is good although the deterministic algorithm underestimates the sweep efficiency beyond the capillary limit ($N_{Ca} \approx 10^{-5}$). At high values of the capillary number trapping of the displaced fluid occurs at the pore level as a result of the growth of small perturbations due to the local anisotropy of the network. At lower values of the capillary number (Figures 4.4c-e and 4.8b-c) capillary forces become significant and motion of the interface results in trapping of the displaced phase and lowering of the sweep efficiency. Finally, in the capillary region motion of the interface is controlled and determined by capillary forces.

In Figure 4.17 the sweep efficiency is plotted against the viscosity ratio. Again the sweep efficiency starts from a low plateau corresponding to the DLA limit and approaches another plateau corresponding to the plug flow region. From Figure 4.5 it is apparent that the stochastic model fails to successfully predict the behaviour of the invading fluid at viscosity ratios close to the instability limit (M=1) due to the noise involved in the simulations. This point is further discussed in Section 4.2. On the other hand, the deterministic algorithm successfully predicts this region and the results are in good agreement with those of Lenormand et al. (1988) (Figure 4.14).

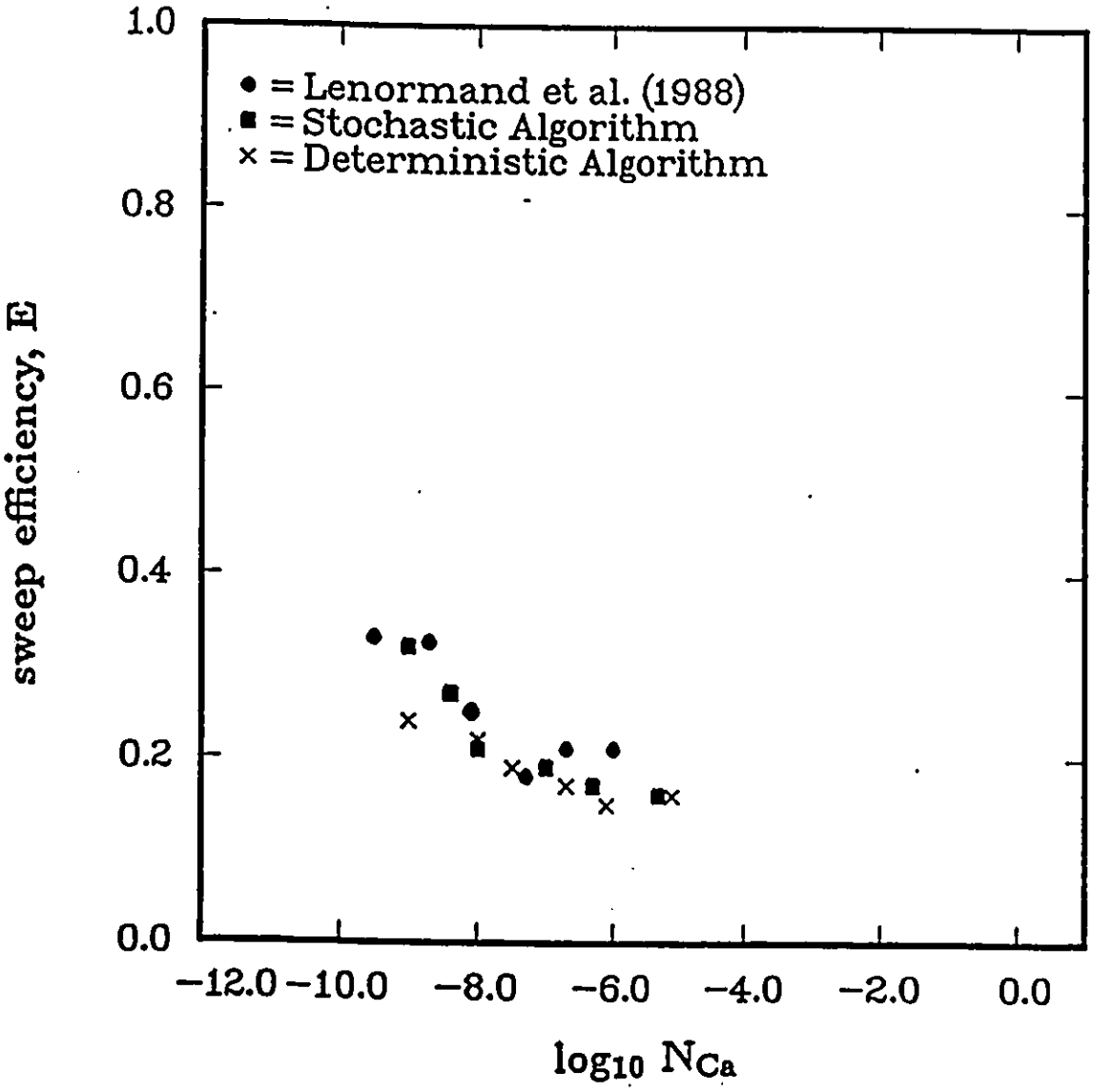

Figure 4.15: The sweep efficiency, E, of the displacement as a function of the logarithm of the capillary number, $log_{10}N_{Ca}$, for $M = 2.0 \times 10^{-5}$. The results available in the literature (Lenormand et al. 1988) are numerical results tested against physical experiments (Figure 4.10).

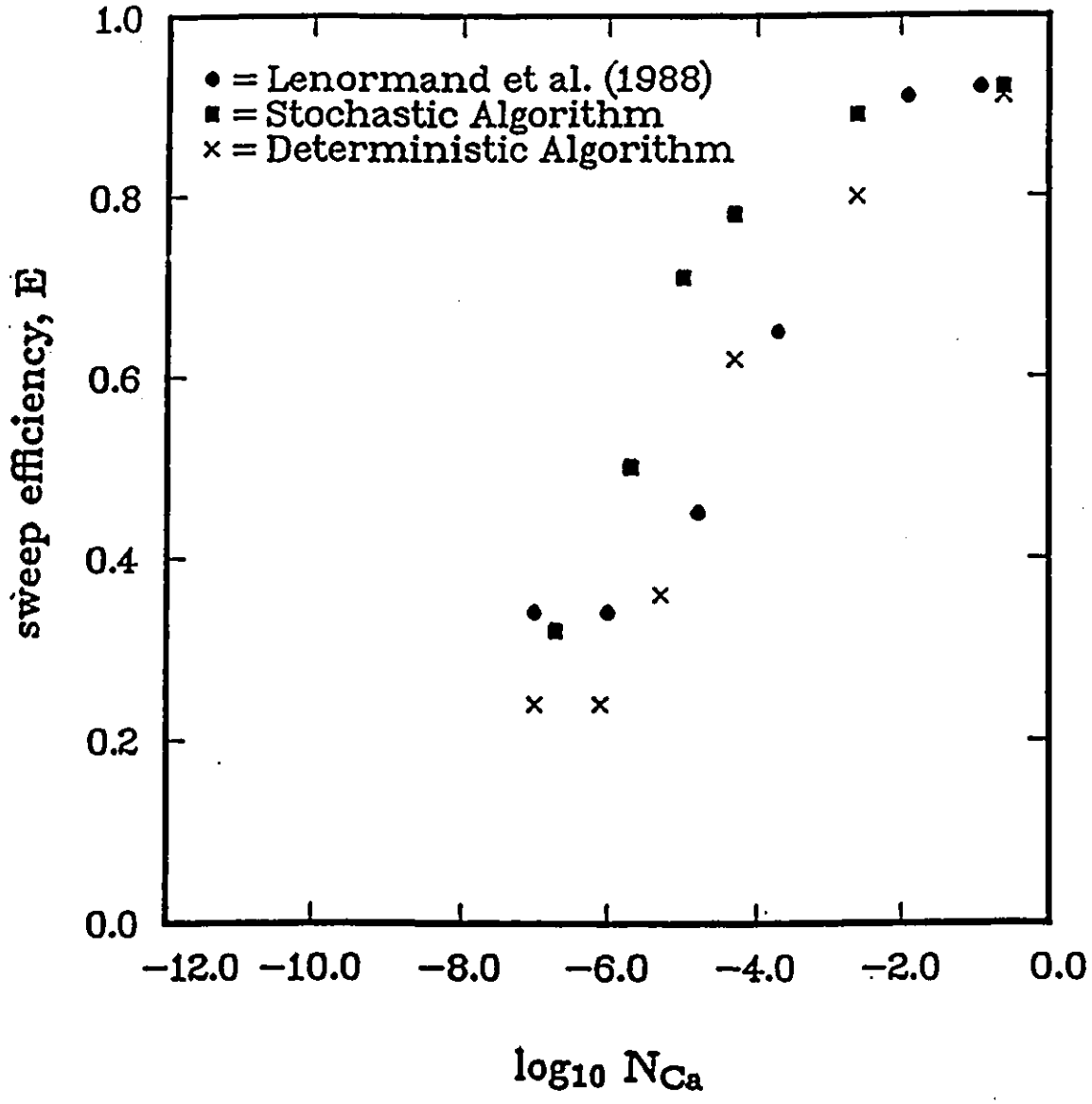

Figure 4.16: The sweep efficiency, E, of the displacement as a function of the logarithm of the capillary number, $log_{10}N_{Ca}$, for M=5.0. The results available in the literature (Lenormand et al. 1988) are numerical results tested against physical experiments (Figure 4.11).

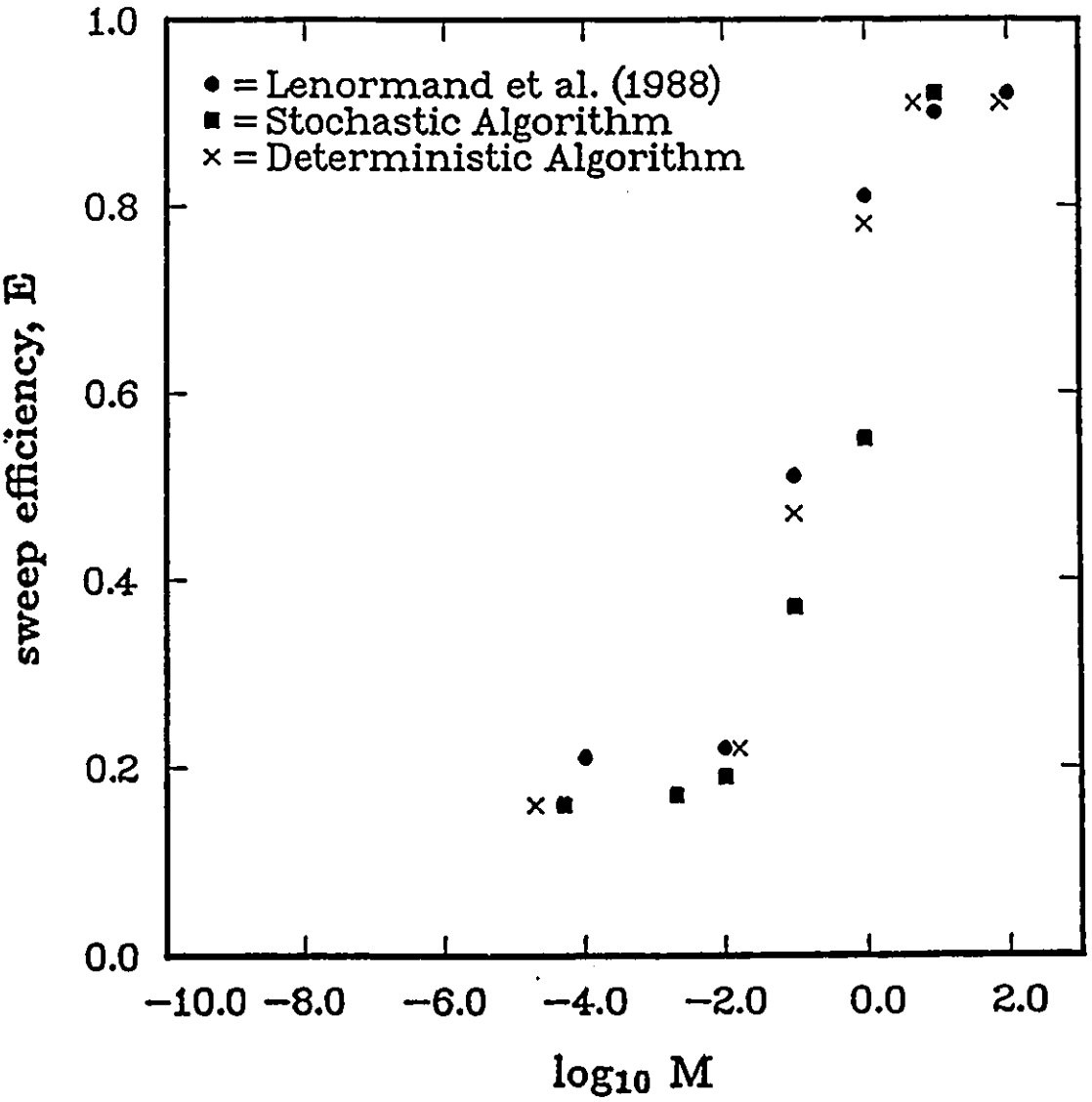

Figure 4.17: The sweep efficiency, E, of the displacement as a function of the logarithm of the viscosity ratio, $log_{10}M$, for $N_{Ca} = 1.0$. The results available in the literature (Lenormand et al. 1988) are numerical results tested against physical experiments.

4.1.3 Fractals - Fractal Dimension of the Invading Cluster

The notion of fractals was introduced in Section 2.1. In the present study the fractal dimension of the cluster of the invading phase is measured for different values of the capillary number and the viscosity ratio. Numerical results from the stochastic algorithm have been analyzed to calculate the fractal dimension. Ranges of the values of the fractal dimension are given in Table 4.1.

A technique suggested by Witten and Sander (1979) is used. According to this technique, squares of different sizes, r_f, are centered on each site of the cluster of the invading fluid and the number of the cluster sites, n, within the squares are counted. Then, the number of sites, n, for each square of size r is averaged over all sites of the cluster. The log_{10} of the average number of cluster sites, n, within each square of size r_f is plotted against $log_{10}r_f$. If the cluster is a fractal, then according to Equation 2.11, one expects the sets of data $(log_{10}n, log_{10}r_f)$ to fit to a straight line with a slope equal to the fractal dimension, D_f. Figures 4.18,19 present typical plots which determine the fractal dimension of the invading cluster. These plots show that the fractal dimension increases with decreasing capillary numbers at a low viscosity ratio, while the opposite is observed at a high viscosity ratio. This is expected since the fractal dimension is a measure of the compactness of the invading cluster. However, the values of the fractal dimension in the DLA and the capillary regions are lower than those predicted by previous studies (Witten and Sander 1981, Lenormand and Zarcone 1985, Chandler et al. 1982, Wilkinson 1983 and others). In the case of DLA, the value predicted by several researchers, namely D_f=1.73,

corresponds to a radial geometry. In the case of invasion percolation, the value of the fractal dimension, D_f=1.82, was determined for a linear geometry and for permeable side-boundaries. The value of the fractal dimension D_f=1.82, found by Lenormand and Zarcone (1985), was determined by a different method from the method used in the present study. Their method was applied to physical experiments in etched networks with impermeable side-boundaries. However, this method is not accurate for linear geometries, as mentioned by the authors themselves. A similar behaviour is observed at a high value of the viscosity ratio.

In conclusion, the notion of fractals can be applied to describe the behaviour of the invading cluster in the porous medium as well as the heterogeneities which are always present in a porous medium (Lenormand and Zarcone 1989, Williams and Dawe 1986).

4.1.4 Effects of Capillary Forces on the Island Size Distribution

Typical simulations have been shown in Figures 4.3 and 4.4 for two particular viscosity ratios and for the range of capillary numbers presented in Table 4.1. When the viscosity of the displacing fluid is less than that of the displaced fluid (M=2×10^{-5}), then at high capillary numbers (Figures 4.3a,b) the fingers grow towards the exit and only a few small islands of displaced fluid are formed. At low capillary numbers, capillary forces become significant and the fingers grow all over resulting in more and larger islands of trapped displaced fluid as the capillary limit is reached (Figure 4.3f). On the other hand, at a high viscosity ratio (M=5) and at high

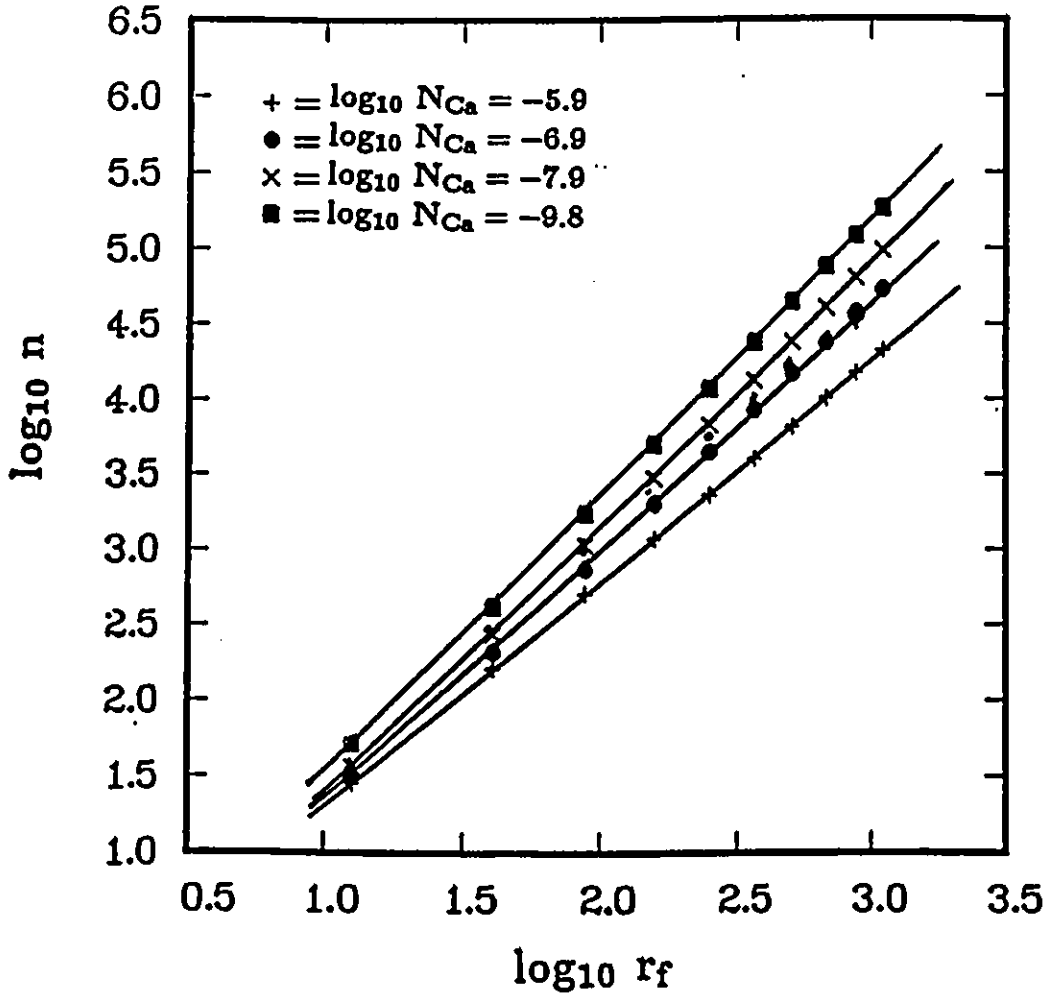

Figure 4.18: The logarithm of the number of cluster sites, $log_{10}n$, as a function of the logarithm of the square size, $log_{10}r_f$, for four different N_{Ca} values at a low viscosity ratio (M=1.0 $\times 10^{-4}$). The slope of each straight line is equal to the fractal dimension of the cluster.

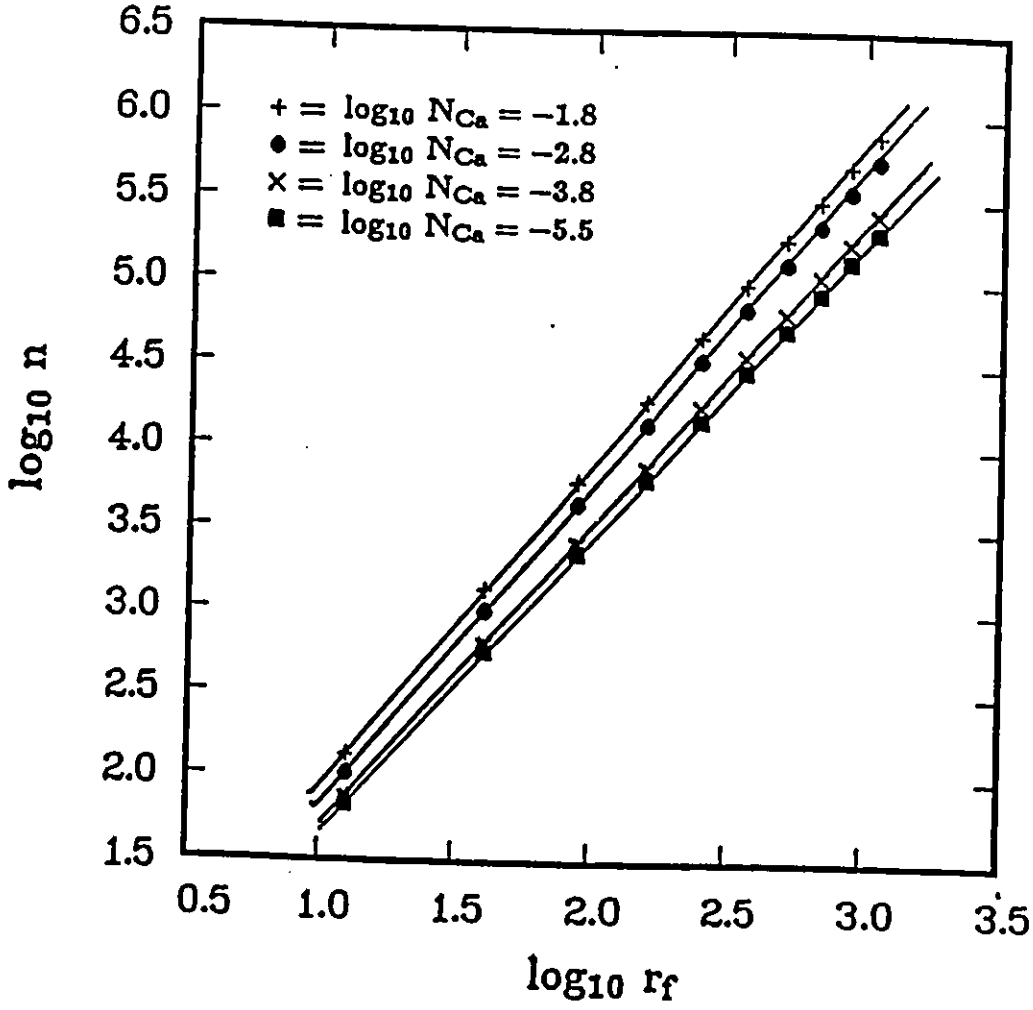

Figure 4.19: The logarithm of the number of cluster sites, $log_{10}n$, as a function of the logarithm of the square size, $log_{10}r_f$, for four different N_{Ca} values at a high viscosity ratio (M=10.0). The slope of each straight line is equal to the fractal dimension of the cluster.

capillary numbers the front is effectively flat and the instabilities are of the pore scale, resulting in a large number of islands of small size (Figure 4.4a,b). At lower capillary numbers (Figures 4.4c-f) the instabilities grow, resulting in fingers and islands of different sizes. The results presented in Table 4.1 in all cases represent the average of 4-6 simulations.

The number of islands of size s_p at the end of each run is represented by $n(s_p)$. The size of an island is characterized in terms of a number of pores (nodes). For evaluation purposes, the islands are grouped into the specific size ranges 1, 2-3, 4-7, 8-15,...., (Sherwood 1986) and the number of islands within a particular size range is given by

$$m(q) = \sum_{s_p=2^{q-1}}^{s_p=2^q-1} n(s_p) \qquad (q = 1, 2, 3, 4, ...) \tag{4.1}$$

where q characterizes the size range.

Following Sherwood's approach (Sherwood 1986), the island size distribution is assumed to satisfy the relation

$$n(s_p) \propto s_p^{-\alpha} \tag{4.2}$$

where α is a function of M and N_{Ca}.

Upon combining Equations (4.1) and (4.2), replacing sums by integrals, and assuming a proportionality constant K, we obtain

$$m(q) = K\frac{2^{(q-1)(1-\alpha)}}{(\alpha-1)}(1-[2(1-2^{-q})]^{1-\alpha})$$

$$\simeq K\frac{2^{(q-1)(1-\alpha)}}{(\alpha-1)}(1-2^{1-\alpha}) \qquad when \qquad 2^{-q} << 1 \tag{4.3}$$

In Figures 4.20a-f and 4.21a-f we plot log_2[n(q)] vs. q (the size range) for the data shown in Figures 4.3a-f and 4.4a-f, respectively. Only islands surrounded completely by the displacing phase are taken into account. The slopes of the best-fitting straight lines in Figures 4.20 and 4.21 correspond to the values of 1-α in Equation (4.3). The values of α determined from these plots are presented in Table 4.5 and they are the average of 4-6 simulations for each case. It may be observed that at a low viscosity ratio and high capillary numbers (Figures 4.3a,b,c), the values of α are quite close to that predicted by Sherwood (1986), namely 2.07. As the capillary number decreases, α tends to an approximate value of 1.95, which corresponds to the capillary limit. For a high viscosity ratio, α decreases from 5.2 at a high capillary number (Figure 4.4a) and tends to a value of 1.95 at low capillary numbers (Figure 4.4f). The high values of α in the stable displacement domain (Figures 4.3a,b) are to be expected since the vast majority of the islands here are of the pore size and only a few islands are of larger size. When decreasing the capillary number more islands of large size are formed and thus the value of α decreases.

To better understand some of the consequences of the above distributions assume that the number of islands of size s is equal to $Ks^{-\alpha}$ (Equation 4.2) and that the largest island is of size $O(N_p^{0.5})$, where N_p is the total number of pores in the network. Then, the total area of the islands is

$$A_t = K \sum_{s_p=1}^{s_p=N_p^{0.5}} s_p^{-\alpha} s_p \simeq \frac{K}{2-\alpha}(N_p^{1-\alpha/2} - 1) \tag{4.4}$$

and the areal density of the islands in the entire network is

$$f = \frac{A_t}{N_p} = \frac{K}{2-\alpha}(N_p^{-\alpha/2} - N_p^{-1}) \tag{4.5}$$

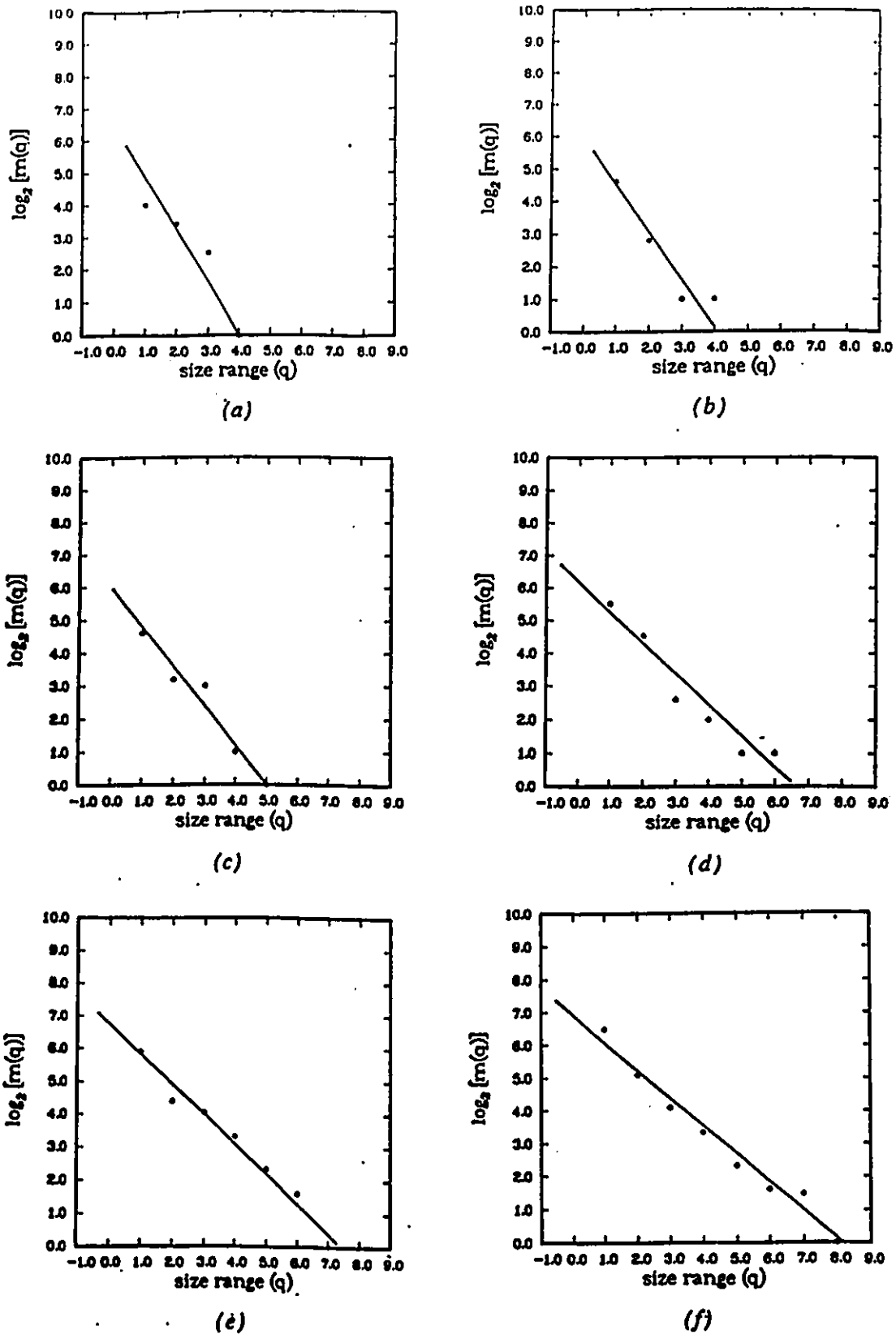

Figure 4.20: $log_2[m(q)]$ as a function of q for $M = 2.0 \times 10^{-5}$ and for: (a) $N_{Ca} = 5.0 \times 10^{-6}$, (b) $N_{Ca} = 5.0 \times 10^{-7}$, (c) $N_{Ca} = 1.0 \times 10^{-7}$, (d) $N_{Ca} = 1.0 \times 10^{-8}$. (e) $N_{Ca} = 5.0 \times 10^{-9}$. (f) $N_{Ca} = 1.0 \times 10^{-9}$.

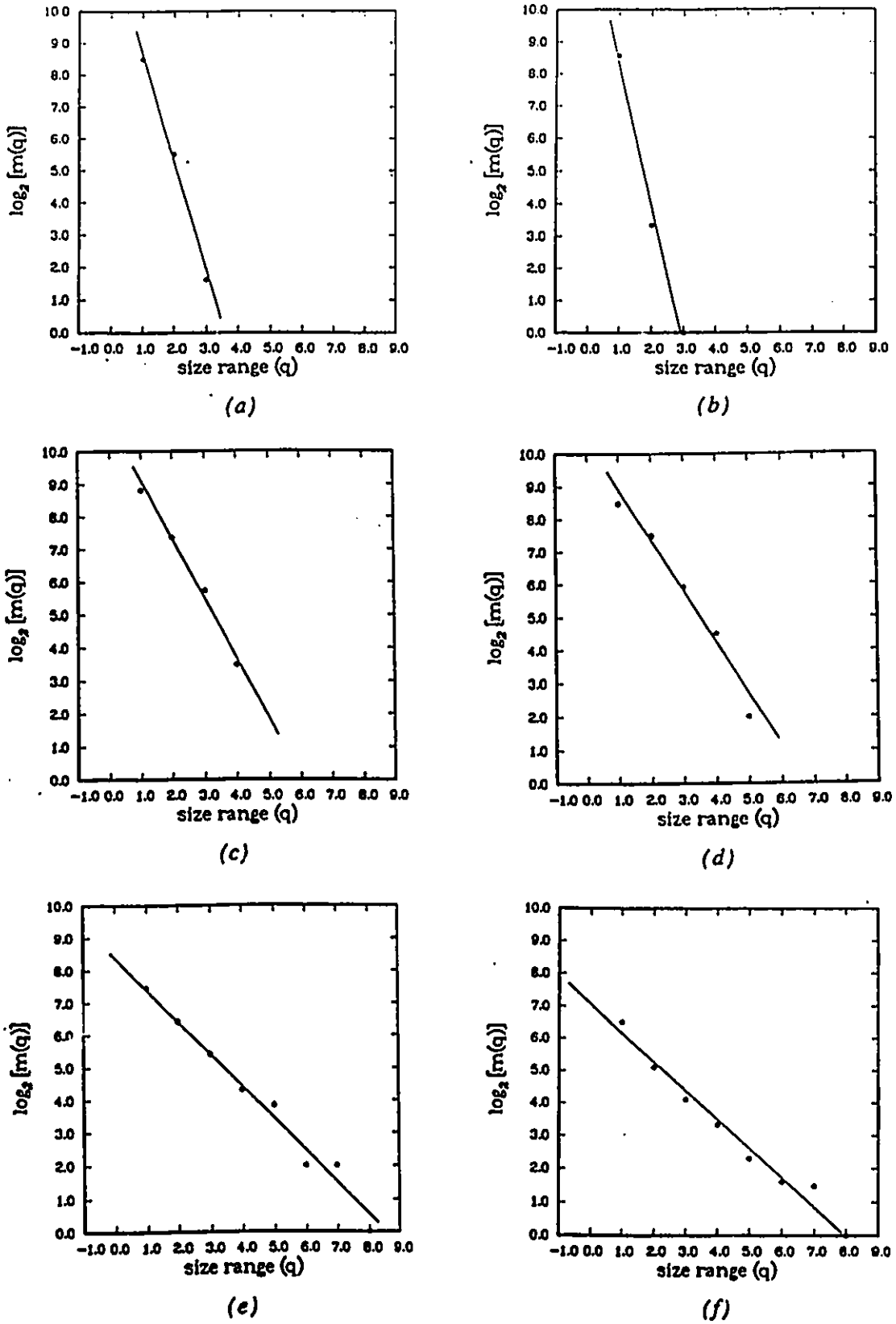

Figure 4.21: $log_2[m(q)]$ as a function of q for M=5.0 and for: (a) $N_{Ca} = 3.0 \times 10^{-1}$. (b) $N_{Ca} = 3.0 \times 10^{-3}$, (c) $N_{Ca} = 5.0 \times 10^{-5}$. (d) $N_{Ca} = 1.0 \times 10^{-5}$, (e) $N_{Ca} = 2.0 \times 10^{-6}$, (f) $N_{Ca} = 2.0 \times 10^{-7}$.

Table 4.5: Results of the Simulations (Stochastic Algorithm)

Figure	N_{Ca}	M	α
4.3a	5.0×10^{-6}	2.0×10^{-5}	2.28
4.3b	5.0×10^{-7}	2.0×10^{-5}	2.26
4.3c	1.0×10^{-7}	2.0×10^{-5}	2.13
4.3d	1.0×10^{-8}	2.0×10^{-5}	2.00
4.3e	5.0×10^{-9}	2.0×10^{-5}	1.97
4.3f	1.0×10^{-9}	2.0×10^{-5}	1.95
4.4a	3.0×10^{-1}	5.0	5.20
4.4b	3.0×10^{-3}	5.0	4.45
4.4c	5.0×10^{-5}	5.0	2.77
4.4d	1.0×10^{-5}	5.0	2.55
4.4e	2.0×10^{-6}	5.0	2.00
4.4f	2.0×10^{-7}	5.0	1.95

According to the last relation, the density of the island area decreases rapidly at high viscosity ratios for large values of α (stable displacement domain) with respect to the size of the network. However, the density decreases more gradually at lower capillary numbers (transition domain) and increases slowly in the capillary domain. At low viscosity ratios the density increases slowly in the DLA and the transition domains and decreases slowly as soon as the capillary limit is reached.

In conclusion, a study has been presented which demonstrates the effects of capillary and viscous forces on the island size distribution. The exponent α strongly depends upon the interplay of viscous and capillary forces and it provides a characteristic measure of trapping of the displaced fluid. Therefore, although trapping of the displaced fluid is a very complicated and apparently unpredictable phenomenon, this study reveals that trapping could be characterized qualitatively by the exponent

α.

4.1.5 Local Anisotropy and Heterogeneity

From the previous results it is apparent that viscous forces and capillary forces and their interplay expressed in terms of the capillary number, N_{Ca}, and the viscosity ratio, M, determine the dynamic behaviour of the invading fluid. However, the role and the effects of the structure of the porous medium on the displacement are not revealed by the numerical experiments presented above.

At this point, the effects of the local anisotropy of the network on the displacement are studied for two limiting cases: (a) DLA, i.e. displacements at a very low value of the viscosity ratio, and (b) viscous fingering at a viscosity ratio close to the instability limit (M=1). The deterministic algorithm is applied for four values of the dispersion, λ, which expresses the degree of local anisotropy. Sample runs are presented in Figures 4.22 and 4.23.

From these results it is observed that in the DLA case at $\lambda = 0.0$ the flow pattern of the invading fluid is finger-like or dendritic. The pressure gradients are higher in the flow direction towards the exit resulting in finger-like growth and relatively little growth of side-branches. Increasing the dispersion, λ, of the uniform size distribution, the flow pattern of the invading fluid becomes ramified. It is also observed that the degree of local anisotropy does not affect the oil sweep efficiency. These results are in good qualitative agreement with the findings, both numerical and experimental, of Chen and Wilkinson (1985) for radial displacement in etched

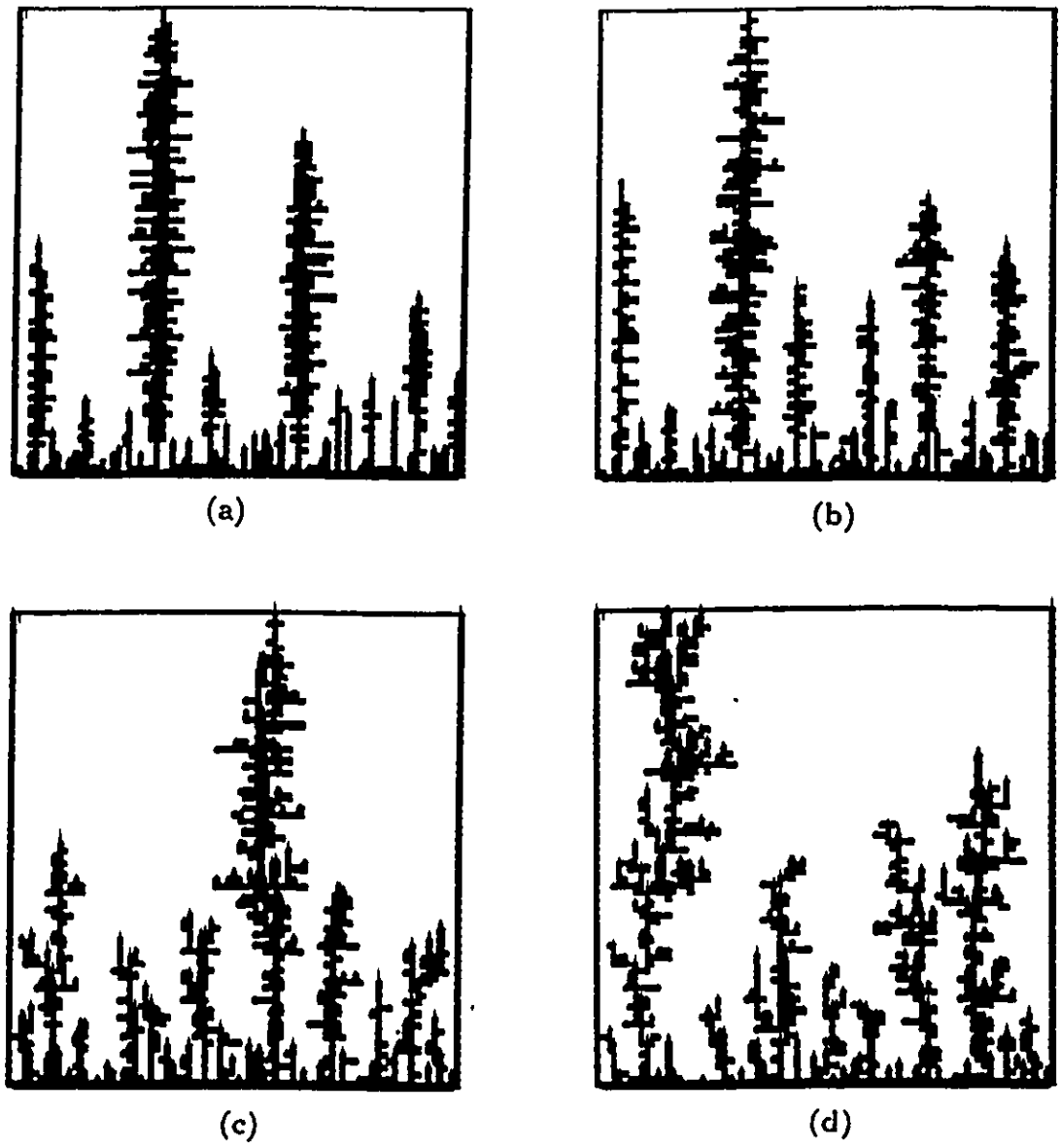

Figure 4.22: Deterministic simulations of DLA (M=2.0 $\times 10^{-5}$, N_{Ca}=1.0 $\times 10^{-4}$) for: (a) $\lambda = 0.0$, (b) $\lambda = 0.25$, (c) $\lambda = 0.50$, (d) $\lambda = 0.75$.

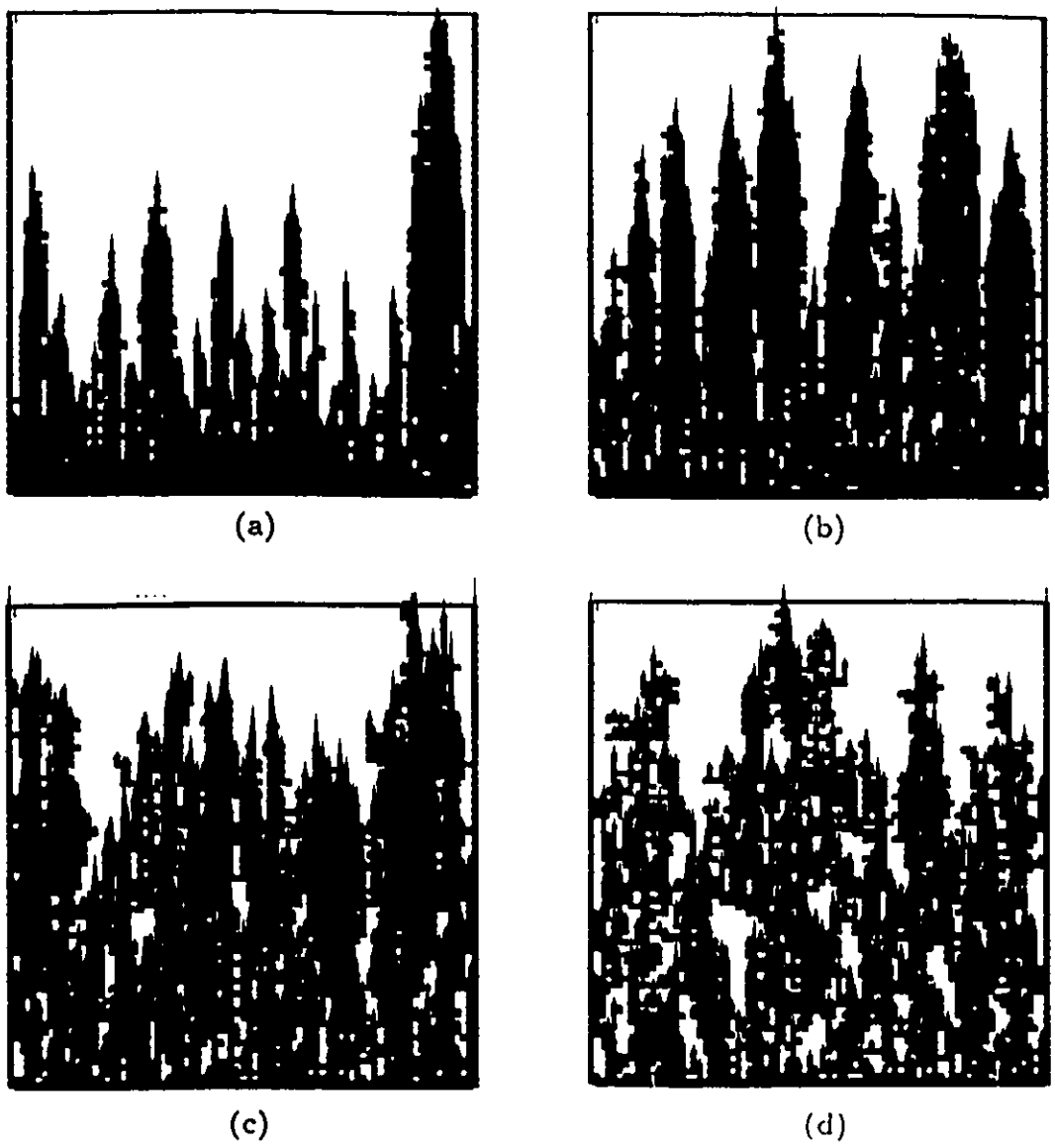

Figure 4.23: Deterministic simulations of viscous fingering (M=0.5, N_{Ca}=1.0 $\times 10^{-3}$) for: (a) $\lambda = 0.0$, (b) $\lambda = 0.25$, (c) $\lambda = 0.50$, (d) $\lambda = 0.75$.

networks. Chen (1989) confirmed these findings by carrying out experiments in an anisotropic Hele-Shaw cell.

In the case of viscous fingering the effects of the anisotropy are similar. However, the sweep efficiency is lower for $\lambda = 0.0$ and increases with increasing λ to approach a constant value. One can also see some similarities between the flow patterns in Figures 4.22a and 4.23a and physical experiments in Hele-Shaw cells.

4.1.6 Effects of Network Size on the Displacement

The invasion percolation algorithm has been used in order to study the effects of the size of the porous medium on the displacement efficiency. Runs were repeated 10 times for a range of sizes of the network with the smallest being 20×20 and the largest 140×140.

Figure 4.24 provides a plot of the logarithm of the sweep efficiency, $log_{10}E$, against the logarithm of the network size, $log_{10}L$. The sets of data $(log_{10}E, log_{10}L)$ fit to a straight line with a slope $D_h = -0.07$ which reveals a hyperscaling relation between E and L similar to Equation (2.12), namely,

$$E \propto L^{D_h} \tag{4.6}$$

A consequence of the above relationship is that $E \rightarrow 0$ as $L \rightarrow \infty$, which is characteristic of a fractal behaviour.

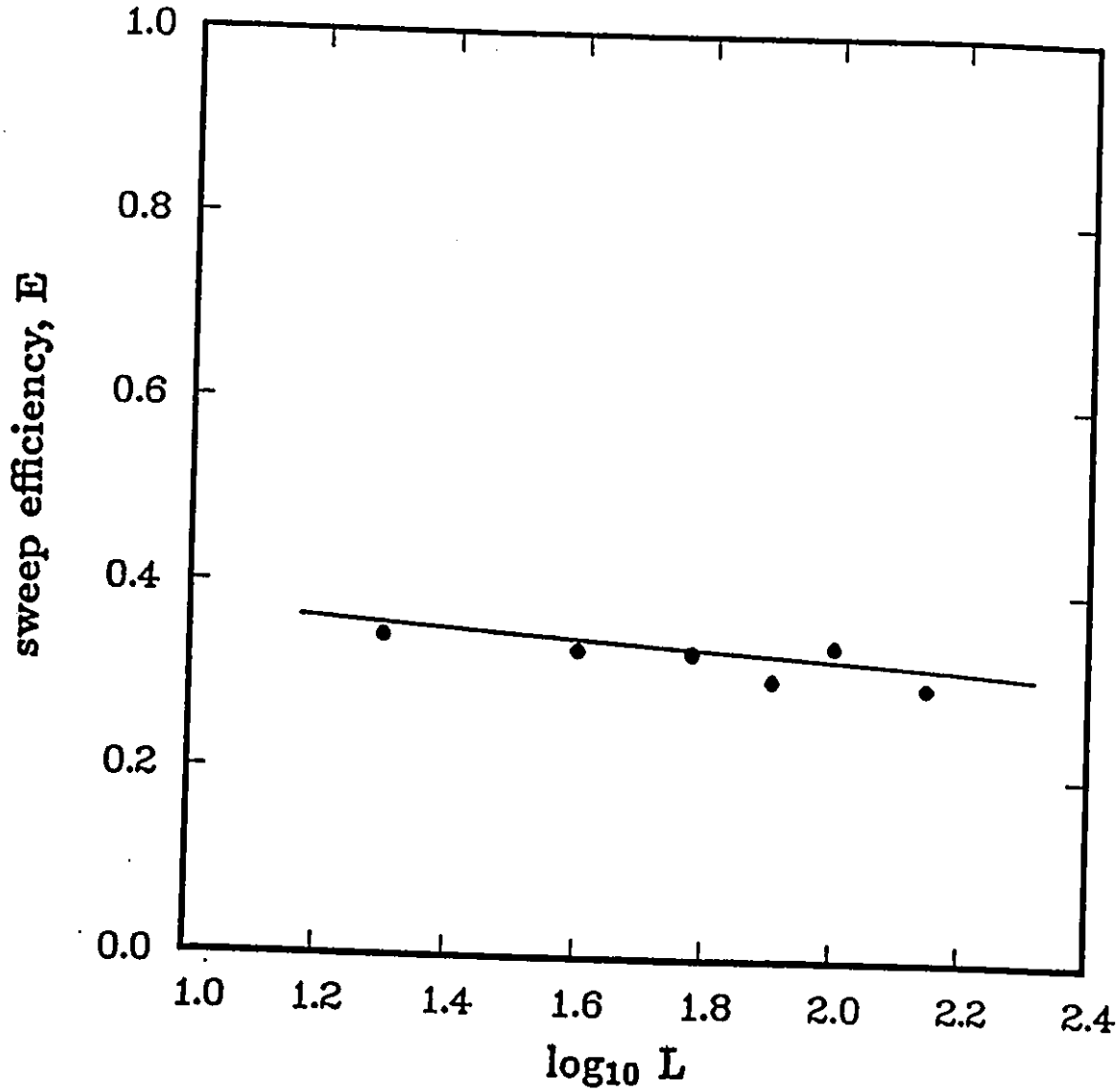

Figure 4.24: The sweep efficiency, E, as a function of the size, L, of the network for M=5.0 and N_{Ca}=1.0 $\times 10^{-10}$. The slope is equal to the hyperscaling exponent D_h.

4.1.7 Conclusions - Implications

At this point some practical implications of the above predictions are discussed with certain reservoir behaviours for different displacement conditions in enhanced oil recovery.

From the above results it is apparent that the highest displacement efficiency is achieved at high values of the capillary number and at favorable values of the viscosity ratio. In actual oil displacement processes one way to increase the viscosity ratio is to increase the viscosity of the displacing fluid by addition of a polymer. This usually happens when the viscosity of the oil is high and high flow rates of the displacing phase are achievable. However, it is true that due to technical limitations high flow rates of the displacing fluid are not always achievable. In this case, due to reservoir heterogeneity and anisotropy capillary fingering is inevitable. A common technique to deal with this problem in the oil industry is surfactant flooding in order to decrease the interfacial tension which results in an increase in the capillary number. Finally, in a displacement of a heavy oil, steam can be used (thermal recovery) to drastically decrease the viscosity of the oil resulting in an increase in the viscosity ratio towards the stability limit.

All the above notions of enhanced oil recovery techniques can be explained and understood, at least qualitatively, by the computer simulations presented above. However, this does not imply that the computer algorithms described in Chapter 3 can provide quantitative macroscopic predictions. They only provide microscopic predictions with some implications that can explain certain reservoir behaviours for

different displacement conditions as has been mentioned above.

4.2 Comparisons with Previous Work

4.2.1 Comparison of the Stochastic Algorithm with Leclerc and Neale's Algorithm

An extensive comparison between the stochastic algorithm described in Section 3.2 and Leclerc and Neale's algorithm is presented below since both algorithms predict the immiscible displacement of a wetting fluid by a non-wetting fluid in a porous medium. In addition, Leclerc and Neale's algorithm was the initiative for the present work and the only attempt that has been made to describe the transitions between the three distinct behaviours of the invading fluid, namely DLA, plug flow and capillary fingering, as they are mapped on the phase diagram. The differences and the advantages, as well as the limitations, of each model are discussed below:

(a) Trapping of the displaced phase accounts for the displacement of an incompressible fluid. In Leclerc and Neale's algorithm trapping of the displaced phase is not taken into account. Simulations with a trapping rule present show a significant difference in the fraction of the invaded pores. Trapping of the displaced phase results in a decrease in the recovery of the displaced phase.

(b) Leclerc and Neale's algorithm can be applied only to isotropic networks, since the transition probabilities of the random walkers are all equal to 0.25. However, finger-like growth of the invading phase is not observed as a result of the

diagonal steps of the random walkers and the next-to-nearest neighbour contacts of the random walkers with the interface. In the present work, the local anisotropy of the network is taken into account by the transition probabilities of the random walkers.

(c) In Leclerc and Neale's algorithm the sticking probability accounts for the capillary pressure and it is defined as the normalized ratio of the intraphase pressure drop which is arbitrary since determination of this intraphase pressure drop requires knowledge of the pressure field. The sticking probability in the present study is assigned only to wetting walkers providing a relative measure of the viscous forces in the invading and displaced phases. The capillary pressure is taken into account only in the transition region towards the capillary region by allowing the interface to move according to the invasion percolation mechanism with a frequency which depends on the phase transition probability.

(d) Leclerc and Neale made use of the DLA and anti-DLA models. Capillary fingering is desribed by the anti-DLA model and the notion of open bonds for percolation. However, at low values of the viscosity ratio and the capillary number motion of the interface occurs by non-wetting walkers (anti-DLA) which implies that pressure gradients in the displaced phase are negligible compared to the pressure gradients in the invading phase, which is not true since $M << 1$. The present algorithm makes use of the three stochastic models, i.e. DLA, anti-DLA and invasion percolation, in order to describe the distinct behaviours of the invading phase as well as the transition from one

region of the phase diagram to another.

(e) Leclerc and Neale's algorithm was applied to radial displacement while the present algorithm is applied to both linear and radial displacements (Kiriakidis et al. 1990a).

(f) Both algorithms are based on the phase diagram (Lenormand 1985) of the immiscible displacement of a wetting fluid by a non-wetting fluid in a porous medium in order to describe the transitions from one region to another.

(g) In the earlier work no attempt was made to predict the transition from DLA to plug flow.

In conclusion, the stochastic algorithm described in this study includes certain features which improve the simulation of the immiscible displacement of a wetting fluid by a non-wetting fluid in a porous medium with respect to Leclerc and Neale's algorithm.

4.2.2 Comparison between the Stochastic and the Deterministic Approaches

A comparison between the stochastic and the deterministic approaches for modelling the immiscible displacement of a wetting fluid by a non-wetting fluid reveals at this point the differences and the limitations in describing certain phenomena as well as the advantages and disadvantages. The following points which are discussed serve a comparison purpose.

(a) The stochastic approach does not provide an explicit solution to the problem, in contrast to the deterministic approach; instead, the solution is approximated by random walkers. The stochastic method approaches the correct pressure field only after a large number of random walkers have been averaged.

(b) According to the stochastic approach, the interface advances only by one pore at a time in a stochastic way. However, in reality advancement of the interface proceeds in a deterministic way and in fact the whole interface moves with local velocities which depend upon the local pressure gradients and the pore structure. Therefore, the deterministic approach provides a solution to the problem which is microscopically closer to the physics of the displacement.

(c) In the stochastic algorithm the interface moves by discrete steps ignoring the channel volume. By contrast, the deterministic algorithm resolves the motion of the interface inside the channels.

(d) According to the stochastic approach, the capillary pressure is taken into account only in the transition region towards capillary fingering. This approach is microscopically incorrect although it leads to a satisfactory agreement with physical experiments. By contrast, the deterministic approach takes into account the capillary pressure directly in solving for the pressure field.

(e) A problem appears when describing the transition from DLA to plug flow by using the stochastic algorithm. Noise is always present in the system due to the stochastic nature of the approach. In certain cases, the interface moves and invades pores which normally would not be invaded. This results in a noise to the solution.

(f) Modelling of two-fluid immiscible displacement flow by the stochastic approach requires a prior knowledge of the phase diagram and its limits. This requirement limits the application of the stochastic algorithm only to drainage displacement flow since no corresponding phase diagram is presently available. However, computer simulations and experiments by Vizika (1989) show that a phase diagram for imbibition displacement flow does exist. However, neither quantitative nor extensive studies have been conducted on this subject.

(g) There are certain quantities in the stochastic algorithm which have to be arbitrarily defined, such as the number of visits, the phase transition probability, the relative permeabilities and even the sticking probabilities. In addition, the physical significance of these parameters is not obvious.

(h) Attempts to include a connate non-wetting phase in stochastic simulations did not provide satisfactory results, especially at low values of the viscosity ratio. Random walkers coming from within the wetting phase avoid the connate phase and they finally stick to the interface far from the connate regions. Therefore, the front rarely approaches the connate regions.

(i) The stochastic algorithm is fast compared to the deterministic one. Typical runs take about 0.5-6 hours (real time). By contrast, typical runs of the deterministic algorithm take about 2-9 days, depending upon the number of iterations. Runs at the capillary limit are very time consuming due to the very high number of iterations required. In both algorithms, a large proportion of the execution time is taken up by the trapping subroutine.

In conclusion, the deterministic algorithm developed in this study better describes the physics of the problem and it is capable of providing quantitative predictions of the behaviour of the invading fluid by directly solving for the pressure field. However, its most serious drawback is the large amount of execution time required in the computer, especially for runs close to the capillary limit. By contrast, the stochastic algorithm is fast and especially in the case of capillary fingering very reliable, but with certain serious limitations as discussed above.

4.2.3 Comparison between the Present Deterministic Algorithm and Other Deterministic Algorithms

The differences and similarities between the different deterministic models in the literature and the present deterministic approach developed in this study are discussed at this point.

All the deterministic models mentioned in Section 2.2 solve for the pressure field in the network by considering the flow conservation equation at each pore in conjunction with appropriate boundary conditions. For the solution of the system of equations the Gauss-Seidel relaxation and overrelaxation techniques are used. The deterministic algorithms of Sherwood and Nittman (1986) and DeGregoria (1985,1986) are applied only to the viscous region from DLA to plug flow. Local heterogeneities of the network are not taken into account. The interface advances in a stochastic manner with a probability which depends on the local pressure gradients. Motion of the interface occurs in discrete steps which is microscopically incorrect as has been mentioned above.

The deterministic algorithm developed in this work makes use of a non-linear approximation proposed by Lenormand et al. (1988). However, motion of the interface is resolved differently. According to Lenormand et al. (1988) a channel with an interface is completely filled with the non-wetting fluid as long as the pressure difference exceeds the capillary pressure. Then, motion of the interface is resolved inside the pores. The whole interface moves along the front within the pores according to a time-step. Blunt and P.King's (1991a,b) algorithm solves the linear problem for the pressure field and moves the interface in a similar way (Lenormand et al. 1988). However, pores previously filled with the invading fluid may become emptied at certain steps of the algorithm. This phenomenon describes better the physics of the real problem and it can lead to the formation of connate regions of the invading fluid within the network which may again become part of the invading phase. Therefore, the main difference between the above two algorithms and the deterministic algorithm described in the present work is in the microscopic motion of the interface at each step of the simulation.

A more realistic model has been proposed by Dias and Payatakes (1986a,b) and also used by Vizika (1989). This model is microscopically more realistic since it takes into account the pressure drop inside the pores and can incorporate a conical shape for the channels. The mathematical model is linear and motion of the interface is resolved in both the channels and the pores. However, the main drawback of the model is the greater amount of execution time required in the computer.

Chapter 5

CONCLUSIONS AND FUTURE WORK

This chapter presents the conclusions of the present study on the displacement of wetting fluid by a non-wetting fluid in a porous medium represented by a two-dimensional network of interconnected capillaries. Recommendations for future work are also given.

5.1 Conclusions

Two computer programs have been developed in order to study the displacement of a wetting fluid by a non-wetting fluid in a porous medium represented by a two-dimensional network of interconnected capillaries.

A stochastic approach has been applied in order to solve the governing equations at the pore level. The stochastic approach is based on the DLA, anti-DLA and invasion percolation models modified in order to incorporate the local anisotropy and heterogeneity of the porous medium, as well as on the notion of the phase diagram for immiscible displacement in porous media. This approach successfully predicts

the transition from one region of the phase diagram to another by making use of a mechanism which takes into account the interplay of viscous and capillary forces in terms of the phase transition probability. The stochastic approach presented in this work has also enabled good predictions of the effects of capillary and viscous forces on the island formation, the island size distribution, the dynamic and fractal behaviour of the displacing fluid and on the oil recovery.

A deterministic approach has also been applied to model the displacement of a wetting fluid by a non-wetting one by using a relaxation technique for solving the governing equations at the pore level and certain rules for the advancement of the interface inside the channels. The deterministic approach successfully predicts the effects of viscous and capillary forces on the dynamic behaviour of the displacing fluid and on the oil recovery, as well as the effects of the local anisotropy and heterogeneity of the porous medium on the dynamic behaviour of the displacing fluid.

A direct comparison between the stochastic and the deterministic approaches has revealed that the deterministic approach is more general since it can be extended in order to model imbibition displacements in porous media. It is also more accurate and better describes the physics of flow in porous media. However, the deterministic algorithm is time consuming in terms of execution time in the computer.

The two computer programs described in the present study can be used in order to gain insight into the role of certain fundamental parameters (such as fluid viscosities, flow rate, wettability, interfacial tension and morphology of the porous medium) on

enhanced oil recovery techniques employed by the oil industry.

5.2 Recommendations for Future Work

The present work could be used as a starting point for further studies leading to a better understanding of the physics of two-fluid immiscible displacement flow in porous media. In particular, the following studies could be conducted:

(a) Extension of the deterministic algorithm to (i) radial displacement and to (ii) the quarter of a five-spot flow geometry displacement of a wetting fluid by a non-wetting fluid. The physics of these problems remains the same and only the boundary conditions and the notation of the channels and pores would need to be changed.

(b) The present deterministic algorithm describes drainage displacement flow in two-dimensional networks (Lenormand et al. 1988). The algorithm could be extended to model displacement flow in quasi-two-dimensional consolidated or unconsolidated porous media.

(c) The deterministic algorithm could be modified in order to model imbibition displacement flow in porous media by solving the linear problem for the pressure field and allowing pores to be invaded by the displaced fluid. Extension to quasi-two-dimensional porous media is also possible. A comparison between imbibition and drainage displacement simulations would be very interesting since it could provide an insight into the role of the wettability on the efficiency of the displacement processes. Furthermore, studies in displacement flow under conditions of mixed wettability and non-uniform permeability are

of considerable interest to the oil industry, since most oil reservoirs exhibit a mixed wettability ranging from strongly water-wet to strongly oil-wet.

(d) The deterministic algorithm could be used for extensive studies of the relative permeabilities. The effects of the wettability, capillary number, connate water, disorder and other parameters on the relative permeabilities of both the displaced and invading phases could be studied by applying the method proposed by Blunt and P.King (1990a).

(e) The effects of gravity on the behaviour of the invading fluid and on the oil recovery could be studied by performing experiments in inclined networks or consolidated porous media. Such studies could reveal the existence of a phase diagram describing the behaviour of the invading fluid as a result of the interplay of viscous, capillary and gravity forces. Similar studies by computer simulations would be another objective.

(f) The stochastic algorithm could be used in order to study disordered and fractal porous media by the DLA or the invasion percolation models. The stochastic algorithm and especially the invasion percolation algorithm, could be applied to three-dimensional networks in order to study disordered and fractal media.

Bibliography

[1] Bakurov, V.G., Gusef, V.I., Izmailov, A.F., and Kessel, A.R., "Dynamical Percolation Model of Oil Displacement by Water in the Oil Reservoir", **J. Phys. A: Math. Gen.**, 23, 2313-2340 (1990).

[2] Ball, R.C., and Brady, R.M., "Large Scale Lattice Effects in Diffusion-Limited Aggregation", **J. Phys. A: Math. Gen.**, 18, L809-L813 (1985).

[3] Blunt, M., and King, P., "Macroscopic Parameters from Simulations of Pore Scale Flow", **Transport in Porous Media**, in press (1991a).

[4] Blunt, M., and King, P., "Relative Permeabilities from Pore Scale Network Modelling", **Transport in Porous Media**, in press (1991b).

[5] Broadbent, S.R., and Hammersley, J.M.,"Percolation Processes I. Crystals and Masses", **Proc. Cambridge Phil. Soc.**, 53, 629-645 (1957).

[6] Chan, D.Y.C., Houghes, B.D., Paterson, L., and Sirakoff, C.,"Simulating Flow in Porous Media", **Phys. Rev. A**, 38, 4106-4120 (1988).

[7] Chandler, R., Koplik, J., Lerman, K., and Wilkinson, J.F., "Capillary Displacement and Percolation in Porous Media", **J. Fluid Mech.**, 119, 249-267 (1982).

[8] Chen, J-D., "Radial Viscous Fingering in Hele-Shaw Cells", **Experiments in Fluids**, 5, 363-371 (1989).

[9] Chen, J-D., and Koplik, J., "Immiscible Displacement in Small Networks", **J. Colloid Interf. Sci.**, 108, 304-329 (1985).

[10] Chen, J.-D., and Wilkinson, J.F., "Pore-Scale Viscous Fingering in Porous Media", **Phys. Rev. Lett.**, 55, 1892-95 (1985).

[11] Chuoke, R.L., van Meers, P., and van der Poel, C., "The Instability of Slow Immiscible Viscous Liquid-Liquid Displacements in Permeable Media", **Trans. AIME**, 216, 188-194 (1959).

[12] Cuiec, L.E., "Evaluation of Reservoir Wettability and its Effects in Oil Recovery", Interfacial Phenomena in Oil Recovery, Marcell Dekker, New York, 319-375 (1990).

[13] Darcy, M., Les Fontaines Publiques de la Ville de Dijon, Dalmont, Paris (1856).

[14] De Gregoria, A.J., "A Predictive Monte Carlo Simulation of Two-Fluid Flow through Porous Media at Finite Mobility Ratios", **Phys. Fluids**, 28, 2933-2935 (1985).

[15] De Gregoria, A.J., "Monte Carlo Simulations of Two-Fluid Flow through Porous Media at Finite Mobility Ratios", **Phys. Fluids**, 29, 3557-3561 (1986).

[16] De Gregoria, A.J., and Schwartz, L.W., "A Boundary-Integral Method for Two-Phase Flow Displacement in Hele-Shaw Cells", **J. Fluid Mech.**, 162, 383-400 (1985).

[17] Dias, M.M., and Payatakes, A.C.,"Network Models for Two-Phase Flow in Porous Media. Part 1. Immiscible Microdisplacement of Non-Wetting Fluids", **J. Fluid Mech.**, 164, 305-336 (1986a).

[18] Dias, M.M., and Payatakes, A.C., "Network Models for Two-Phase Flow in Porous Media. Part 2. Motion of Oil Ganglia", **J. Fluid Mech.**, 164, 337-358 (1986b).

[19] Dullien, F.A.L., Porous Media, Fluid Transport and Pore Structure, Academic Press, New York (1979).

[20] Fatt, I., "The Network Model of Porous Media I. Capillary Pressure Characteristics", **Trans. AIME**, 207, 44-159 (1956a).

[21] Fatt, I., "The Network Model of Porous Media II. Dynamic Properties of a Single Size Tube Network", **Trans. AIME**, 207, 160-163 (1956b).

[22] Fatt, I., "The Network Model of Porous Media III. Dynamic Properties with Tube Radius Distribution", **Trans. AIME**, 207, 164-181 (1956c).

[23] Fernandez, J.F., and Narayan, K.A., "Diffusion-Limited Aggregation with Surface Tension: Scaling of Viscous Fingering", **Phys. Rev. Lett.**, 64, 2133-2136 (1990).

[24] Forrest, S.R., and Witten, T.A., "Long-Range Correlations in Smoke-Particle Aggregates", **J. Phys. A: Math. Gen.**, 12, 1210-1218 (1979).

[25] Greenkorn, R., Flow Phenomena in Porous Media, Marcel Dekker, New York (1983).

[26] Hele-Shaw, J.H.S., "The Flow of Water", **Nature**, 58, 34-36 (1898).

[27] Homsy, G.M., "Viscous Fingering in Porous Media", **Ann. Rev. Fluid Mech.**, 19, 271-311 (1987).

[28] Jha, K.N., "Enhanced Oil Recovery-An Introduction", **Chemistry in Canada**, 19-26 (Sept. 1973).

[29] Kadanoff, L.P., "Simulating Hydrodynamics: A Pedestrian Model", **J. Stat. Phys.**, 39, 267-283 (1985).

[30] Kertesz, J., and Vicsek, T., "Diffusion-Limited Agregation and Regular Patterns: Flactuations versus Anisotropy", **J. Phys. A: Math. Gen.**, 19, 2257-262 (1986).

[31] King, M.J., and Scher, H., "Probability Approach to Multiphase and Multicomponent Fluid Flow in Porous Media", **Phys. Rev. A**, 35, 929-932 (1987).

[32] King, P.R., "The Fractal Nature of Viscous Fingering in Porous Media", **J. Phys. A: Math. Gen.**, 20, L529-L534 (1987).

[33] Kiriakidis, D.G., Neale, G.H., and Mitsoulis, E., "Numerical Simulations of Radial Displacement of a Wetting Fluid by a Non-Wetting Fluid in a Porous Medium", **J. Phys. A: Math. Gen.**, 23, 5089-5094 (1990a).

[34] Kiriakidis, D.G., Mitsoulis, E., and Neale, G.H., "Modelling of Two-Phase Flow in Porous Media", **6th Int. Conf. Inst. Fr. Petr.**, Arles, France (1990b).

[35] Kiriakidis, D.G., Mitsoulis, E., Neale, G.H., "Linear Immiscible Displacement of a Wetting Fluid by a Non-Wetting Fluid in Porous Media", **Can. J. Chem. Eng.**, 69, 557-563 (1991).

[36] Kiriakidis, D.G., Neale, G.H., and Mitsoulis, E., "Effects of Capillary Forces on the Island Size Distribution for Immiscible Displacement Flow in Porous Media", **J. Phys. A: Math. Gen.** (1991b in press).

[37] Kirkpatrick, S.,"Percolation and Conduction", **Rev. Mod. Phys.**, 45, 574-588 (1973).

[38] Koplik, J. and Lasseter, J.J., "One and Two-Phase Flow in Network Models of Porous Media", **Chem. Engng. Commun.**, 26,

285-295 (1986).

[39] Laidlow, W.G., Hamilton, G.R., Flewweling, R.B., and Wilson, W.G., "Fractal Patterns of Fluid Domains for Displacement Processes in Porous Media", **J. Stat. Phys.**, 53, 713-732 (1988).

[40] Lake, W.L., Enhanced Oil Recovery, Prentice Hall, New Jersey (1989).

[41] Larson, R.G., Scriven, L.E., and Davis, H.T., "Percolation of Residual Phases in Porous Media", **Nature**, 268, 409-418 (1977).

[42] Larson, R.G., Scriven, L.E., and Davis, H.T., "Percolation Theory of Two-Phase Flow in Porous Media", **Chem. Eng. Sci.**, 36, 57-73 (1981).

[43] Larson, R.G., Davis, H.T., and Scriven, L.E., "Displacement of Residual Non-Wetting Fluid from Porous Media", **Chem. Eng. Sci.**, 36, 75-85 (1981).

[44] Leclerc, D.F., and Neale, G.H., "Monte-Carlo Simulations of Radial Displacement of Oil from a Wetted Porous Medium: Fractals, Viscous Fingering and Invasion Percolation", **J. Phys. A: Math. Gen.** , 20, 2979-2994 (1988).

[45] Lefebvre du Prey, E.I., "Factors Affecting Liquid-Liquid Relative Permeabilities in a Consolidated Porous Medium", **Soc. Pet. Eng. J.**, 13, 39-47 (1973).

[46] Lenormand, R., "Differents Mechanismes de Deplacement Visqueux et Capillaires en Milieu Poreux: Diagram de Phase", **C.R. Acad. Sci. Paris**, 301, 247-250 (1985).

[47] Lenormand, R., "Pattern Growth and Fluid Displacements through Porous Media", **Physica A**, 140, 114-123 (1986a).

[48] Lenormand, R. "Scaling Laws for Immiscible Displacements with Capillary and Viscous Fingering", **SPE 15390, 61st Annual Tech. Conf. and Exhib. of SPE**, New Orleans LA, Oct 5-8 (1986b).

[49] Lenormand, R., "Applications of Fractal Concepts in Petroleum Engineering", **Physica D**, 38, 230-234 (1989a).

[50] Lenormand, R., "Flow through Porous Media: Limits of Fractal Patterns", **Proc. R. Soc. London A**, 423, 159-168 (1989b).

[51] Lenormand, R., and Boris, S., "Description d' un Mechanisme de Convection de Liaison Destine a l' Etude du Drainage avec Piegage en Milieux Poreux", **C.R. Acad. Sci. Paris B**, 291, 279-283 (1980).

[52] Lenormand, R., Zarcone, C., and Sarr, A.," Mechanisms of the Displacement of One Fluid by Another in a Network of Capillary Ducts", **J. Fluid. Mech.**, 135, 337-353 (1983).

[53] Lenormand, R., Zarcone, C., "Invasion Percolation in an Etched Network: Measurement of a Fractal Dimension", **Phys. Rev. Lett.**, 54, 2226-2229 (1985a).

[54] Lenormand, R., and Zarcone, C., "Two-Phase Flow Experiments in a Two-Dimensional Permeable Medium", **PhysicoChem. Hydrodyn.**, 6, 497-505 (1985b).

[55] Lenormand, R., Touboul, E., and Zarcone, C., "Numerical Models and Experiments on Immiscible Displacements in Porous Media", **J. Fluid Mech.**, 189, 165-187 (1988).

[56] Lenormand, R., and Zarcone, C., "Capillary Fingering: Percolation and Fractal Dimension", **Transport in Porous Media**, 4, 599-612 (1989).

[57] Liang, S., "Random Walk Simulations of Flow in Hele-Shaw Cells", **Phys. Rev. A**, 33, 2663-2674 (1986).

[58] Maloy, K.I., Feder, J., and Jossang, T., "Viscous Fingering Fractals in Porous Media", **Phys. Rev. Lett.**, 55, 2688-2691 (1985).

[59] Mandelbrot, B.B., The Fractal Geometry of Nature, Freeman S. Francisco (1982).

[60] Mandelbrot, B.B., "Fractal Geometry: what it is and how does it do?", **Proc. R. Soc. London A**, 423, 3-16 (1989).

[61] McCarthy, J.F., "Invasion Percolation on a Random Lattice", **J. Phys. A: Math. Gen.**, 20, 3465-3469 (1987).

[62] McKean, H.C., and Dawe, R.A., "Numerical Simulations of Displacement in Systems Containing a Lens of Heterogeneity", **J. Can. Petr. Tech.** , 29, 88-93 (1990).

[63] McLean, J.W., and Saffman, P.G., "The Effect of Surface Tension on the Shape of Fingers in a Hele-Shaw Cell", **J. Fluid Mech.**, 102, 455-469 (1981).

[64] Meakin, P., "Diffusion-Controlled Cluster Formation in Two, Three, and Four Dimensions", **Phys. Rev. A**, 27, 604-607 (1983a).

[65] Meakin, P., "Diffusion Controlled Cluster Formation in 2-6 Dimensional Space", **Phys. Rev. A**, 27, 1495-1507 (1983b).

[66] Meakin, P., and Deutch, J.M., "The Formation of Surfaces by Diffusion-Limited Annihilation", **J. Chem. Phys.**, 85, 2320-2325 (1986).

[67] Meakin, P., and Vicsek, T., "Diffusion-Limited Aggragation with Radial Bias", **J. Phys. A: Math. Gen.**, 20, L171-L175 (1987).

[68] Meakin, P., and Tolman, S., "Diffusion-Limited Aggregation", **Proc. R. Soc. London A**, 423, 133-148 (1989).

[69] Mohanty, K.K., Davis, H.T., and Scriven, L.E., "Physics of Oil Entrapment in Water-Wet Rocks", **SPE Reserv. Engng**, 113-128 (Feb. 1987).

[70] Morrow, N.R., "Wettability and its Effects on Oil Recovery", **SPE Reserv. Engng.**, 1476-1484 (Dec. 1990).

[71] Nasr-el-Din, H.A., Khulbe, K.C., Hornof, V., and Neale, G.H., "Effects of Interfacial Reaction on the Radial Displacement of Oil by Alkaline Solutions", **Rev. Inst. Fr. Petr.**, 45, 231-243 (1990).

[72] Ni, L.W., Hornof, V., and Neale, G.H., "Radial Fingering in a Porous Medium", **Rev. Inst. Fr. Petr.**, 41, 217-228 (1986).

[73] Nittmann, J., Daccord, G., and Stanley, E.H., "Fractal Growth of Viscous Fingers: Quantitative Characterization of a Fluid Instability Phenomenon", **Nature**, 314, 141-144 (1985).

[74] Nittmann, J., and Stanley, E.H., "Tip Splitting without Interfacial Tension and Dendritic Growth Patterns Arising from Molecular Anisotropy", **Nature**, 321, 663-668 (1986).

[75] Odeh, A.S., "Effect of Viscosity Ratio on Relative Permeability", **Trans. AIME**, 216, 346-353 (1959).

[76] Paterson, L., Hornof, V., and Neale, G.H., "Visualization of a Surfactant Flood of an Oil saturated Porous Medium", **Soc. Pet. Eng. J.**, 24, 325-327 (1984).

[77] Paterson, L., "Radial Viscous Fingering in a Hele-Shaw Cell", **J. Fluid Mech.**, 113, 513-540 (1981).

[78] Paterson, L., "Diffusion-Limited Aggregation and Two-Fluid Displacement in Porous Media", **Phys. Rev. Lett.**, 52, 1621-1624

(1984).

[79] Paterson, L., "Simulations of Fluid Displacement in Heterogeneous Porous Media", **J. Phys. A: Math. Gen.**, 20, 2179-2185 (1987).

[80] Paterson, L., Hornof, V., and Neale, G.H., "Water Fingering into an Oil-Wet Porous Medium Saturated with Oil or Connate Water Saturation", **Rev. Inst. Fr. Petr.**, 39, 517-521 (1984).

[81] Payatakes, A.C., "Dynamics of Oil Ganglion during Immiscible Displacement in Water-Wet Porous Media", **Ann. Rev. Fluid. Mech.**, 14, 365-393 (1982).

[82] Payatakes, A.C., and Dias, M.M., "Immiscible Microdisplacement and Ganglion Dynamics in Porous Media", **Rev. Chem. Engng.**, 2, 85-174 (1984).

[83] Peters, E.J., and Flock, D.L., "The Onset of Instability during Two-Phase Immiscible Displacement in Porous Media", **Soc. Pet. Eng. J.**, 21, 249-258 (1981).

[84] Pool, R., "Fractal Fracas", **Science**, 249, 363-364 (1990).

[85] Ramakrishnan, T.S., and Wasan, D.T., "Two-Phase Distributions in Porous Media: an Application of Percolation Theory", **Int. J. Multiphase Flow**, 12, 357-388 (1986).

[86] Rudnick, J., and Gaspari, G., "The Shape of Random Walks", **Science**, 127, 384-389 (1987).

[87] Ryan, J.T., and Neale, G.H., "Two-Phase Flow through Fractures in Porous Media", **Can. J. Chem. Eng.**, 55, 471-472 (1975).

[88] Saffman, P.G., and Taylor, G.I., "The Penetration of a Fluid into a Porous Medium or a Hele-Shaw Cell Containing a More Viscous Liquid", **Proc. R. Soc. London, Ser.A**, 245, 312-339 (1958).

[89] Sahimi, M., and Yortsos, Y.C., "Pattern Formation in Viscous Fingering: a Diffusion-Limited Aggregation Approach", **Phys. Rev. A**, 32, 3762-3764 (1985).

[90] Sahimi, M., and Siddiqui, H., "The Effect of Morphological Disorder on Viscous Fingering and Diffusion-Limited Aggregation in a Porous Medium", **J. Phys. A: Math. Gen.**, 20, L89-L96 (1987).

[91] Scheidegger, A.E., The Physics of Flow through Porous Media, University of Toronto Press (1974).

[92] Sherwood, J.D., "Island Size Distribution in Stochastic Simulations of the Saffman-Taylor Instability", **J. Phys. A: Math. Gen.**, 19, L195-l200 (1986).

[93] Sherwood, J.D., and Nittmann, J., "Gradient Governed Growth: the Effect of Viscosity Ratio on Stochastic Simulations of the Saffman-Taylor Instability", **J. Physique**, 47, 15-22 (1986).

[94] Shreider, J.A. Methods of Statistical Calculations: The Monte Carlo Method, Prentice Hall, New York (1963).

[95] Siddiqui, H., Cluster Aggregation and Fluid Displacement Processes in Porous Media, Ph.D. Thesis, University of Southern California, USA (1989).

[96] Stalkup, F.I., "Displacement of Oil by Solvent at High Water Saturation", **SPE J.**, 10, 337-348 (1970).

[97] Stauffer, D., Introduction to Percolation Theory, Taylor and Francis, London (1985).

[98] Tang, C., "Diffusion-Limited Aggregation and the Saffman-Taylor Problem", **Phys. Rev. A**, 31, 1977-1979 (1985).

[99] Tayal, P., and Narayan, K.A., "Visualization of Water and Surfactant Floods in Oil-Saturated Porous Media", **Experiments in**

Fluids, 9, 337-344 (1990).

[100] Tryggavson, G., and Aref, H., "Numerical Experiments in Hele-Shaw Flow with a Sharp Interface", **J. Fluid Mech.**, 136, 1-30 (1983).

[101] Turkevitch, L., and Scher, H., "Occupancy Probability Scaling in Diffusion-Limited Aggregation", **Phys. Rev. Lett.**, 55, 1026-1029 (1985).

[102] Vicsek, T., "Pattern Formation in Diffusion-Limited Aggregation", **Phys. Rev. Lett.**, 53, 2281-2284 (1984).

[103] Vizika, O., Immiscible Microdisplacements in Porous Media, Ph.D. Thesis, University of Patras, Greece (1989).

[104] Wilkinson, D., "Percolation Model of Immiscible Displacement in the Presence of Buoyancy Forces", **Phys. Rev. A**, 30, 520-521 (1986).

[105] Wilkinson, D., and Barsony, M., "Monte-Carlo Studies of Invasion Percolation in Two and Three Dimensions", **J. Phys. A: Math. Gen.**, 17, 2129-2135 (1984).

[106] Wilkinson, D., and Willemsen, J.F., "Invasion Percolation: A New Form of Percolation Theory", **J. Phys. A: Math. Gen.**, 16, 3365-3376 (1983).

[107] Williams, J.K., and Dawe, R.A., "Fractals: An Overview of Potential Applications to Transport in Porous Media", **Transport in Porous Media**, 1, 201-209 (1986).

[108] Witten, T.A., and Sander, L.M., "Diffusion-Limited Aggregation, a Kinetic Critical Phenomenon", **Phys. Rev. Lett.**, 47, 1400-1403 (1981).

[109] Witten, T.A., and Sander, L.M., "Diffusion-Limited Aggregation", **Phys. Rev. B**, 27, 5686-5697 (1983).

[110] Yanuka, M., Dullien, F.A.L, and Elrick, D.E., "Percolation Processes and Porous Media. I. Geometrical and Topological Model of Porous Media Using a Three-Dimensional Joint Pore-Size Distribution", **J. Colloid Interf. Sci.**, 112, 24-41 (1986).